COMPUTATIONAL MODELLING OF THE ANGIOPOIETIN AND TIE INTERACTIONS.

Thesis submitted for the degree of

Doctor of Philosophy

at the University of Leicester

by

Deborah O. A. Alawo

Department of Cardiovascular Sciences

University of Leicester

September 2013

Computational modelling of the angiopoietin and Tie interactions.

Deborah O. A. Alawo

Abstract

Angiopoietins have been shown to regulate the vascular states of development and quiescence. Activation of this signalling pathway through their receptor tyrosine kinase, Tie2, is involved in angiogenesis and vascular protection. Regulation of this pathway is under tight control and has many complex factors which regulate its activation, defects in which cause many pathological conditions such as; vascular disease, sepsis and cancer. There are several factors which are integrated to control the Tie2 signalling pathway at the level of the receptor and these mechanisms are poorly understood. Computational and mathematical modelling can be used to understand the regulation of this pathway.

The aim of this project was to construct a quantitative model of the angiopoietin and Tie interactions at the endothelial cell surface. A schematic representation of the interactions was produced in the CellDesigner modelling program. Ordinary differential equations were used to describe the system and change of states over time. Parameters required for the simulation of the model were identified and most were obtained from the literature, while others were quantified through experiments. The model was converted for use in MATLAB to simulate the angiopoietin time-courses and concentration-dependent studies. Quantitative Western blotting was used to measure the relative levels of receptor activation in endothelial cells stimulated with angiopoietin(s). Subsequently simulation results were compared to experimental data to validate the model.

In summary this project has established a model similar to physiological conditions which is valid for Ang1 and potentially for Ang2 interactions. This simplified model of Ang1 and Ang2 interactions with Tie2 on the endothelial cell surface provides a foundation on which further analysis, and additional receptor modelling can be performed and expanded. The model can also be used to test hypotheses, generate new predictions, and identify new therapeutic targets for many diseases.

Acknowledgements

First and foremost I would like to thank my supervisor Professor Nick Brindle for giving me the opportunity to do this multidisciplinary PhD project and whose guidance and support was invaluable. To my engineering collaborators; Professor Declan Bates, Dr Svetlana Amirova, Dr Adam Spargo and Dr Matthew Turner, for their initial support in constructing the model and teaching me the basics of MATLAB.

I also thank the past and present members of the Brindle lab; TJ, Eyad, Nisha, Djalil and Mandeep. With special thanks to the Postdocs Dr Harprit Singh and Dr Tariq Tahir for all their advice and assistance with experiments. Also to the Cardiovascular Sciences technical staff Julie Chamberlain and Jonathan Barber for their initial assistance with the HUVECs.

Finally I would like to thank my family and friends for their constant positive encouragement and support throughout the years.

Contents

List of Figures

Chapter 5

Results: Model simulations and validation without dephosphorylation

Chapter 6

Results: Model simulations and validation with dephosphorylation

List of Tables

List of Appendices

Appendices

List of Abbreviations

Ang- Angiopoietin

Ang1- Angiopoietin-1

Ang2- Angiopoietin-2

BSA- Bovine serum albumin

CCD- charge-coupled device

DAPI- 4',6-diamidino-2-phenylindole

ECM- Extracellular matrix

EGFR- Epidermal growth factor receptor

FCS- Fetal calf serum

HPTP-β- Human protein tyrosine phosphatase beta

HUVECs- Human umbilical vein endothelial cells

MMP- Matrix metalloproteinase

nTie2- new Tie2

ODE- Ordinary differential equation

PBS- Phosphate buffered saline

PFA- Paraformaldehyde

PMA- Phorbol-12-myristate-13-acetate

RTK- Receptor tyrosine kinase

SB- Sample buffer

sTie- Soluble Tie

TBS- Tris buffered saline

Tie- Tyrosine kinase with immunologlobulin and epidermal growth factor homology domains

TNF-α – Tumour necrosis factor alpha

Tx100- Triton-X 100

VEGF- Vascular endothelial growth factor

Chapter 1: Introduction

1.1. Angiogenesis

Angiogenesis is the formation of new blood vessels from pre-existing capillaries. It is required for vascular formation during embryonic development, wound healing and the reproductive cycle in women. However activation of angiogenesis can also contribute to pathological conditions such as tumour growth, chronic inflammation and hypoxic/ischemic conditions (Folkman, 1995; Griffioen & Molema, 2000).

1.2. Angiopoietins

Angiopoietins (Ang) are protein growth factors which play a role in angiogenesis, vascular development and quiescence. There are 4 members of the angiopoietin family; Ang1, Ang2, Ang3, Ang4. Ang1 and Ang2 are the most studied of this family (Thomas & Augustin, 2009) and although they have ~60% homology in their amino acid sequence (Maisonpierre *et al.*, 1997) they cause different effects on the cell which will be discussed later (Section 1.6) (Fiedler *et al.*, 2003; Maisonpierre *et al.*, 1997; Davis *et al.*, 1996).

The protein structure of angiopoietins mainly consists of an amino terminal superclustering domain, a coiled-coil domain and a carboxy terminal fibrinogen-like domain (Figure 1.1) (Moss, 2013). The amino terminal and coiled-coil domains are required for angiopoietin superclustering and oligomerisation which are essential for receptor activation. A short linker separates this domain from the fibrinogen-like domain which contains the receptor binding region (Kim *et al.*, 2005)

Angiopoietins are ligands of the Receptor Tyrosine Kinase, Tie2 (Davis *et al.*, 1996; Maisonpierre *et al.*, 1997; Valenzuela *et al.*, 1999).

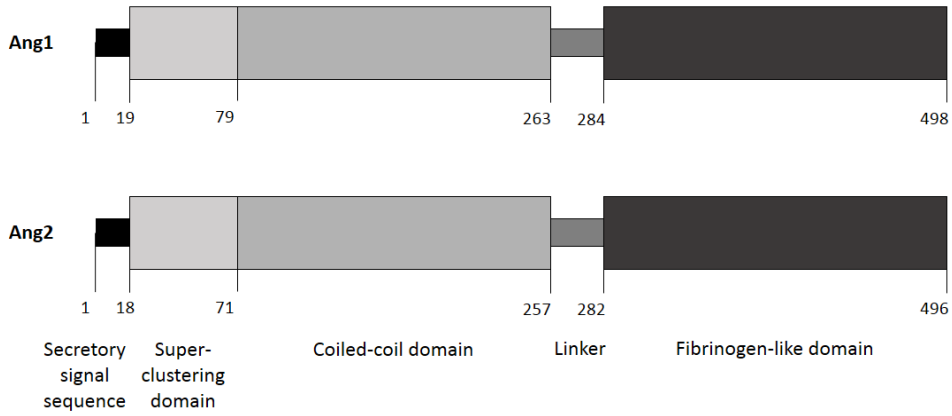

Figure 1.1: Schematic diagram of the protein structure of Ang1 and Ang2
The domains of Ang1 and Ang2 are highly conserved. It consists of a secretory signal sequence (amino acids 1-19 for Ang1 and 1-18 for Ang2), a super clustering domain (amino acids 20-79 for Ang1 and 19-71 for Ang2), a coiled-coil domain (amino acids 80-263 for Ang1 and 72-257 for Ang2), a short linker (amino acids 264-284 for Ang1 and 258-282 for Ang2), and a carboxy-terminal fibrinogen-like domain (amino acids 285-498 for Ang1 and 283-496 for Ang2) (adapted from Moss, 2013).

Angiopoietin-1

Angiopietin-1 (Ang1) is a 70kDa glycoprotein which binds to its receptor, Tie2, and activates the receptor, when present in a tetrameric or higher multimeric form (Davis *et al.*, 1996; Kim *et al.*, 2005; Davis *et al.*, 2003). It is expressed in pericytes, smooth muscle cells, fibroblasts and tumour cells, (Davis *et al.*, 1996; Stratmann *et al.*, 1998; Sugimachi *et al.*, 2003). Over expression of Ang1 in mice has been shown to promote vessel formation (Suri *et al.*, 1998), and prevent vascular leakage (Thurston *et al.*, 1999; Thurston *et al.*, 2000).

Ang1 plays an important role in embryonic angiogenesis where it is needed for the organization and maturation of newly formed vessels, whilst in developed vasculature Ang1 plays an important role in vascular homeostasis, the maintenance of vessels, and protection (Koh, 2013). The vascular protective effects of Ang1 promote the survival of blood vessels, and prevent vascular inflammation by inhibition of vascular leakage and suppression of inflammatory gene expression (Brindle *et al.*, 2006).

Angiopoietin-2

Angiopoietin-2 (Ang2) is also a ~70kDa glycoprotein expressed in endothelial cells which can bind to Tie2 (Maisonpierre *et al.*, 1997). Ang2 expression is modulated by many factors including hypoxia and vascular endothelial growth factor (VEGF), and increased during vascular remodelling. It is present at low concentrations in the endothelium where the release of Ang2 can cause destabilisation (Fagiani & Christofori, 2013).

Ang2 can also activate Tie2 when present at high concentrations or during prolonged periods, and is considered to be a partial agonist of Tie2 as its agonist activity is much lower than Ang1 (Kim *et al.*, 2000; Teichert-Kuliszewska *et al.*, 2001; Bogdanovic *et al.*, 2006; Yuan *et al.*, 2009). Moreover as Ang1 and Ang2 can compete for the same site on Tie2 (figure 1.2), Ang2 can act as a competitive antagonist to Ang1 by replacing the full agonist activity of Ang1 to the partial agonist activity of Ang2 (Bogdanovic *et al.*, 2006; Yuan *et al.*, 2007). The opposing effects of Ang2 can destabilize the endothelium (Scharpfenecker *et al.*, 2005). Over expression of Ang2, high serum, and high plasma levels of Ang2 have been linked to various types of cancers and inflammation (sepsis) (Parikh, 2013; Thurston & Daly, 2012).

Ang2 is stored in Weibel–Palade Bodies and released following endothelial cell activation or in the presence of phorbol esters, thrombin and histamine (Fiedler *et al.*, 2004; Fagiani & Christofori, 2013).

Angiopoietin-3 and Angiopoietin-4

Not much is known about angiopoietin-3 (Ang3) and angiopoietin-4 (Ang4) however Ang3 has been found to be an antagonist of the receptor while Ang4 is an agonist (Figure 1.2) (Valenzuela *et al.*, 1999; Lee *et al.*, 2004; Kim *et al.*, 1999; Nishimura *et al.*, 1999).

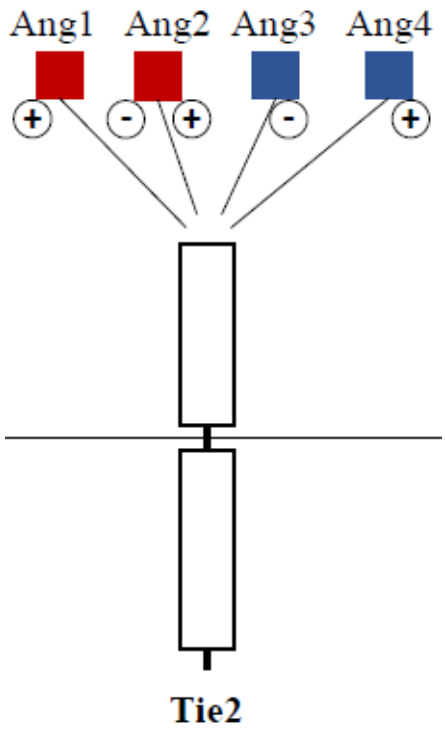

Figure 1.2: Tie2 receptor tyrosine kinase and the angiopoietins
The activity of angiopoietins on binding to Tie2 (+ agonist to Tie2, - antagonist to Tie2). Ang1 and Ang2 (highlighted in red) are the best characterised of the angiopoietin family. (Adapted from Yancopoulos et al., 2000).

1.3. Tie receptors

Tie is a receptor tyrosine kinase with immunoglobulin (Ig) and epidermal growth factor homology domains. There are 2 known types of Tie receptors: Tie1 and Tie2, and they have ~76% homology in their amino acid sequence (Sato *et al.*, 1993).

Tie1

Tie1 is an orphan receptor and exists in a preformed complex with Tie2 (Tie1:Tie2) where it regulates Tie2 phosphorylation and activation by acting as an inhibitory co-receptor (Marron *et al.*, 2000; Marron *et al.*, 2000; Seegar *et al.*, 2010). The extracellular domain of Tie1 can be proteolytically cleaved by metalloprotease in response to phorbol ester, PMA (phorbol-12-myristate-13-acetate), vascular endothelial growth factor (VEGF), tumour necrosis factor-alpha (TNF-α) or shear stress (Yabkowitz *et al.*, 1997; Yabkowitz *et al.*, 1999). The remaining truncated form of Tie1 can also be cleaved (by γ-secretase), and this intracellular domain may contribute to Tie2 signal transduction (Marron *et al.*, 2007). Activation of the Tie1 pathway is thought to modulate blood vessel morphogenesis (Yuan *et al.*, 2007). Transcription of Tie1 is upregulated during hypoxia and by VEGF (known angiogenic stimuli) and in areas of vascular formation; wounds, ovarian follicles and tumours (Korhonen *et al.*, 1992; McCarthy *et al.*, 1998).

Tie2

Tie2 (also called Tek) is the receptor of all 4 angiopoietins. Tie2 is expressed by endothelial cells (Schnurch & Risau, 1993), endothelial precursor cells (Dumont *et al.*, 1992), hematopoietic cells (Shaw *et al.*, 2004), and also in some tumour cells (Brown *et*

al., 2000) where it is upregulated during tumour angiogenesis (Peters *et al.*, 1998; Takahama *et al.*, 1999).

Mice embryos deficient in Tie2 die between embryonic day 10.5 and 12.5 due to defects in the remodelling and maturation of the primary capillary plexus (Dumont *et al.*, 1994; Sato *et al.*, 1995). Ang1 deficient mice die (E12.5) as a result of a similar vascular development problem to Tie2-deficient mice (Suri *et al.*, 1996). Conversely mutations of the Tie2 RTK that cause increased Tie2 activity lead to subsequent venous malformations (Vikkula *et al.*, 1996). Therefore the Ang1-Tie2 signalling pathway is important in the development and maturation of embryonic vasculature.

In normal physiological conditions Tie2 can also be cleaved by matrix metalloprotease (MMP-14) to produce a soluble form of the receptor (Reusch *et al.*, 2001; Onimaru *et al.*, 2010). Studies have shown that increased concentrations of soluble Tie2 (sTie2) are present in many cardiovascular diseases (Chung *et al.*, 2003). It has also been shown in mice to inhibit ischemia-induced retinal neovascularisation (Takagi *et al.*, 2003).

1.4. Ang1-Tie2 signalling

Ang1 must be in a multimeric structure to activate Tie2 (Kim *et al.*, 2005). Multimeric Ang1 binds to Tie2 and clusters the receptor to form a tetrameric structure. This tetramerisation activates the receptors by transphosphorylation of the kinase domains and initiates the Tie2 signalling pathway (Barton *et al.*, 2006). Activation of the Tie2 receptor

can stimulate the pathway for either vascular quiescence or angiogenesis which can depend on the inter-endothelial cell adhesions (Saharinen *et al.*, 2008).

In mature vasculature where there are many cell-cell adhesions (i.e. in highly confluent cells and quiescent endothelium), binding of Ang1 to Tie2 causes Tie2 to relocate to sites of cell-cell contacts. The Ang1 is also able to bind to Tie2 of adjoining cells which results in Tie2 trans-association (Fukuhara *et al.*, 2008; Fukuhara *et al.*, 2010). Activation of trans-associated Tie2 results in vascular quiescence. In the absence of cell-cell contacts (sparse and angiogenic endothelium), characteristic of endothelial cells undergoing angiogenesis, Ang1 binds to Tie2 and also to the extracellular matrix (ECM). This anchors Tie2 to the ECM (Saharinen *et al.*, 2008; Fukuhara *et al.*, 2008). Activation of ECM anchored Tie2 results in angiogenesis.

1.4.1. Activation of trans-associated Tie2 in mature vasculature.

Ang1 binds to Tie2 inducing tetramerisation and Tie2 autophosphorylation which leads to the phosphorylation of the p85 subunit of phosphatidylinositol 3-kinase (PI3K) and activation of Akt/PKB (Protein Kinase B). Akt activation can phosphorylate and activate the forkhead transcription factor, FOXO-1, a strong inducer of Ang-2 expression. Activation of Akt also stimulates the phosphorylation and thereby the inhibition of pro-apoptotic proteins, including the Bcl-2-associated death promoter (BAD) and procaspase-9. In addition, Akt promotes cell survival by upregulation of survivin, which is an apoptosis inhibitor, Figure 1.3 (Thomas & Augustin, 2009). The anti-inflammatory

effects of Ang1 may be mediated by this pathway (Kim *et al.*, 2000; Kim *et al.*, 2002). Thus stimulation of the trans-associated Tie2 by Ang1 can maintain vascular quiescence.

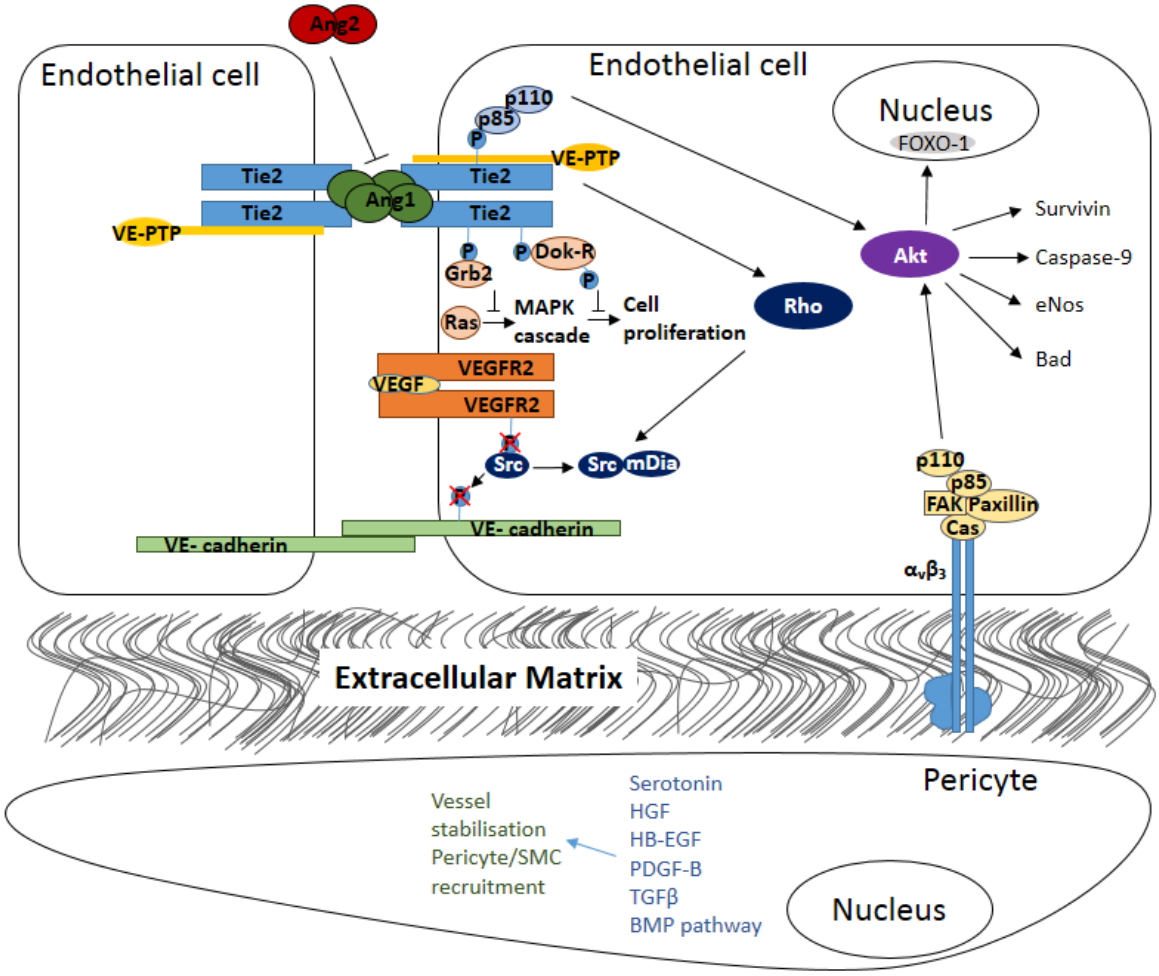

Figure 1.3: Activation of trans-associated Tie2 in mature vasculature
The activation of trans-associated Tie2 in mature vasculature with cell-cell contact. Stimulation of the Ang1-Tie2 signalling pathway (via PI3K/Akt activation) maintains vascular quiescence and cell survival (adapted from Thomas and Augustin 2009).

1.4.2. Activation of ECM-anchored Tie2 during angiogenesis.

Ang1 can anchor Tie2 to the ECM when endothelial cells lose cell-cell contact. ECM-anchored Tie2 activation can stimulate the formation of focal adhesion complexes, which activate focal adhesion kinase (FAK). FAK promotes cell migration (Thomas & Augustin, 2009) (Figure 1.4) and proliferation via the extracellular signal-regulated kinase 1/2 (ERK 1/2) pathway (Abdel-Malak *et al.*, 2009). This results in angiogenesis (Fukuhara *et al.*, 2008; Saharinen *et al.*, 2008).

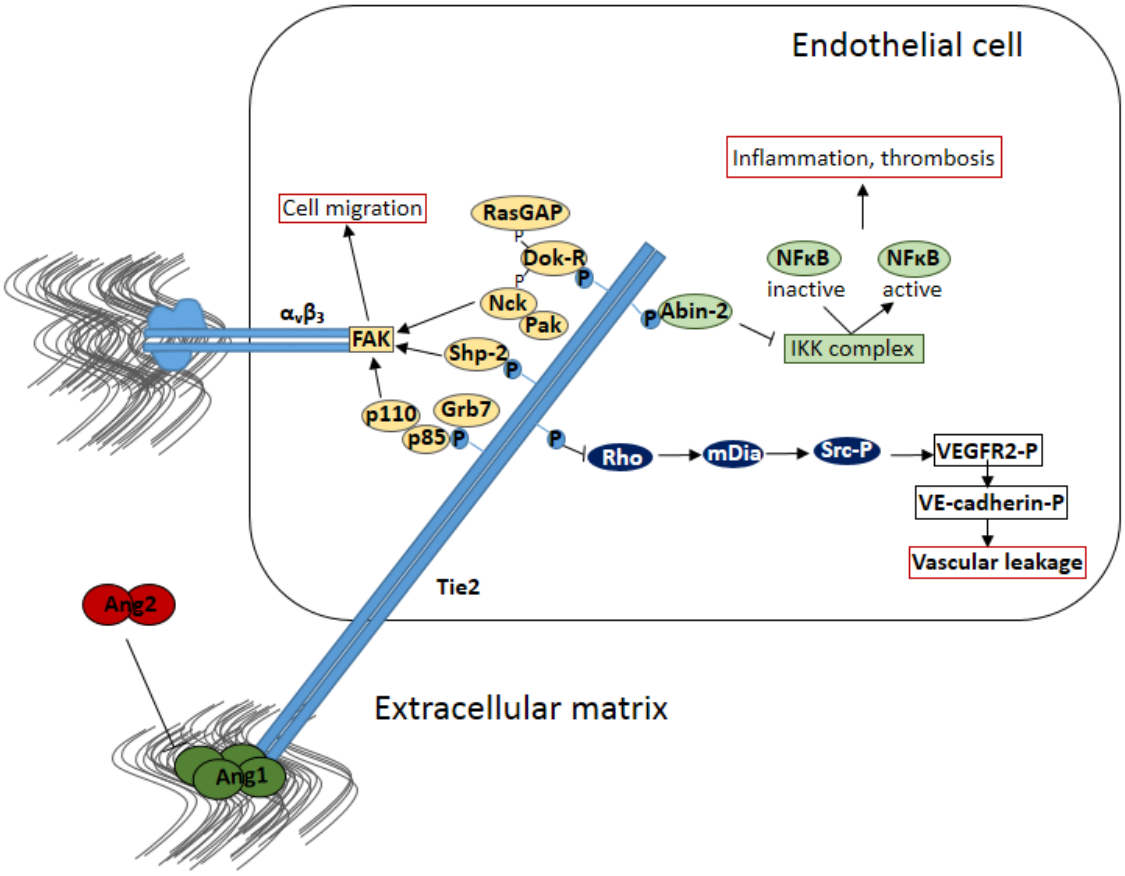

Figure 1.4: Activation of ECM-anchored Tie2 during angiogenesis
The Ang1-Tie2 signalling pathway (via activation of ECM-anchored Tie2) in the absence of cell-cell contacts which activates focal adhesion kinase (FAK) and cell migration and subsequent angiogenesis (adapted from Thomas and Augustin 2009).

1.5. Regulation of Tie2 signalling

There are several factors that can regulate the activation of the Ang-Tie signalling pathway at the level of the Tie2 receptor (Singh *et al.*, 2011):

1. Ang1:Ang2 ratio
2. Tie1:Tie2 and Tie2:Tie2 balance
3. Tie1 cleavage status
4. Tie2 cleavage status
5. Soluble Tie2 extracellular domain (sTie2)

Ang1 : Ang2 ratio

One regulator of Tie2 activation is the ratio of its ligands; Ang1 and Ang2. A ratio in favour of Ang1, due to constitutive expression of Ang1 and suppression of Ang2, activates the Tie2 pathway and maintains vascular quiescence. Whereas a ratio in favour of Ang2 following endothelial activation, competes with Ang1 for Tie2 binding and decreases the activity of the receptor, this destabilizes the endothelium and increases the cell's response to cytokines. The presence of other stimuli (e.g. VEGF) can determine whether the vasculature switches back to a quiescent state or induces an angiogenic response (Fiedler & Augustin, 2006). Therefore, the Ang1:Ang2 ratio is important in controlling the functional status of the vasculature.

Studies have shown that Ang2 is up-regulated in highly vascular tumours (Tanaka *et al.*, 1999; Holash *et al.*, 1999; Holash *et al.*, 1999). This suggests that a ratio in favour of Ang-2 may be linked to tumour angiogenesis and plays a role in the angiogenic switch between angiogenesis and vascular regression (Tait & Jones, 2004).

Tie1:Tie2 vs Tie2:Tie2

The balance between the homo-oligomeric Tie2:Tie2 and the hetero-oligomeric Tie1:Tie2 complex can also regulate Tie2 signalling. The Tie1:Tie2 complex is likely to be in equilibrium with free Tie1 and free Tie2 on the endothelial cell membrane.

$$\text{Tie1:Tie2} \leftrightarrow \text{Tie1} + \text{Tie2}$$

Binding of Ang1 to Tie2:Tie1 has been shown to dissociate the hetero-oligomeric complex and this shifts the equilibrium towards the right allowing more Tie2:Tie2 clusters to form and stimulate Ang1-Tie2 signalling (Hansen *et al.*, 2010; Seegar *et al.*, 2010).

In addition, the presence of Tie1 has been shown to regulate the binding of Ang1 to the complexed Tie2. Hansen and colleagues demonstrated that Ang1 and Ang2 bind differently to Tie2 at the cell surface due to the presence of Tie1 (Hansen *et al.*, 2010). Tie1 can partially occlude Ang1 binding to Tie2 (Marron *et al.*, 2007), thus Ang1 favours binding to Tie2 complexes without Tie1 (Hansen *et al.*, 2010). Hence cleavage of Tie1 and suppression of Tie1 expression increases Ang1 binding to Tie2 (Hansen *et al.*, 2010).

Conversely Ang2 binding to Tie2 is not affected by the presence of Tie1, however the presence of Tie1 can determine the agonist/antagonist role for Ang2 and will be discussed further in Section 1.6 (Seegar *et al.*, 2010).

Tie1 cleavage

As studies have shown that Tie1 acts as an inhibitory co-receptor to Tie2 the cleavage of Tie1 can affect Tie2 signalling (Marron *et al.*, 2007; Seegar *et al.*, 2010). The Tie1 ectodomain can be cleaved by MMP in response to VEGF, inflammatory stimuli (e.g.TNF), shear stress and phorbol esters (Yabkowitz *et al.*, 1997; Yabkowitz *et al.*, 1999). The Tie1 ectodomain is shed from the Tie1:Tie2 complex and increases access of Ang1 to Tie2 on the surface of the endothelial cells. Therefore cleavage of Tie1 promotes Tie2 activation and Tie2 downstream signalling (Hansen *et al.*, 2010).

Tie2 cleavage

Cleavage of Tie2 also regulates Tie2 signalling. The extracellular domain of Tie2 can also be proteolytically cleaved by MMP in response to VEGF, PMA and activated Akt or constitutively cleaved after a certain period of time (Reusch *et al.*, 2001; Findley *et al.*, 2007; Onimaru *et al.*, 2010). Therefore full-length Tie2 on the endothelial cell membrane loses its ability to bind Ang1 or Ang2 and thus produces a lower cell response and vessel destabilisation.

Soluble Tie2 extracellular domain

The cleavage of the Tie2 extracellular domain results in a 75-kDa soluble Tie2 (sTie2) protein, which is shed from the cell membrane, and is soluble in the medium surrounding the cell (Reusch *et al.*, 2001). This domain can regulate Tie2 signalling as it is able to compete with full-length Tie2 to bind to Ang1/Ang2 (Findley *et al.*, 2007). Thus sTie2 can act as an inhibitor as less Ang1/Ang2 binds to full-length Tie2.

1.6. Ang1 and Ang2 opposing effects on Tie2 signalling

As previously mentioned Ang1 and Ang2 have similar protein structures however they have opposing functions on Tie2 signalling. There are five potential factors that can affect the functional difference between Ang1 and Ang2;

1. The binding affinity of the angiopoietin for the Tie2 receptor.
2. The oligomerisation state of the angiopoietin.
3. The difference in receptor binding domains.
4. The molecular structure.
5. Additional interactions with other receptors or co-receptors.

Binding affinity

It is widely accepted that Ang1 binds to Tie2 with same affinity as Ang2. Studies have shown that Ang1 and Ang2 can bind to the extracellular domain of soluble Tie2 with similar binding affinity.

Davis et al., (1996) estimated the binding affinity (K_D) of Ang1 and Ang2 to Tie2 to be ~3.7 nM whereas Maisonpierre et al., (1997) estimated the binding affinity for both ligands to be ~3 nM.

However Yuan et al. (2009) have demonstrated that Ang2 binds to Tie2 with ~20 fold-lower affinity when compared to Ang1. Hence it has been suggested that the partial agonist activity of Ang2 may be due to its lower binding affinity of Ang2 for Tie2.

Oligomerisation

Oligomerisation of Tie2 clusters the receptor's kinase domains closer together which facilitates trans-phosphorylation and activation of the receptors (Kim *et al.*, 2009). Hence an oligomeric angiopoietin is required to aid the oligomerisation of the receptor. The oligomeric state of the angiopoietins has been shown to have an effect on the strength of Tie2 activation (Cho *et al.*, 2004).

Native Ang1 predominantly exists in a tetrameric or higher order form which can aggregate Tie2 and induces multiple auto- and transphosphorylations to occur at the tyrosine kinase domain (Kim *et al.*, 2005; Procopio *et al.*, 1999). Native Ang2 is predominantly found in a dimeric form with higher order forms also present at low amounts (Procopio *et al.*, 1999; Kim *et al.*, 2005; Kim *et al.*, 2009).

Studies suggest that a tetrameric or higher form of Ang1 is required to activate Tie2 (Kim *et al.*, 2005). Therefore the low oligomeric forms of Ang2 may limit the Ang2 ability to activate Tie2 as Ang2 has only been shown to weakly activate Tie2 (Yuan *et al.*, 2009).

Oligomeric variants of Ang1 and Ang2 have been produced to cluster angiopoietins together to form multimeric structures (mainly pentameric forms) (Cho *et al.*, 2004; Kim *et al.*, 2009). The amino terminal superclustering and coiled-coil domains of the angiopoietin were replaced with a short coiled-coil domain of cartilage oligomeric matrix protein (COMP). These variants (COMP-Ang1 and COMP-Ang2) are more potent than their native forms at phosphorylating Tie2 and activating downstream signalling *in vitro* and *in vivo* (Cho *et al.*, 2004; Kim *et al.*, 2009). A comparison of the effects of COMP-Ang1 and COMP-Ang2 demonstrated similar effects which suggests that the oligomeric

state of angiopoietins could be a possible factor for Tie2 activation difference between Ang1 and Ang2 (Cho *et al.*, 2004; Kim *et al.*, 2009).

Receptor binding domains

Ligand binding to most receptor tyrosine kinases induce a structural change in the receptor's ectodomain which promotes oligomerisation and activation of the receptor and downstream signalling pathways (Hubbard & Till, 2000). The crystal structure of Ang1 and Ang2 have recently been compared in studies to analyse the angiopoietin receptor binding domain and Tie ligand binding region (Barton *et al.*, 2006; Yu *et al.*, 2013). It has been suggested that the binding mechanism of angiopoietins to Tie2 is different to most receptor tyrosine kinases in that they use a lock-and-key mechanism for ligand recognition (Barton *et al.*, 2006). The angiopoietin and Tie2 binding surfaces are complementary and binding does not induce conformational changes or rearrangement of domains in either partner (Barton *et al.*, 2006; Yu *et al.*, 2013).

The crystal structure of Ang1 and Ang2 show that both have similar receptor binding domains which consist of three domains; A, B and P. The P domain has been identified as the interface of Tie2 binding which allows the angiopoietins to bind to Tie2 in a similar manner (Barton *et al.*, 2005; Barton *et al.*, 2006). This suggests that ligand presentation does not determine the functional difference between Ang1 and Ang2 (Yu *et al.*, 2013).

Molecular structure

Further examination of the angiopoietin P domain has identified a β6-β7 loop near the receptor binding region which could possibly determine the functional difference between Ang1 and Ang2 (Yu *et al.*, 2013). The loop in Ang1 contains a TAG sequence which is not conserved in Ang2. The study by Yu et al., (2013) constructed an Ang2 chimera containing the Ang1 loop (with the TAG sequence) and assessed its function in cellular assays. The Ang2 chimera was found to behave similar to native Ang1 by dissociating the Tie1:Tie2 complex which increases Tie2 clustering and induces Tie2 signalling (Seegar *et al.*, 2010; Yu *et al.*, 2013). Conversely, the Ang1 chimera containing the Ang2 loop (with PQR sequence) did not activate Tie2 signalling. This suggests that the β6-β7 loop in the P domain of angiopoietins may be responsible for the differences in functional activity.

Additional interactions

The additional interactions of angiopoietins and Tie2 with other receptors or co-receptors have also been shown to influence the opposing functions of Ang1 and Ang2.

As previously discussed, Tie1 can interact with Tie2 to form a heterodimeric Tie1:Tie2 complex and acts as an inhibitory co-receptor (Marron *et al.*, 2000; Marron *et al.*, 2007; Seegar *et al.*, 2010). A study by Marron and colleagues demonstrated that cleavage of the Tie1 ectodomain and down regulation of Tie1 can each increase binding of Ang1 to Tie2 and enhance activation of Tie2 (Marron *et al.*, 2007). Thus the presence of Tie1 can regulate Tie2 phosphorylation and activation by inhibiting Ang1 binding to Tie2. A further study on the effects of Tie1 on Ang1 and Ang2 regulation demonstrated that the

cleavage of the Tie1 ectodomain and down regulation of Tie1 do not affect the ability of Ang2 to bind to Tie2 or increase the Ang2 agonist activity (Hansen *et al.*, 2010). Furthermore Ang1 has been shown to disrupt the Tie1:Tie2 complex and increase Tie2 signalling whereas Ang2 has no effect (Seegar *et al.*, 2010; Yu *et al.*, 2013). Hence the Tie1 co-inhibitory receptor can be a possible factor for the opposing functions of Ang1 and Ang2 in Tie2 activation.

Ang1 and Ang2 can also bind to integrins (Carlson *et al.*, 2001; Saharinen *et al.*, 2005; Felcht *et al.*, 2012). Although Ang1 and Ang2 bind to integrins with a lower affinity than to Tie2. Angiopoietin binding integrins are involved in different cellular responses to stimulation.

These different types of regulation and factors affecting Ang1 and Ang2 function can make it difficult to predict which of these mechanisms are the most important for regulating angiogenesis. For that reason computational modelling can be used to model and simulate these mechanisms at the level of the Tie2 receptor on endothelial cells.

1.7. Computational and mathematical modelling

Computational modelling is a method which can be used to study the individual reactions in a biological system and the effect of the interactions on the behaviour of the system. Some of the different types of systems which have been modelled include metabolic pathways (Bakker *et al.*, 1997; Papin *et al.*, 2003), functional genomics (Stoll *et al.*, 2001) and signalling pathways (Kholodenko *et al.*, 1999). These biological systems can be modelled and the equations input and simulated on a computer to study the complex interactions of the system (Di Ventura *et al.*, 2006).

Mathematical modelling is used to make testable predictions and gain insight to a biological system's behaviour (Orton *et al.*, 2005). This analysis of biological systems can help us to understand how an individual pathway functions when interacting with other pathways, to estimate parameters and validate the proposed mechanism, and also to identify major regulatory components and therefore new targets for pharmacological intervention (Eungdamrong & Iyengar, 2004).

1.8. The Modelling Process

There are five steps involved in modelling a biological system; identification, definition, simulation, validation and analysis (see Figure 1.5) (Orton *et al.*, 2005).

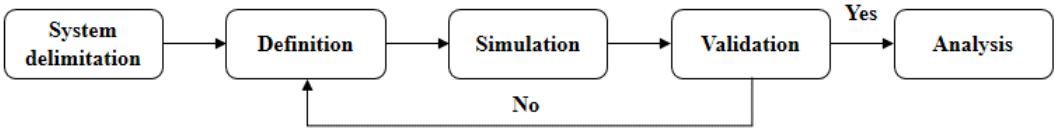

Figure 1.5: The process of modelling a biological system
The five steps to modelling. The first step is system delimitation which involves identifying the system to model. The next step is defining the model using rate equations (mathematical modelling) which represent the system. The model is then simulated and the simulation results are validated. If the model is valid, it can be analysed further for robustness. If the model is not valid then the model is checked for errors and re-defined (adapted from Orton *et al.*, 2005).

System delimitation

The first step to modelling is identifying the biological system to model. The interactions and chemical reactions between the components in the network are drawn as a schematic diagram (Kitano *et al.*, 2005).

Definition

Once the biological system has been identified, a kinetic model using rate equations can be produced to represent the behaviour of the system. The most common method of modelling biochemical pathways is by a set of coupled ordinary differential equations (ODEs) (Aldridge *et al.*, 2006). There are 2 sets of equations that are developed for this type of model; a set of ODEs to describe the system behaviour (system kinetic equations) and a set of algebraic equations used to describe the rates of change of specific variables (rate law equations) (Holmes, 2008).

First the set of ODEs are developed to represent the change of substrate concentration (e.g. A) over time (t), d[A]/dt. The set of ODEs have specific kinetic reaction rates and rate equations which show how the reaction occurs over time (Orton *et al.*, 2005). These rate equations are formed using a kinetic rate law, either mass action or Michaelis-Menten to model the behaviour of the reactions.

The law of mass action refers to a process being directly proportional to the concentration of the variable. Mass action rate equations are written as a rate constant (k) times the concentration of the substrate (S).

For example, a reaction of A converting to B (A → B) would be described by ODE and mass action kinetics as:

$$\frac{d[A]}{dt} = -k[A]$$

Where d[A]/dt is the rate of change in concentration of A.

In the case of cell surface receptor binding models (Lauffenburger and Linderman, 1993), where the reversible reaction of the association of the ligand (L) and the receptor (R) forms the ligand-receptor complex (LR), the interaction is shown as:

$$L + R \underset{k_{off}}{\overset{k_{on}}{\rightleftharpoons}} LR$$

Where k_{on} ($M^{-1}min^{-1}$) is the association rate constant, and k_{off} (min^{-1}) is the dissociation rate constant (Krohn & Link, 2003).

At equilibrium when the association rate equals the disassociation rate, the equilibrium dissociation constant, K_D (M), can be defined as:

$$K_D = \frac{k_{off}}{k_{on}} = \frac{[L][R]}{[LR]}$$

(Krohn & Link, 2003)

Thus, the mass-action equation to describe the ODE of the rate of change of the ligand-receptor complex over time is:

$$\frac{d[LR]}{dt} = k_{on}[L][R] - k_{off}[LR]$$

(Lauffenburger and Linderman, 1993)

The Michaelis-Menten rate law (see formula below) can be derived from the mass-action rate law, and is used for enzymatic kinetic reaction modelling e.g. for phosphorylation and dephosphorylation. Where Vmax is the max velocity and Km is the concentration of substrate at half Vmax.

$$V = \frac{V_{max}}{K_m + [S]}$$

The rate equations generate a list of parameters (e.g. rate constants and initial concentrations) needed to simulate the model. The values of kinetic parameters are obtained from the literature or databases such as the enzyme database, BRaunschweig ENzyme Database (BRENDA) (Chang *et al.*, 2009). Parameters can also be determined from quantitative experimental data. Once the mathematical model is produced and the parameters have been determined a computational model is constructed in modelling software (e.g. CellDesigner or MATLAB).

CellDesigner is a software with a graphical user interface which allows the modelling and simulation of biological networks. Networks can be drawn in CellDesigner based on a schematic diagram and the quantitative characteristics of the network e.g. rate equations and parameters can be input. The model can then be simulated by changing the parameter values and solving the mathematical equations to produce a simulation results plot which can help the user to understand the behaviour of the model (Funahashi *et al.*, 2003; Funahashi *et al.*, 2008). The model is stored using the Systems Biology Markup Language (SBML), a standard for representing models of biochemical and gene-regulatory networks (Hucka *et al.*, 2003) which makes the model compatible with other modelling software, and allows the user to download published models from BioModels database for use in CellDesigner (Li *et al.*, 2010). The SBML enables CellDesigner to integrate with other simulation software e.g. Complex Pathway Simulator (COPASI) (Hoops *et al.*, 2006) and the analysis software, MATLAB (MATrix LABoratory) (Schmidt & Jirstrand, 2006; Keating *et al.*, 2006).

Simulation

Simulation of the model solves the ODEs using the specified parameters e.g. the initial concentrations and reaction rates. The simulation can produce simulation results plots on the changes in reactant concentration over time (Kriete and Eils, 2005; Funahashi *et al.*, 2008; Funahashi *et al.*, 2003). The initial parameter values can also be changed to simulate different conditions in the system.

Validation

Simulation of the model generates hypotheses and a proposed mechanism which can be tested by cellular experiments. This comparison between *in silico* and *in vivo/in vitro* experiments is needed to validate the model. If the model is valid, it can be analysed further; if it is not, the model can be redefined and checked for errors (Figure 1.5) (Orton *et al.*, 2005).

Analysis

Before the proposed mechanism can be accepted, the robustness of the model needs to be analysed. Robustness is the insensitivity of a model to changes in parameter values (Kitano, 2002; Kitano, 2002; Aldridge *et al.*, 2006). The sensitivity analysis is a technique used to determine the robustness of a model in response to parameter variation (Zi, 2011). It can be performed in MATLAB, an engineering software package used for numerical computation and analysis (Ashino *et al.*, 2000). A sensitivity analysis can be used to identify the key parameters which have the greatest influence on the system (Orton *et al.*, 2008).

1.9. The purpose of robust modelling

After the model has been validated and refined, more *in silico* simulation experiments can be performed to test hypotheses and generate new predictions. Computational modelling also allows the analysis and manipulation of key components and parameters in the system. This will enable the user to understand the behaviour of the system without having to perform costly experiments (Kell and Knowles, 2006).

1.10. Example of receptor signalling modelling

Kholodenko and colleagues constructed an ODE-based mathematical model of the epidermal growth factor receptor (EGFR) signalling pathway in CellDesigner to quantify the short term signalling pattern in isolated rat hepatocytes, see figure 1.6 (Kholodenko *et al.*, 1999). Parameters for each kinetic equation were obtained from the literature or derived from basic physico-chemical quantities.

To validate the model, the simulated time courses of EGFR phosphorylation and the phosphorylation of their adaptor proteins; Shc (Src homology and collagen homology), Grb2 (growth factor receptor bound protein 2) and PLCγ (phospholipase Cγ), were compared to laboratory experiments to show that the model represents the system in isolated rat hepatocytes and to identify which kinetic constants have the biggest influence on the system. The time course results showed that the EGFR phosphorylation and the phosphorylation of its adaptor proteins occurred within 15 - 30 seconds after stimulation with EGF. Following this activation period, the concentrations of the phosphorylated proteins; EGFR, Grb2 co-precipitated with EGFR, and PLCγ decreased over time, whereas the levels of Shc and Grb2 co-precipitated with Shc increased.

Sensitivity analysis of the model showed that it was robust to the changes of many kinetic constants and sensitive to the changes of the adaptor proteins concentrations. Principally the Shc/Grb2 ratio was suggested to be the key regulator of the EGFR signalling response (Kholodenko *et al.*, 1999).

The development of this model has made it possible to predict the change in EGFR-activated proteins concentrations over time and has been used as a foundation for other EGFR signalling models e.g. (Resat *et al.*, 2003; Schoeberl *et al.*, 2002).

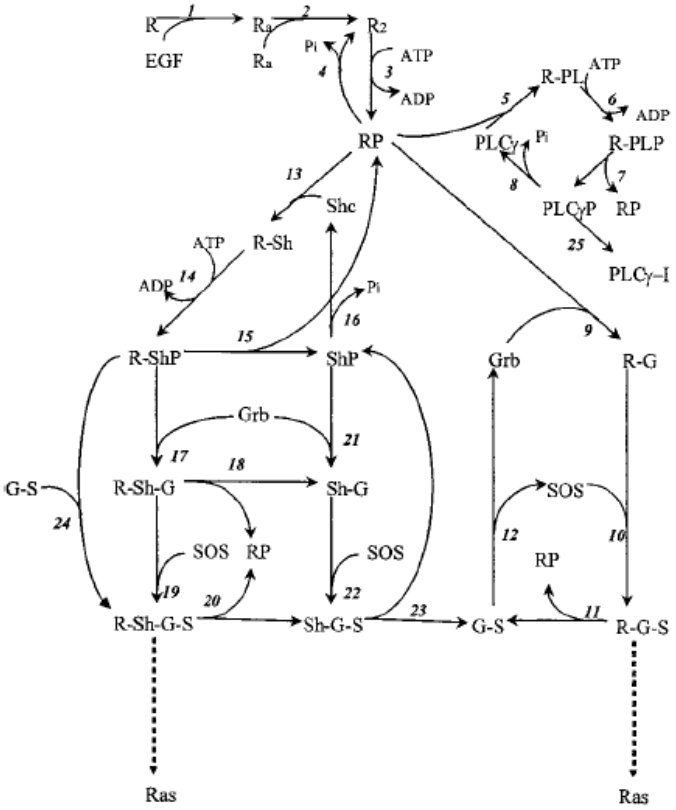

Figure 1.6: Schematic representation of the EGFR signalling pathway
The kinetic model of short-term EGFR signalling was based on these 25 protein interactions (Kholodenko *et al.*, 1999).

1.11. Aim

The Ang-Tie signalling pathway plays a role in vascular quiescence and angiogenesis, and is under complex regulation by multiple factors which are integrated to control its activation. To understand the behaviour of this system at the level of the receptor, computational and mathematical modelling can be used to model and simulate these interactions *in silico*.

The aim for this project is to construct a robust quantitative computer model of the Ang-Tie interactions at the endothelial cell surface.

First the system to be modelled will be identified by producing a schematic diagram of the angiopoietin and Tie interactions and regulatory mechanisms. The system will be defined using ODE mathematical modelling and constructed in CellDesigner software. All parameters needed to simulate the model will be obtained from the literature or quantified using a suitable quantitative detection method (e.g. immunofluorescence or Western blotting). The model will be simulated in MATLAB to produce simulation plots of the change in state concentration over time. Validation of the model will be analysed by measuring Tie2 receptor activation in endothelial cells using the selected quantitative method and comparing the results to simulations.

Chapter 2: Methods

2.1. General materials and reagents

All chemicals were of analytical grade and obtained from Sigma-Aldrich (Poole, UK) or Fisher Scientific (Loughborough, UK) unless otherwise stated.

Tissue culture plastics were obtained from Greiner Bio One or SPL Life Sciences.

2.2. Cell culture

Human umbilical vein endothelial cells (HUVECs) were obtained from Promocell (experiments in Chapter 4) or Invitrogen (experiments in Chapter 5). Promocell HUVECs were maintained in Medium 199 supplemented with 20% foetal bovine serum (FBS), 2 mM L-glutamine, 5units/ml heparin and 100 ug/ml endothelial cell growth supplement. Invitrogen HUVECs were maintained in Medium 200 supplemented with Low Serum Growth Supplement (Invitrogen); 2% v/v FBS, 1 µg/ml hydrocortisone, 10 ng/ml human epidermal growth factor, 3 ng/ml basic fibroblast growth factor, 10 µg/ml heparin. For experiments in Chapter 6, Invitrogen HUVECs were maintained on 2% gelatin coated flasks with 2% v/v FBS added to the complete medium (Medium 200 with Low Serum Growth Supplement). Preliminary experiments suggested that the medium made no difference to the cells (data not shown). Cells were incubated at 37^{o}C (Galaxy R+, RSBiotech) and passaged when they reached confluency.

2.2.1. Passage and plating

Confluent HUVECs were washed with phosphate buffered saline (PBS) and incubated with 2% Trypsin-EDTA for 2 minutes at room temperature. The trypsin was inactivated and removed from the cells by adding complete medium and centrifuging the cells at 180g for 7 minutes (Jouan CR422). The pellet of cells was resuspended in complete medium and split into flasks or plated. The splitting of cells from a flask to a 6 well plate was performed 18 hours prior to sample preparation. All experiments were performed with HUVECs between passages 3-5.

2.2.2. Freezing and storage

Confluent flasks ($80cm^2$) of HUVECs were washed with PBS and trypsinised (as described in section 2.2.1- Passage and plating). Cells were resuspended in freezing medium consisting of; 40% complete medium 200, 50% FCS and 10% DMSO, and placed into sterile freezing vials (2 vials per flask). The vials were kept in a polystyrene box at -80^{o}C for 2 days before finally storing in liquid nitrogen. For culturing cells from liquid nitrogen, frozen vials were thawed at 37^{o}C and plated in a flask with complete medium. Cells used for experiments in Chapter 6 were plated on 2% gelatin coated flasks with 2% FCS added to complete medium.

2.3. Immunofluorescence

Immunofluorescence is a staining method used to label specific antigens in samples using primary antibodies. Secondary antibodies bound to fluorochromes can be used to visualize the presence and localization of specific antigens using fluorescence microscopy, and the levels of fluorescence can be quantified using a combined Cell^R/Scan^R system.

2.3.1. Preparing cell samples for immunofluorescence staining

HUVECs for immunofluorescence were grown to 50% confluency on 22 mm coverslips (ThermoScientific) in 6 well plates to characterise the ECM-anchored Tie2 (angiogenic state)**.** HUVECs were incubated in serum-free Medium 199 for 4 hours before treatment with recombinant human angiopoietin-1 (R&D Systems) for 30 minutes. To fix the samples, cells were rinsed with PBS (140 mM NaCl, 2.7 mM KCl, 10 mM $NaHPO_4$, 1.8 mM KH_2PO_4, pH 7.3), fixed with 4% w/v paraformaldehyde (in PBS, 1M NaOH, pH 7) and incubated for 15 minutes (all incubations were maintain at +37^{o}C, no CO_2, unless stated otherwise). Samples were then stained by immunofluorescence (section 2.3.2) or stored at +4^{o}C.

2.3.2. Immunofluorescence staining

Fixed samples were washed three times for 5 minutes with tris-buffered saline, TBS, (250 mM Tris, 144 mM NaCl, pH 7.4). All washes were carried out on a rocker at room temperature to remove excess PFA. As the protein to be detected is inside the cell, the cell membrane was permeablized with 90% methanol (in TBS) on ice for 30 minutes

followed by antigen retrieval with 0.5% v/v SDS (in TBS) for 5 minutes at room temperature to enhance the level of immunofluorescence (Robinson & Vandre, 2001). After treatment the cells were washed three times with TBS for 5 minutes.

Free protein binding sites were blocked with 2% w/v bovine serum albumin (BSA) with TBS-Tx100 (0.1% v/v Tx-100 in TBS) incubated for 10 minutes to prevent non-specific binding. The coverslips were inverted onto parafilm with 50 µl of the primary antibody (Affinity-Purified Rabbit Anti-Phospho-Tie-2 (Y992) Antibody (R&D Systems) (1:200 dilution) and incubated in a moist box for 1 hour at +37^{o}C. The coverslips were returned to the wells and washed three times for 5 minutes with TBS. The cells were incubated with the secondary fluorescent conjugated antibody, Cy™3-conjugated AffiniPure Donkey Anti-Rabbit IgG (Jackson ImmunoResearch Laboratories, Inc), and as before the coverslips were inverted onto parafilm with 50 µl of 1:1000 secondary antibody and incubated in a moist box for 1 hour at +37^{o}C. The coverslips were returned to the wells and washed three times for 10 minutes with TBS-Tx100 to remove excess antibody.

To visualise individual cell nuclei, the nuclei were counterstained with DAPI (4',6-diamidino-2-phenylindole) (Sigma-Aldrich), a blue fluorescent probe which binds to the minor groove of double stranded DNA. Coverslips were inverted onto parafilm with DAPI (50µl/coverslip of a 1:1000 dilution in PBS) and incubated in a moist box in a dark cupboard for 10 minutes. Coverslips were returned to the well and washed three times for 2 minutes with TBS. Cells were rinsed with dH_2O to prevent crystallization of the sample and then mounted onto a slide (Thermo Electron Coroporation, Shandon Double Frost Microscope Slides) with anti-fading mounting medium (Vectashield, VectorLabs). The edges of the coverslips were sealed with clear nail polish to prolong storage.

2.3.3. Detection and quantification of immunofluorescence staining

Fluorescence of cells was visualised using an inverted fluorescence microscope (Nikon Eclipse TE2000-U) with an oil-immersion objective. Cy3 has a red fluorescence and excites at 550 nm and emits at 570 nm and DAPI has a blue fluorescence and excites at 345 nm and emits at 455 nm. Slides were stored in the dark at 4^{o}C.

The levels of fluorescence in the cells were quantified using an Olympus IX81 microscope and combined Cell^{R}/Scan^{R} system.

2.4. Cell sample preparation

Materials:

Phosphate Buffered Saline (PBS): 140 mM NaCl, 2.7 mM KCl, 10 mM $NaHPO_4$, 1.8 mM KH_2PO_4, pH 7.3

3 x Sample Buffer (3xSB): 50 mM Tris pH 6.8, 2% SDS, 10% Glycerol, 5 mM EDTA pH6.8, 0.1% Bromophenol Blue

2 x SBDTT (Sample Buffer DTT): 3xSB diluted with dH_2O, 30 mg 1,4-Dithiothreitol (DTT)

Methods:

HUVECs were plated on a 6 well plate at either $1x10^5$ or $2x10^5$ (~50-60% confluency) cells per well 18 hours prior to cell lysis.

HUVECs were washed in PBS, lysed with 70 µl 2xSBDTT and sonicated (Soniprep 150 MSE) for 10 seconds. The cell lysates were boiled at 95^oC for 6 minutes and centrifuged for 1 minute at 13,000rpm. Cell lysate samples were kept at +4^oC until immediate use in Sodium Dodecyl Sulphate-Polyacrylamide Gel Electrophoresis (SDS-PAGE) or stored at -20^oC for prolonged periods.

2.4.1. Quantification of Tie1 and Tie2 in HUVECs

For the quantification of Tie experiments, HUVECs were plated and samples were collected as describe above (Section 2.4).

2.4.2. Ang1 or Ang2-induced Tie2 phosphorylation

For Ang1 or Ang2-induced phospho-Tie2 western blotting, HUVECs were serum-starved with serum-free Medium 199 or Medium 200 incubated for one hour and treated with 1 mM sodium orthovanadate (vanadate) for 5 minutes (unless stated otherwise), followed by stimulation with recombinant human angiopoietin-1 (R&D Systems) (concentration as described in experiment) for 15 minutes (or at specified times during time-course experiments) prior to collection. Then HUVECs were washed with PBS, lysed, sonicated and boiled as described above (Section 2.4).

2.4.3. Ang1 and Ang2 competitive inhibition of Tie2 phosphorylation

For experiments of Ang1 and Ang2 effects on phospho-Tie2 western blotting, HUVECs were serum-starved with serum-free Medium 199 or Medium 200 incubated for one hour and treated with recombinant human angiopoietin-2 (R&D Systems) (concentration as described in experiment) for 5 minutes, followed by stimulation with recombinant human angiopoietin-1 for 15 minutes. To collect the samples from the wells the HUVECs were washed with PBS, lysed, sonicated and boiled as described above (Section 2.4).

2.4.4. Ang1 and sTie2 effects on Tie2 phosphorylation

For experiments of Ang1 and sTie2 effects on phospho-Tie2 western blotting, HUVECs were serum-starved with serum-free Medium 199 or Medium 200 incubated for one hour, during this time sTie2 was incubated with recombinant human angiopoietin-1 for 15 minutes. After one hour the cells were treated with 1 mM vanadate for 5 minutes, followed by stimulation with the sTie2 (100, 200, 500, or 1000 ng/ml) and 50 ng/ml

recombinant human angiopoietin-1 (R&D Systems) for 15 minutes. To collect the samples from the wells the HUVECs were washed with PBS, lysed, sonicated and boiled as described above (Section 2.4).

2.5. Western Blotting and antibody probing

2.5.1. Sodium Dodecyl Sulphate-Polyacrylamide Gel Electrophoresis

Materials:

Resolving gel: 1.0 mm or 1.5 mm

Reagent	7.5%	10%
30% Acrylamide/Bisacrylamide (Biorad)	5.0 ml	6.7 ml
2M Tris pH8.8	3.7 ml	9.6 ml
dH_2O	10.9 ml	3.7 ml
20% Sodium Dodecyl Sulphate (SDS)	100 µl	100 µl
10% Ammonium Persulphate (APS)	134 µl	134 µl
Tetramethylethylenediamine (TEMED) (Sigma)	14 µl	14 µl

Stacking gel: 10 lanes or 15 lanes

Reagent	5%
30% Acrylamide/Bisacrylamide (Biorad)	3.3 ml
1M Tris pH6.8	2.5 ml
dH_2O	13.7 ml
20% Sodium Dodecyl Sulphate (SDS)	100 µl
10% Ammonium Persulphate (APS)	200 µl
Tetramethylethylenediamine (TEMED) (Sigma)	20 µl

10x Protein Electrophoresis Buffer: 250 mM Glycine, 25 mM Tris-base, 0.1% (w/v) SDS

Recombinant human Tie-1/FC Chimera (R&D Systems)

Recombinant human Tie-2/FC Chimera (R&D Systems)

Precision Plus Protein Kaleidoscope Standard (Biorad)

Spectra Multicolor broad range protein ladder (Pierce)

Method:

For quantification of proteins, the cell lysate samples (45 µl) were loaded into a 7.5%, 1.5 mm gel alongside the Protein Kaleidoscope Standard molecular mass marker (8 µl) and various concentrations of recombinant Tie1 or Tie2 (for quantification of Tie experiments). The proteins were resolved by sodium dodecyl sulphate-polyacrylamide gel electrophoresis (SDS-PAGE) in 1x protein electrophoresis buffer at 100V for 2 hours.

For detection of phosphorylation, the cell lysate samples were loaded into a 12%, 1.0 mm gel (30 µl) alongside the Spectra protein ladder (8 µl). The proteins were resolved by SDS-PAGE in 1x protein electrophoresis buffer at 130V for 1 hour and 30 minutes.

2.5.2. Western Blotting: Transfer to membrane

Proteins were transferred onto a nitrocellulose membrane (Hybond™ ECL™, GE Healthcare) or PVDF membrane (Hybond-P, GE Healthcare) in 1x Transfer buffer, overnight at 0.15 amps.

2.5.3. Western Blotting: Antibody probing

Materials:

Amersham Hybond™ ECL™ Nitrocellulose membrane (GE Healthcare Life Sciences)

Amersham Hybond-P™ PVDF Membrane (GE Healthcare Life Sciences)

20% Triton X-100 (Tx-100) (Sigma-Aldrich)

10x Protein Transfer Buffer: 25 mM Tris-HCl pH 8.3, 0.15M Glycine, 20% (v/v) Methanol

TBS-TX100: 50 mM Tris, 150 mM NaCl, 0.1% TritonX-100

5% Milk: 1g Marvel powdered milk and 20 ml 0.1% Tx-100-TBS

5% BSA: 1g Bovine Serum Albumin (BSA) and 20 ml 0.1% Tx-100-TBS

Developer solution: 10 ml of 100 mM Tris-HCl pH 8.5, 22 µl of 90 mM p-Coumaric Acid in DMSO, 50 µl of 250 mM Luminol (5-Amino-2,3-dihydro-1,4-phthalazinedione) in DMSO, 3 µl 30% H_2O_2 (added just before use)

Anti-human Tie-1 extracellular domain-specific goat IgG (R&D Systems)

Anti- human Tie-2 extracellular domain-specific goat IgG (R&D Systems)

p-Tie-2 (Tyr 992) Antibody (Santa Cruz Biotechnology)

Anti-Goat HRP: Polyclonal Rabbit anti-Goat Immunoglobulins/HRP (Dako)

Anti-Rabbit HRP: Polyclonal Goat anti-Rabbit Immunoglobulins/HRP (Dako)

Method:

Non-specific protein-protein interactions were blocked with 5% Marvel powdered milk, or 5% BSA (for anti-phospho-Tie2 detection) for 1 hour. The blot was probed with the relevant primary antibodies (anti-Tie 1, anti-Tie 2, anti-phospho-Tie2) in their respective blocking solutions and incubated on a rocker; at +4^{o}C overnight, or at +37^{o}C for one hour, or at room temperature for one hour. Following incubation blots were washed three times for 10 minutes per wash with TBS-Tx100 to remove unreacted antibody (all washes were carried out on a rocker at room temperature). The immuno-labelled proteins were detected with horseradish peroxidise-conjugated secondary antibodies (anti-goat, anti-mouse, anti-rabbit) all in 5% Marvel powdered milk, which were incubated on a rocker at room temperature for 1 hour and then washed three times for 10 minutes (per wash) with TBS-Tx100 to remove excess antibody. The blot was left in the developer solution for 1 minute then the proteins were detected by chemiluminescence using either film or CCD imager (Matthews *et al.*, 1985).

Primary antibody	**Incubation**	**Secondary antibody**	**Incubation**
Tie1 (R&D Systems)	1:1000 in 5% milk 4^{o}C overnight or 37^{o}C for 1 hour	Goat IgG/HRP (Dako)	1:1000 in 5% milk room temperature for 1 hour
Tie2 (R&D Systems)			
pY^{992} Tie2 (Santa Cruz)	1:1000 in 5% BSA 4^{o}C overnight or 37^{o}C for 1 hour	Rabbit IgG/HRP (Dako)	1:1000 in 5% milk room temperature for 1 hour

2.5.4. Detection and quantification using film and ImageJ

For detection using a film, the blot was exposed to film (Thermo Scientific CL-XPosure Film) and developed (AGFA Curix 60 Developer machine). The films were scanned (HP Scanjet 4500c) at 300dpi and saved in .tif format. The densities of the bands were quantified with Wright Cell Imaging Facility Image J software (Schneider *et al.*, 2012). The relevant bands were outlined and plots for each lane were generated. The background was corrected by marking the baseline of the curve and the area under the curve was measured.

2.5.5. Detection and quantification using a CCD imager and MultiGauge

For detection using a cooled charge-coupled device (CCD) imager, a CCD camera (Fujifilm LAS-4000) was used to acquire images of the blots at specified exposure times. The blots were imported into MultiGauge Software where the lanes and bands were selected and profile plots of the lanes were produced. The background was detected automatically and the region intensities of the bands were quantified in linear arbitrary units. The values of the region intensities minus the background intensities were used for analysis.

2.5.6. Stripping of membrane

In order to reprobe a blot for an alternative protein, blots were stripped with 1x Stripping Mild (10x Stripping Mild (Millipore)) for 10 minutes on a rocker. The membrane was then blocked and reprobed with another antibody (as described in Section 2.5.3). Blots

originally probed for phosphorylated Tie2 were stripped and reprobed for total Tie2 to normalise phosphorylation results.

2.6. Conjugation of pY992-Tie2 to BSA

A standard of phosphorylated Y992 Tie2 protein was required to produce a standard calibration curve to quantify the amount of Tie2 phosphorylation. To do this the primary amine (lysine) of the pY992-Tie2 was conjugated to the sulphydryl (cysteine-34) of bovine serum albumin (BSA) through the BMPS crosslinker (Thermo-Scientific).

The pY992 protein was dissolved in conjugation buffer (2 mM EDTA in PBS) and a preliminary test was carried out to check the absorbance and fraction number by eluting the protein through the column. The absorbance was measured at 280 nm using a nano-spectrometer. The BMPS crosslinker was dissolved in DMSO and combined in excess with the pY992 protein (so all protein is bound to linkers) and incubated for 30 minutes at room temp. Excess cross-linker was removed by running through a desalting column (Sephadex-G10, beads were swollen overnight before experiment) and the fractions contain protein was determined using nano-spectrophotometer (Abs = 280 nm). The pY992-BMPS protein was combined with BSA protein (1:1, 1 BSA bound to protein) and incubated overnight at +4^{o}C. To stop the conjugation reaction, a buffer containing reduced cysteine was added at a concentration several times greater than the sulphydryls of the pY992 protein. Western blotting was used to verify the efficiency of conjugation.

2.7. Normalisation of experimental data

The levels of phosphorylation were normalised to the levels of Tie2 by stripping and reprobing the blot for Tie2 (as described in section 2.5.6).

To normalise the effect of Ang in experiments for comparison with simulation results, the basal level of phosphorylation was normalised to zero for the initial level of phosphorylation before stimulation with Ang. Hence the basal to maximum phosphorylation is relative to the change of time point or concentration.

2.8. Statistical analysis

Data are expressed as the mean ± standard error of the mean (SEM).

Statistics were performed using GraphPad Prism 6 Software. A Student's *t* test was performed to determine the significance of the means of two groups in experiments. A one-way analysis of variance (ANOVA) was performed to determine the significance of the means of more than two groups to the control in experiments. A two-way ANOVA was performed to determine the significance of the experiments to the simulation. A *P* value of <0.05 was considered statistically significant.

2.9. Computational modelling

Two scripts of the full mathematical model were prepared in MATLAB R2010a (The MathWorks). The first script is the main script which contains the parameter values, initial concentrations of states and the required simulation plot (time-course of chosen

state). The second script contains the equations for the reaction rates and the ordinary differential equations (ODE).

To simulate the model main script was used to modify the parameter values, state concentrations, the length of time that the model should simulate, and output details to produce the relevant simulated state time-course plot.

The initial concentrations of the states (Ang1, Ang2 and sTie2) were changed to the appropriate values in nanomolar. If a state was not to be included in a simulation this value was set as zero. For steady state simulations this was set at 18000 seconds (five hours) and for other simulations required for validation this was set at 1800 seconds (30 minutes).

When the main script was run, a code included in both scripts linked the two scripts together and the equations were integrated using the ODE solver. Once the simulation was completed a simulation plot of the state concentration over time was produced. As the script was not produced to simulate multiple state concentrations in one run, (e.g. for an Ang1 concentration dependent curve) a time-course simulation for each concentration was performed, and the concentration of phosphorylated Tie2 was obtained at the 15 minute time point. These values were plotted manually in GraphPad Prism 6 Software.

Chapter 3: Computational modelling of the angiopoietin and Tie interactions

3.1. System delimitation

This project aims to model the angiopoietin-Tie interactions and various regulatory features at the endothelial cell surface. Schematic diagrams of the angiopoietin-1 and angiopoietin-2 interactions with Tie were produced (figures 3.1 and 3.2) to clarify the key reactions to be modelled, which entail the following:

1. Tie1 and Tie2 in equilibrium with the Tie1:Tie2 heterodimer at initial conditions with no ligand interaction. Tie1 and Tie2 cleavage will not be modelled.
2. Ang1 binds to Tie2 (Ang1.Tie2) and causes tetramerisation of the receptor through consecutive free Tie2 bindings; dimerisation, trimerisation and tetramerisation (Ang1(Tie2)4). The receptors in the complex are autophosphorylated by their tyrosine kinase domain forming a phosphorylated Ang1.Tie2 tetramer (Ang1(Tie2)4.P). The activated receptor is downregulated by subsequent internalisation and degradation, or by dephosphorylation through the human protein tyrosine phosphatase beta (HPTP-β). New internal Tie2 (nTie2) is replenished to the cell surface.
3. Ang2 binds to Tie2 (Ang2.Tie2) in a similar manner as Ang1. There are three different oligomeric forms of Ang2; dimeric (Ang2)2, trimeric (Ang2)3, and tetrameric (Ang2)4. Each Ang2 binds to Tie2 and subsequently recruits free Tie2 to form its respective Tie2 oligomeric complex. Only the tetrameric form of Ang2 can tetramerize Tie2 and therefore become phosphorylated to form a phosphorylated Ang2.Tie2 tetramer ((Ang2)4(Tie2)4.P). The phosphorylated

complex is dephosphorylated by HPTP-β. Ang2 oligomeric forms can also bind to Tie2 in the preformed Tie1:Tie2 heterodimer. New internal Tie2 (nTie2) is replenished to the cell surface.

4. Ang1 and Ang2 can also bind to soluble Tie2 (sTie2) which is present in the medium.

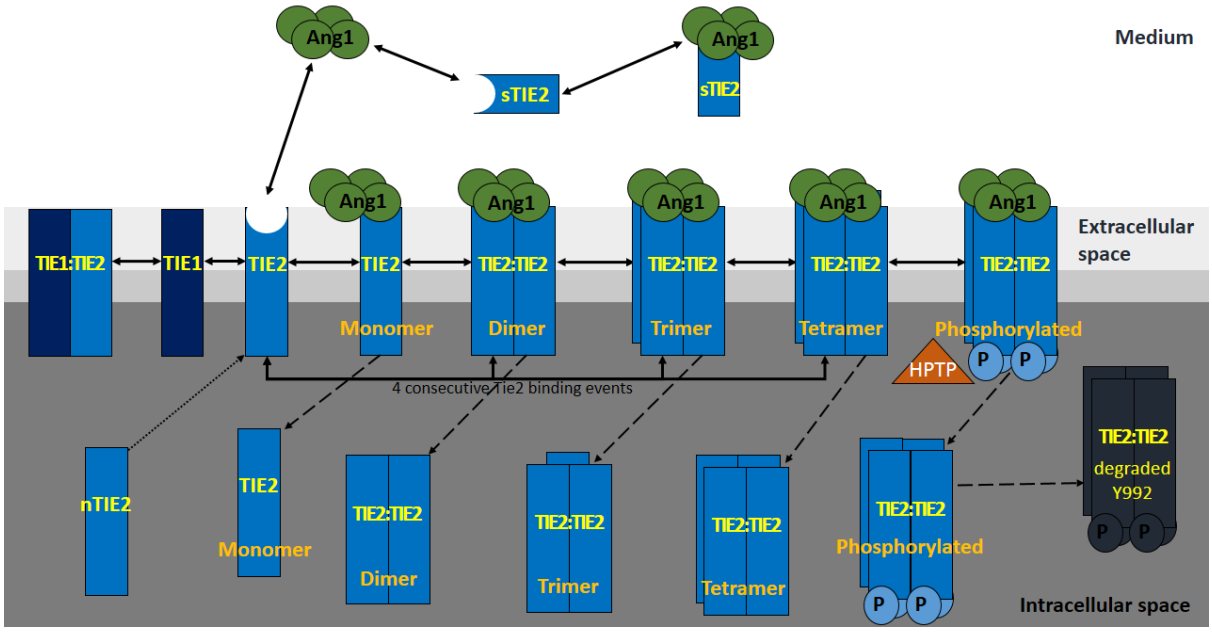

Figure 3.1- Schematic diagram of Ang1 interactions and Tie2 reactions to be modelled
Ang1 (tetramer) can bind to Tie2 to form a monomer. The monomeric complex can recruit free Tie2 to form a dimer, trimer and tetramer. Only the tetrameric Ang1-Tie2 complex can be phosphorylated and dephosphorylated by human protein tyrosine phosphatase beta (HPTP). All Ang1-Tie2 complexes can be internalised following which the phosphorylated form is degraded. New Tie2 (nTie2) replenishes Tie2 to the cell surface. Tie1 and Tie2 can heterodimerize to form the Tie1:Tie2 complex. Ang1 can also bind to soluble Tie2 (sTie2).

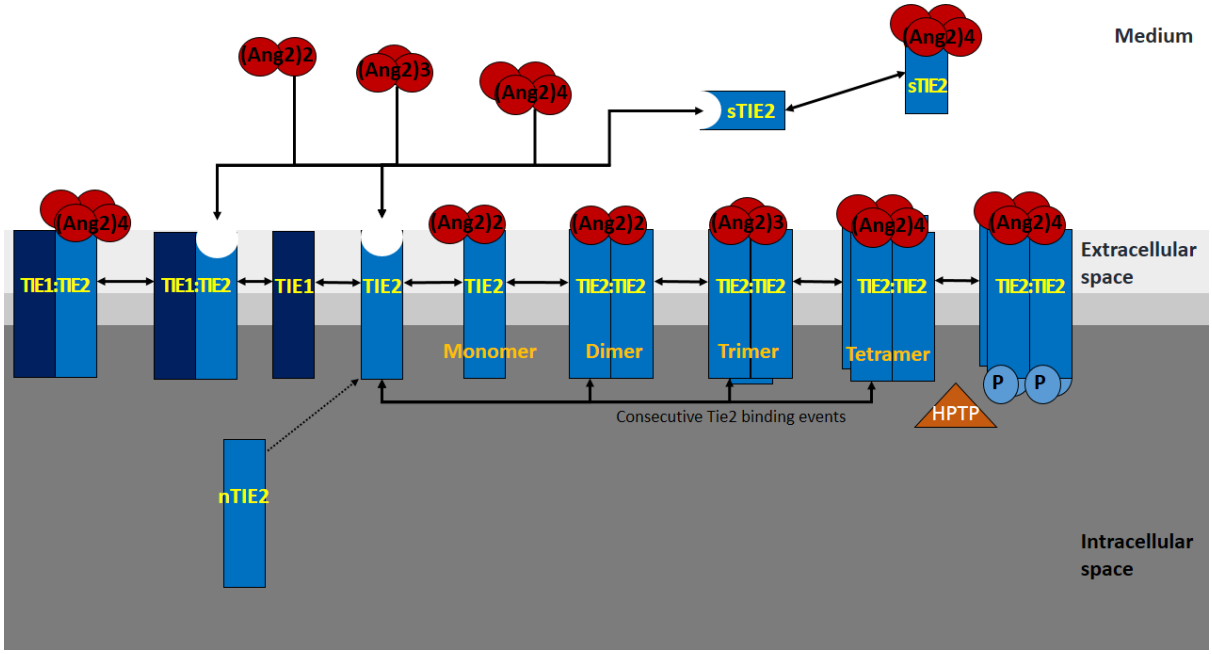

Figure 3.2- Schematic diagram of Ang2 interactions and Tie2 reactions to be modelled
Ang2 is present in 3 forms; dimeric (Ang2)2, trimeric (Ang2)3 and tetrameric (Ang2)4. All forms can bind to Tie2 to form a monomer and recruit free Tie2 to form the respective complex of Ang2 with Tie2. Only the tetrameric (Ang2)4.(Tie2)4 complex can be phosphorylated and dephosphorylated by human protein tyrosine phosphatase beta (HPTP). New Tie2 (nTie2) replenishes Tie2 to the cell surface. Tie1 and Tie2 can heterodimerize to form the Tie1:Tie2 complex. All Ang2 forms can also bind to Tie2 in the Tie1:Tie2 complex and to soluble Tie2 (sTie2).

3.2. The schematic diagram of model reactions

The schematic diagrams of the angiopoietin-1 and angiopoietin-2-Tie interactions (figures 3.1 and 3.2) were used to produce a schematic diagram of the model reactions in CellDesigner™ (Figure 3.3). CellDesigner uses this representation of the model as a graphical user interface, for simplifying the modification of reactions, states and parameters, and the input of rate equations. The three compartments (extracellular, extracellular space and intracellular) identify the areas where the reactions take place. The model incorporates 32 reactions and 37 different states.

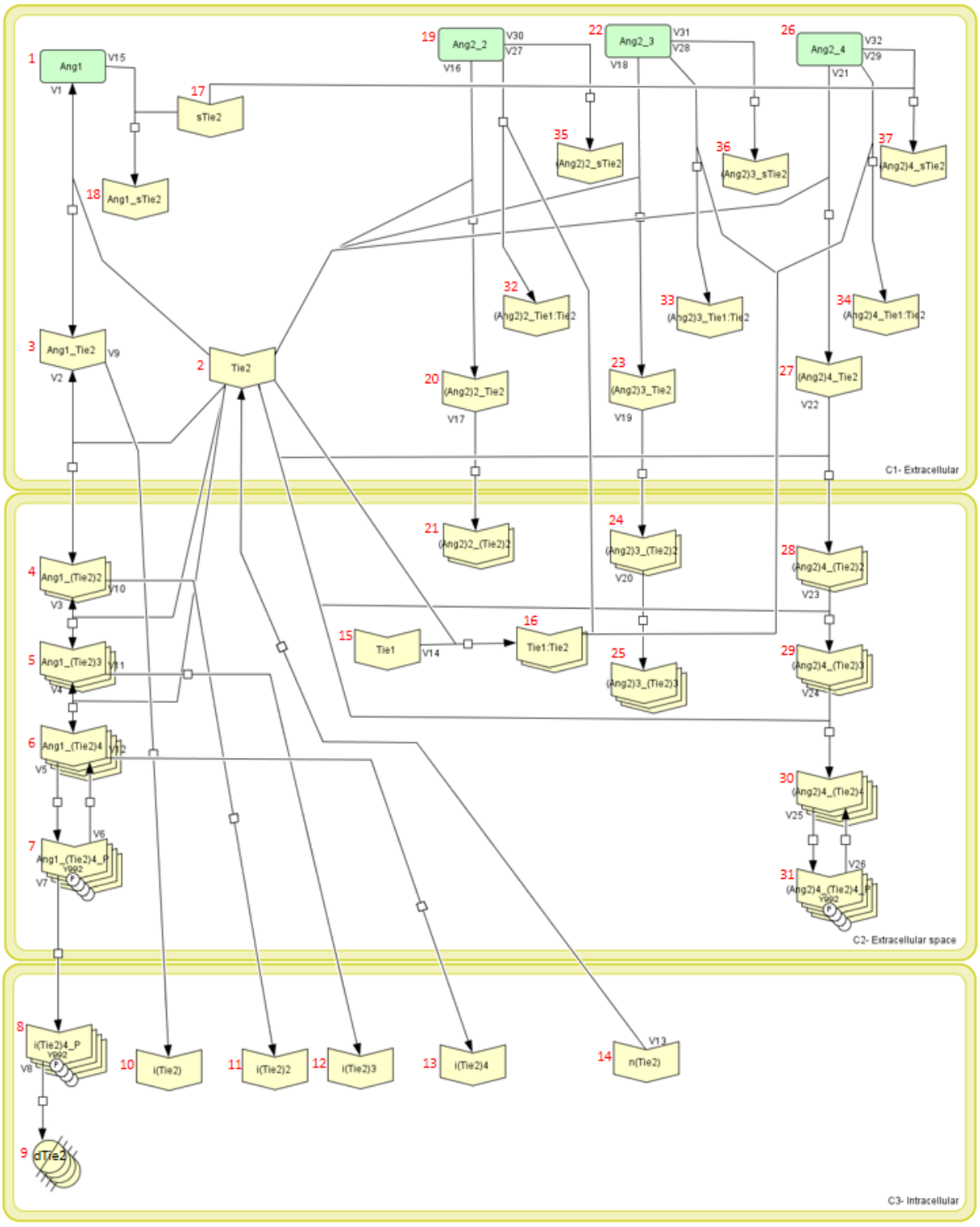

Figure 3.3: The schematic diagram produced in CellDesigner™.
Computational representation of all the model reactions produced in CellDesigner™. This diagram shows that there are 37 states (numbered in red) and 32 kinetic reaction rates (numbered in black). The 3 compartments identify where the reactions occur.

3.3. Model assumptions

The concentration of states can be variable or fixed. Variable states will be changed in experiments and simulations whereas fixed states will not be changed.

3.3.1. Variable states

Ang1

Ang1 exists predominantly as higher order multimers and in this model is assumed to be present only in the tetrameric form (Procopio *et al.*, 1999). The concentration of this state will be varied in the model to reproduce the validation experiments.

Ang2

Ang2 is present predominantly as a dimer however trimeric and tetrameric forms have also been shown to exist (Kim *et al.*, 2005). The relative percentages of Ang2 oligomeric forms were calculated to be; 75% dimeric, 16% trimeric and 9% tetrameric. The concentration of this state will be varied in the model to reproduce the validation experiments. The relative concentrations of each Ang2 oligomeric state for simulation is shown in Appendix 1.

Soluble Tie2

Soluble Tie2 (sTie2) is the soluble truncated extracellular form of Tie2 which can bind both Ang1 and Ang2 (Reusch *et al.*, 2001; Findley *et al.*, 2007). The sTie2 used in

experiments is a dimeric wildtype produced by Professor Nicholas Brindle and Teonchit Nuamchit. The concentration of this state will be varied in the model to reproduce the validation experiments.

3.3.2. Fixed states

Tie1, Tie2, Tie1:Tie2 and internal Tie2

The concentrations of these states at initial conditions will not be changed in the model as the experiments required for validation will use primary cell line HUVECs plated at a known fixed amount ($2x10^5$ cells per well). Therefore the concentrations of these states in the model and in experiments are assumed to be the same at initial conditions. The Tie1:Tie2 heterodimer is assumed to be pre-formed as demonstrated in the literature (Marron *et al.*, 2000). Cleavage of Tie1 and Tie2 will not be modelled as preliminary simulations have shown this induces further complexity to the model. In addition the cleavage-inducing factors (VEGF and PMA) will not be incorporated or added to experiments.

Intermediate states

The intermediates states are all the other states in the model apart from Ang1, Ang2, soluble Tie2, Tie1, cell surface Tie2, Tie1:Tie2 and internal Tie2. The initial concentrations of the states formed after binding and before phosphorylated states will be considered as zero. This is due to the model assumption that these states are ligand induced. Moreover these states are difficult to quantify experimentally.

3.3.3. Kinetic reactions and rate constant parameter values

There is minimal data on quantified kinetic reaction rates of the Ang-Tie system. Hence the EGFR system which is also a previously modelled RTK system will be used as a guide for parameter values (Kholodenko *et al.*, 1999).

Ang1 binding to Tie2

The binding affinity K_D for Ang1 binding to Tie2 has been determined in two separate studies (Davis *et al.*, 1996; Maisonpierre *et al.*, 1997). The first study examined Ang1 binding to the extracellular domain of soluble Tie2 and showed the binding affinity K_D to be ~3.7 nM (Davis *et al.*, 1996). The second study examined an Ang1 variant binding to the extracellular domain of soluble Tie2 which was found to be ~3 nM (Maisonpierre *et al.*, 1997).

However as the association rate constant (k_{on}) and dissociation rate constant (k_{off}) have not been quantified in the literature or were performed in isolation, this model will primarily use the equilibrium dissociation constant (K_D) and k_{off} determined by Dr Kathryn Steele (Steele, 2013). The K_D and k_{off} for the angiopoietins binding to Tie2 was determined using binding studies for both Ang1 and Ang2 in the chicken B cell line-DT40. Moreover the K_D values provided are similar to the values described previously (Davis *et al.*, 1996; Maisonpierre *et al.*, 1997).

The vales for these parameters are shown in Table 3.1. The k_{on} for Ang2 was calculated from the K_D and k_{off}. As Ang1 and Ang2 both compete for binding to Tie2, the association rate for Ang1 was assumed to be the same as Ang2. Using this value and the K_D for Ang1 it was possible to calculate the dissociation constant for Ang1 which was difficult to measure in vitro.

Parameter	Value
Ang2 K_D	1.026 ± 0.23 nM
Ang1 K_D	0.456 ± 0.17 nM
Ang2 k_{off}	0.0096 ± 0.002 s^{-1}

Table 3.1: Binding kinetics of Ang1 and Ang2 to Tie2
The dissociation constant (K_D) for Ang1 and Ang2, and the dissociation rate constant (k_{off}) for Ang2 in the DT40 cell line was determined by Dr Kathryn Steele (Steele, 2013).

Tie2 oligomerisation

The model was initially simulated under the assumption that Tie2 is pre-clustered on the cell surface (Bogdanovic *et al.*, 2006). However preliminary simulations indicated that the rate of phosphorylation occurred rapidly after binding and peaked earlier than the 15-20 minutes as demonstrated in the literature (Yuan *et al.*, 2007; Maliba *et al.*, 2008). Hence the model was redefined to assume the tetramerisation of monomeric Tie2 which would reduce the rate of phosphorylation.

The redefined model for Ang1-Tie2 interactions assumes that binding of tetrameric Ang1 to Tie2 induces the formation of an Ang1-Tie2 tetramer by receptor clustering (Barton *et al.*, 2006). Thus oligomerisation of Tie2 is ligand-induced where one tetrameric Ang1

can bind to four Tie2 monomers. The reactions for oligomerisation take place only in the extracellular space containing the Tie2 ectodomain, the concentrations of Tie2 for oligomerisation reactions need to be scaled up as it is a much smaller volume than the medium (refer to section 3.4). The rate at which the Ang1-Tie2 binds to the three additional Tie2 monomers is assumed to occur very fast and would depend on the amount of Tie2 present in the cell membrane. Therefore the rate of oligomerisation is limited by the diffusion of Tie2. The parameters used for the rate equations are the diffusion rates for Epidermal Growth Factor Receptor (EGFR) (Kholodenko *et al.*, 1999). There is no data in the literature to prove that binding of an additional Tie2 occurs any faster thus the same values were used for trimerisation and tetramerisation.

Tie2 phosphorylation and dephosphorylation

In this model only the tetramerized Tie2 complex can autophosphorylate the receptor when induced by tetrameric Ang1 or Ang2, as it has been shown that monomeric and dimeric forms of the ligand cannot induce phosphorylation of Tie2 (Barton *et al.*, 2006). The kinetics of phosphorylation in this model is assumed to be similar to the EGFR model (by Kholodenko and colleagues) where the concentration of ATP is higher than the Michaelis constant of receptor tyrosine kinase for ATP (Kholodenko *et al.*, 1999). For the phosphorylation reaction, the rate equation is a pseudo-first-order reaction using the law of mass-action kinetics, which was also used to model phosphorylation of the EGFR (Kholodenko *et al.*, 1999).

The dephosphorylation reaction is modelled using Michaelis-Menten kinetics as this is an enzymatic reaction catalysed by human protein tyrosine phosphatase beta (HPTP-β) and vascular endothelial phosphatase (VE-PTP) which are known to dephosphorylate the Tie2 receptor (Yacyshyn *et al.*, 2009; Winderlich *et al.*, 2009). The Vmax and Km parameters required for the dephosphorylating reaction are for the HPTP-β using the EGFR phosphotyrosyl peptide as a substrate which is assumed to be similar for Tie2 (Cho *et al.*, 1993).

Internalised Tie2 states

A study has shown that Ang1 stimulation induces a fast rate of Tie2 internalisation and Ang1 is released back to the extracellular space (Bogdanovic *et al.*, 2006). In this model Ang1 binding to Tie2 also induces Tie2 internalisation of each Ang1-Tie2 oligomeric complex, whereas Ang2 does not induce internalisation (refer to section 3.9). To simplify the model it is assumed that internalisation of the complex does not release Ang1 or Ang2, allowing them to bind with another Tie2. Tie2 has been shown to be internalised via clathrin-coated pits possibly to down regulate the receptor activation and facilitate downstream signalling (Bogdanovic *et al.*, 2009). The internalisation parameter has not been determined in the literature for angiopoietins however as the EGFR is also internalised through clathrin-coated pits for which there are many parameters available in literature the average value for EGFR internalisation will be used (Table 3.2) (Waterman & Yarden, 2001).

Internalisation value (mean ± SD)	Parameter	Reference
0.70 ± 0.09 min^{-1}	0.012 s^{-1}	(Haigler *et al.*, 1980; Gex-Fabry & DeLisi, 1984)
0.10 ± 0.05 min^{-1}	0.0017 s^{-1}	(Brown *et al.*, 1979; Gex-Fabry & DeLisi, 1984)
0.001 s^{-1}	0.001 s^{-1}	(Hatakeyama *et al.*, 2003)
0.15 min^{-1}	0.0025 s^{-1}	(Shankaran *et al.*, 2007)
1.0 min^{-1}	0.017 s^{-1}	(Starbuck & Lauffenburger, 1992)
	0.00684 s^{-1}	Average of ligand-induced rates

Table 3.2: Potential internalisation parameters
Internalisation values for the epidermal growth factor receptor which like Tie2 is also internalised into the cell through clathrin-coated pits. Values are the mean ± standard deviation. The average values of these parameters will be used for the model.

Degradation of phosphorylated Tie2

Once the receptor is phosphorylated and internalised it is thought that the Tie2 is degraded. It has been suggested that Tie2 degradation may regulate the magnitude and duration of Ang1 signalling (Bogdanovic *et al.*, 2006). Degradation is a complex step to model mathematically, thus this model will assume that degradation occurs in one step which removes the Tie2 from the system. The rate of phosphorylated Tie2 degradation has not been quantified in the literature.

Replenishment of cell surface Tie2

Preliminary experiments by Dr Tariq Tahir showed that the concentration of Tie2 on the cell surface is constant at basal conditions, and that the original level of Tie2 is not replenished to initial levels even 2 hours after ligand removal. Therefore to maintain this

equilibrium in the model the replenishment of new Tie2 (nTie2) is only added to the model when there is ligand-induced internalisation or Tie2 degradation. The nTie2 does not represent newly synthesized Tie2 but is the Tie2 within the cell already formed at initial conditions, and waiting to be transported to the cell surface during ligand stimulation. This way the original level of total Tie2 is not increased, and is only replaced by preformed internal Tie2. In this model the rate of internalisation is equal to the rate of replenishment of Tie2 within the cell, however as the nTie2 is also able to bind ligands and be degraded it doesn't replenish Tie2 back to the initial cell surface concentration.

Tie1:Tie2 heterodimerisation

There are no studies in the literature which have determined the rate of Tie1 and Tie2 heterodimerisation and dissociation. Therefore the dissociation constant was assumed to be the same as Tie2:Tie2 dissociation, and the association rate will be calculated using the rate equation at steady state when Tie1 and Tie2 are in equilibrium with the Tie1:Tie2 complex. As the dimerisation reaction happens between the ectodomains of Tie1 and Tie2 (Seegar *et al.*, 2010), this reaction also occurs in the extracellular space similar to Tie2:Tie2 oligomerizaton. Hence the state concentrations are scaled to represent the reaction between Tie1 and Tie2 occurring in this compartment (refer to section 3.4).

Ang1 binding to sTie2

The concentrations of sTie2 dimer to be simulated are much higher than the concentrations for Ang1 and Ang2 and this saturates the system with sTie2. Hence it is assumed that only one Ang1 or Ang2 can bind to one sTie2, and that once bound it can no longer bind to Tie2, and any additional binding to sTie2 will not be modelled. It is

assumed that sTie2 has the same binding affinities and rate constants as full length Tie2, and can therefore compete with full length Tie2 in binding both ligands.

Ang2 binding to Tie2 and oligomerisation

The binding affinity K_D for Ang2 binding to extracellular soluble Tie2 was shown to be similar to Ang1 at ~3.7 nM and 3 nM (Davis *et al.*, 1996; Maisonpierre *et al.*, 1997). The K_D and dissociation constant for Ang2 binding was also determined by Dr Kathryn Steele as shown in Table 3.1. The k_{on} for Ang2 was calculated from the K_D and k_{off}. The binding of oligomeric Ang2 to Tie2 induces the formation of the respective oligomeric Tie2 complex, in a similar fashion to Ang1, and only the tetrameric complex can be phosphorylated. Furthermore it has been shown that Ang2 induced internalisation is very slow, as 90 minutes after stimulation a majority of receptors are still present at the cell surface, hence Ang2-induced internalisation will not be modelled (Bogdanovic *et al.*, 2006).

Ang2 binding to Tie1:Tie2

It has been suggested that Ang2 can also bind to Tie2 in the Tie1:Tie2 complex, and is not affected by Tie1 (Hansen *et al.*, 2010). Therefore it is assumed that this is similar to Ang2 binding to a Tie2 monomer.

3.4. Scaling of Tie2 in the extracellular space

The reactions of ligand binding to Tie2 occur in the extracellular medium which has a volume of $1x10^{-3}$ litres. Once the ligand is bound this induces subsequent binding of free Tie2 to form oligomers. However as the free Tie2 is not freely moving in the extracellular medium but is anchored to the cell membrane, this reaction of oligomerisation takes place in a much smaller volume (Figure 3.4). Upon ligand binding receptor tyrosine kinases have been suggested to oligomerize at the ectodomain (Barton *et al.*, 2006; Hubbard & Till, 2000). Therefore the volume that this reaction takes place is in the extracellular space outside the cell membrane and within the reach of the Tie2 ectodomain. Figure 3.4 illustrates the Tie2 ectodomain and its dimensions; 90 x 65 x 50 Å (Barton *et al.*, 2006). From this the reach of the Tie2 ectodomain is calculated to be 9nm. The surface area of a HUVEC stated in the literature is $400x10^{-9}$ m^2 ($4x10^{11}$ nm^2) (Bai *et al.*, 2008) and 10,400 um^2 ($1x10^{10}$ nm^2) (Lee *et al.*, 2007), thus for the calculation the area was assumed to be $4x10^8$ nm^2. To calculate the extracellular space volume per cell, the surface area was multiplied by the reach of the Tie2 ectodomain (9 nm) and halved, assuming that half the cell surface is exposed to the medium. The total volume per well (of a 6 well plate) was calculated by multiplying the volume per cell by the total amount of cells per well ($2x10^5$ cells per well), and was converted to litres. The ratio between the extracellular medium ($1x10^{-3}$ L) and extracellular space ($3.6x10^{-10}$ L) is $2.8x10^6$. Therefore the concentrations of Tie2 and Tie1 involved in the oligomerisation reactions (occur in the extracellular space) were scaled up by multiplying them by the factor of $2.8x10^6$.

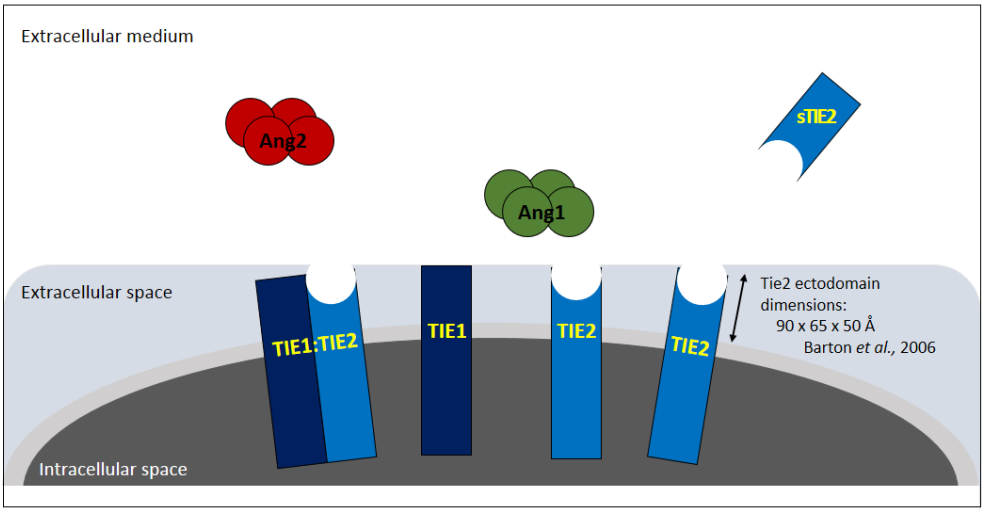

Figure 3.4: The extracellular space and Tie2 ectodomain.
The diagram illustrates the 3 different compartments in the model; the extracellular medium, the extra cellular space and the intracellular space. The angiopoietin ligands and soluble Tie2 (sTie2) are freely moving in the extracellular medium and the receptors Tie1 and Tie2 are anchored to the cell membrane. The Tie2 ectodomain in the extracellular space has the dimensions of 90 x 65 x 50 Å (Barton *et al.*, 2006).

3.5. Derivation of the kinetic model

3.5.1. Kinetic equations

A list of kinetic equations to describe the behaviour of the Ang-Tie interactions was produced using the schematic diagram (Figure 3.3) and modified ODEs from the previously described EGFR model by (Kholodenko *et al.*, 1999) (Table 3.3). Each ODE equation for the change in state concentration over time is assigned a reaction rate which is either mass-action or Michaelis-Menten kinetics (Table 3.4- Ang1 modelling, Table 3.5- Ang2 modelling).

State number	State	Time-course for concentration	Kinetic reaction rates
1	Ang1	d[Ang1]/dt =	$-V_1$
2	Tie2	d[Tie2]/dt =	$-V_1-V_2-V_3-V_4+V_{13}-V_{14}-V_{16}-V_{17}-V_{18}-V_{19}-V_{20}-V_{21}-V_{22}-V_{23}-V_{24}$
3	Ang1.Tie2	d[Ang1.Tie2]/dt =	$V_1-V_2-V_9$
4	Ang1.(Tie2)2	d[Ang1.(Tie2)2]/dt =	$V_2-V_3-V_{10}$
5	Ang1.(Tie2)3	d[Ang1.(Tie2)3]/dt =	$V_3-V_4-V_{11}$
6	Ang1.(Tie2)4	d[Ang1.(Tie2)4]/dt =	$V_4-V_5+V_6-V_{12}$
7	Ang1.(Tie2)4.P	d[Ang1.(Tie2)4.P]/dt =	$V_5-V_6-V_7$
8	i.Ang1.(Tie2)4.P	d[i.Ang1.(Tie2)4.P]/dt =	V_7-V_8
9	d.Ang1.(Tie2)4.P	d[d.Ang1.(Tie2)4.P]/dt =	V_8
10	i.Ang1.Tie2	d[i.Ang1.Tie2]/dt =	V_9
11	i.Ang1.(Tie2)2	d[i.Ang1.(Tie2)2]/dt =	V_{10}
12	i.Ang1.(Tie2)3	d[i.Ang1.(Tie2)3]/dt =	V_{11}
13	i.Ang1.(Tie2)4	d[i.Ang1.(Tie2)4]/dt =	V_{12}
14	nTie2	d[nTie2]/dt =	$-V_{13}$
15	Tie1	d[Tie1]/dt =	$-V_{14}$
16	Tie1:Tie2	d[Tie1:Tie2]/dt =	$V_{14}-V_{27}-V_{28}-V_{29}$
17	sTie2	d[sTie2]/dt =	$V_{15}-V_{30}-V_{31}-V_{32}$
18	Ang1.sTie2	d[Ang1.sTie2]/dt =	V_{15}
19	(Ang2)2	d[(Ang2)2]/dt =	$-V_{16}-V_{27}-V_{30}$
20	(Ang2)2.Tie2	d[(Ang2)2.Tie2]/dt =	$-V_{16}-V_{17}$
21	(Ang2)2.(Tie2)2	d[(Ang2)2.(Tie2)2]/dt =	V_{17}
22	(Ang2)3	d[(Ang2)3]/dt =	$-V_{18}-V_{28}-V_{31}$
23	(Ang2)3.Tie2	d[(Ang2)3.Tie2]/dt =	$V_{18}-V_{19}$
24	(Ang2)3.(Tie2)2	d[(Ang2)3.(Tie2)2]/dt =	$V_{19}-V_{20}$
25	(Ang2)3.(Tie2)3	d[(Ang2)3.(Tie2)3]/dt =	V_{20}

26	(Ang2)4	d[(Ang2)4]/dt =	$-V_{21}-V_{29}-V_{32}$
27	(Ang2)4.Tie2	d[(Ang2)4.Tie2]/dt =	$V_{21}-V_{22}$
28	(Ang2)4.(Tie2)2	d[(Ang2)4.(Tie2)2]/dt =	$V_{22}-V_{23}$
29	(Ang2)4.(Tie2)3	d[(Ang2)4.(Tie2)3]/dt =	$V_{23}-V_{24}$
30	(Ang2)4.(Tie2)4	d[(Ang2)4.(Tie2)4]/dt =	$V_{24}-V_{25}+V_{26}$
31	(Ang2)4.(Tie2)4.P	d[(Ang2)4.(Tie2)4.P]/dt =	$V_{25}-V_{26}$
32	(Ang2)2.Tie1:Tie2	d[(Ang2)2.Tie1 :Tie2]/dt =	V_{27}
33	(Ang2)3.Tie1:Tie2	d[(Ang2)3.Tie1 :Tie2]/dt =	V_{28}
34	(Ang2)4.Tie1:Tie2	d[(Ang2)4.Tie1 :Tie2]/dt =	V_{29}
35	(Ang2)2.sTie2	d[(Ang2)2.sTie2]/dt =	V_{30}
36	(Ang2)3.sTie2	d[(Ang2)3.sTie2]/dt =	V_{31}
37	(Ang2)4.sTie2	d[(Ang2)4.sTie2]/dt =	V_{32}

Table 3.3: Kinetic equations comprising the computational model

ODE equations which form the mathematical model and describe the behaviour of the system. The time-courses of the different state concentrations are governed by kinetic reaction rates which are full described by their rate equations. Reactions for Ang1 modelling are in black and reactions for Ang2 modelling are in blue.

Reaction	Rate Equation	Parameter
V_1	Ang1 binds to Tie2	
	k_1[Ang1][Tie2]	k_1
	$-k_{-1}$[Ang1.Tie2]	k_{-1}
V_2	Formation of Ang1.Tie2 dimer	
	k_2([Ang1.Tie2]*2800000)*([Tie2]*2800000)	k_2
	$-k_{-2}$[Ang1.(Tie2)2]	k_{-2}
V_3	Formation of Ang1.Tie2 trimer	
	k_3[Ang1.(Tie2)2]*([Tie2]*2800000)	k_3
	$-k_{-3}$[Ang1.(Tie2)3]	k_{-3}
V_4	Formation of Ang1.Tie2 tetramer	
	k_4[Ang1.(Tie2)3]*([Tie2]*2800000)	k_4
	$-k_{-4}$[Ang1.(Tie2)4]	k_{-4}
V_5	Phosphorylation of Ang1.Tie2 tetramer	
	k_5[Ang1.(Tie2)4]	k_5
	$-k_{-5}$[Ang1.(Tie2)4.P]	k_{-5}
V_6	Dephosphorylation of Ang1.Tie2 tetramer	
	$\frac{kv_6 \quad (Ang1.(Tie2)4.P)}{k_7 + (Ang1.(Tie2)4.P)}$	kv_6 k_6
V_7	Internalisation of the phosphorylated Tie2 tetramer	
	k_7[i.Ang1.(Tie2)4.P]	k_7
V_8	Degradation of the internalised phosphorylated Tie2 tetramer	
	k_8[d.Ang1.(Tie2)4.P]	k_8
V_9	Internalisation of Tie2 monomer	
	k_9[i.Ang1.(Tie2)]	k_9
V_{10}	Internalisation of Tie2 dimer	
	k_{10}[i.Ang1.(Tie2)2]	k_{10}
V_{11}	Internalisation of Tie2 trimer	
	k_{11}[i.Ang1.(Tie2)3]	k_{11}
V_{12}	Internalisation of Tie2 tetramer	
	k_{12}[i.Ang1.(Tie2)4]	k_{12}
V_{13}	Replenishment of cell surface Tie2	
	k_{13}[nTie2]	k_{13}
V_{14}	Formation of Tie1.Tie2 heterodimer	
	$k_{14(}$[Tie1] *2800000) * ([Tie2] *2800000)	k_{14}
	$-k_{-14}$[Tie1:Tie2]	k_{-14}
V_{15}	Ang1 binds to sTie2	
	k_{15}[Ang1][sTie2]	k_{15}
	$-k_{-15}$[Ang1.sTie2]	k_{-15}

Table 3.4: Rate equations for the kinetic reaction rates for Ang1 model interactions
The rate equations for each kinetic reaction rate of the system identified in chapter 3.1. The dephosphorylation equations use Michaelis-Menten kinetics whereas the rest are mass-action kinetics. Each equation has parameters which need to be quantified.

	Rate Equation	**Parameter**
V_{16}	(Ang2)2 binds to Tie2 k_{16}[(Ang2)2][Tie2] $-k_{-16}$[(Ang2)2.Tie2]	 k_{16} k_{-16}
V_{17}	Formation of (Ang2)2.Tie2 dimer k_{17}([(Ang2)2.Tie2]*2800000)*([Tie2]*2800000) $-k_{-17}$[(Ang2)2.(Tie2)2]	 k_{17} k_{-17}
V_{18}	(Ang2)3 binds to Tie2 k_{18}[(Ang2)3][Tie2] $-k_{-18}$[(Ang2)3.Tie2]	 k_{18} k_{-18}
V_{19}	Formation of (Ang2)3.Tie2 dimer k_{19}([(Ang2)3.Tie2]*2800000)*([Tie2]*2800000) $-k_{-19}$[(Ang2)3.(Tie2)2]	 k_{19} k_{-19}
V_{20}	Formation of (Ang2)3.Tie2 trimer k_{20}[(Ang2)3.(Tie2)2]*([Tie2]*2800000) $-k_{-20}$[(Ang2)3.(Tie2)3]	 k_{20} k_{-20}
V_{21}	(Ang2)4 binds to Tie2 k_{21}[(Ang2)4][Tie2] $-k_{-21}$[(Ang2)4.Tie2]	 k_{21} k_{-21}
V_{22}	Formation of (Ang2)4.Tie2 dimer k_{22}([(Ang2)4.Tie2]*2800000)*([Tie2]*2800000) $-k_{-22}$[(Ang2)4.(Tie2)2]	 k_{22} k_{-22}
V_{23}	Formation of (Ang2)4.Tie2 trimer k_{23}[(Ang2)4.(Tie2)2]*([Tie2]*2800000) $-k_{-23}$[(Ang2)4.(Tie2)3]	 k_{23} k_{-23}
V_{24}	Formation of (Ang2)4.Tie2 tetramer k_{24}[(Ang2)4.(Tie2)3]*([Tie2]*2800000) $-k_{-24}$[(Ang2)4.(Tie2)4]	 k_{24} k_{-24}
V_{25}	Phosphorylation of (Ang2)4.Tie2 tetramer k_{25}[(Ang2)4.(Tie2)4] $-k_{-25}$[(Ang2)4.(Tie2)4.P]	 k_{25} k_{-25}
V_{26}	Dephosphorylation of (Ang2)4.Tie2 tetramer $\frac{kv_{26}\ ((Ang2)4.(Tie2)4.P)}{k_{26} + ((Ang2)4.(Tie2)4.P)}$	 kv_{26} k_{26}
V_{27}	(Ang2)2 binds to Tie1:Tie2 k_{27}[(Ang2)2][Tie1:Tie2] $-k_{-27}$[(Ang2)2.Tie1:Tie2]	 k_{27} k_{-27}
V_{28}	(Ang2)3 binds to Tie1:Tie2 k_{28}[(Ang2)3][Tie1:Tie2] $-k_{-28}$[(Ang2)3.Tie1:Tie2]	 k_{28} k_{-28}
V_{29}	(Ang2)4 binds to Tie1:Tie2 k_{29}[(Ang2)4][Tie1:Tie2] $-k_{-29}$[(Ang2)4.Tie1:Tie2]	 k_{29} k_{-29}
V_{30}	(Ang2)2 binds to sTie2 k_{30}[(Ang2)2][sTie2] $-k_{-30}$[(Ang2)2.sTie2]	 k_{30} k_{-30}
V_{31}	(Ang2)3 binds to sTie2 k_{31}[(Ang2)3][sTie2] $-k_{-31}$[(Ang2)3.sTie2]	 k_{31} k_{-31}

V_{32}	(Ang2)4 binds to sTie2 k_{32}[(Ang2)4][sTie2] $-k_{-32}$[(Ang2)4.sTie2]	 k_{32} k_{-32}

Table 3.5: Rate equations for the kinetic reaction rates for Ang2 model interactions
The rate equations for each kinetic reaction rate of the system identified in chapter 3.1. The dephosphorylation equations use Michaelis-Menten kinetics whereas the rest are mass-action kinetics. Each equation has parameters which need to be quantified. Oligomeric forms of Ang2; (Ang2)2 dimeric, (Ang2)3 trimeric, (Ang2)4 tetrameric.

3.5.2. Parameters

The list of rate equations generates a set of parameters which need to be quantified before the model can be simulated. The rate constants for each reaction and the concentrations of the different states at initial conditions were obtained from the literature and are described in Table 3.6 for modelling Ang1 interactions and Table 3.7 for modelling Ang2 interactions. Parameters and state concentrations which are not available in the literature or in databases will need to be determined by quantitative experiments and these are indicated in Table 3.8.

Parameters (kinetic rate constants) for modelling Ang1 interactions				
Reaction	**Notation**	**Value**	**Units**	**References**
Ang1.Tie2 binding Monomer	k_1	0.0094	$nM^{-1}s^{-1}$	Experimental data Dr K. Steele (Steele, 2013)
	k_{-1}	0.0043	s^{-1}	
Ang1.(Tie2)2 Dimer	k_2	0.5	$nM^{-1}s^{-1}$	(Kholodenko *et al.*, 1999) Diffusion limit
	k_{-2}	0.1	s^{-1}	
Ang1.(Tie2)3 Trimer	k_3	0.5	$nM^{-1}s^{-1}$	
	k_{-3}	0.1	s^{-1}	
Ang1.(Tie2)4 Tetramer	k_4	0.5	$nM^{-1}s^{-1}$	
	k_{-4}	0.1	s^{-1}	
Ang1.Tie2.P phosphorylation	k_5	1	$nM^{-1}s^{-1}$	(Kholodenko *et al.*, 1999)
	k_{-5}	0.01	s^{-1}	
Ang1.Tie2.P dephosphorylation	kv_6	43	µmol/ min/mg	(Cho *et al.*, 1993) HPTP-β
	k_{-6}	104000	nM	
Ang1.Tie2.P internalisation	k_7	0.00684	s^{-1}	Average parameter value for multiple references
Tie2.P degradation	k_8	?		
Tie2 internalisation	k_9	0.00684	s^{-1}	Average parameter value for multiple references
(Tie2)2 internalisation	k_{10}	0.00684	$[s^{-1}$	
(Tie2)3 internalisation	k_{11}	0.00684	s^{-1}	
(Tie2)4 internalisation	k_{12}	0.00684	s^{-1}	
nTie2 replenishment	k_{13}	0.00684	s^{-1}	Same as internalisation
Tie1:Tie2	k_{14}	?		
	k_{-14}	?		
Ang1 binding sTie2	k_{15}	0.0094	$nM^{-1}s^{-1}$	Same as Ang1 binding to Tie2
	k_{-15}	0.0043	s^{-1}	

Table 3.6: Reaction constants for Ang1 modelling

Values for each of the reaction constants were taken from the literature. "?" indicates missing data.

Parameters (kinetic rate constants) for modelling Ang2 interactions				
Reaction	**Notation**	**Value**	**Units**	**References**
(Ang2)2.Tie2 binding Monomer	k_{16}	0.0094	$nM^{-1}s^{-1}$	Experimental data Dr K. Steele (Steele, 2013)
	k_{-16}	0.0096	s^{-1}	
(Ang2)2.(Tie2)2 Dimer	k_{17}	0.5	$nM^{-1}s^{-1}$	(Kholodenko *et al.*, 1999) Diffusion limit
	k_{-17}	0.1	s^{-1}	
(Ang2)3.Tie2 binding Monomer	k_{18}	0.0094	$nM^{-1}s^{-1}$	Experimental data Dr K. Steele (Steele, 2013)
	k_{-18}	0.0096	s^{-1}	
(Ang2)3.(Tie2)2 Dimer	k_{19}	0.5	$nM^{-1}s^{-1}$	(Kholodenko *et al.*, 1999) Diffusion limit
	k_{-19}	0.1	s^{-1}	
(Ang2)3.(Tie2)3 Trimer	k_{20}	0.5	$nM^{-1}s^{-1}$	(Kholodenko *et al.*, 1999) Diffusion limit
	k_{-20}	0.1	s^{-1}	
(Ang2)4.Tie2 binding Monomer	k_{21}	0.0094	$nM^{-1}s^{-1}$	Experimental data Dr K. Steele (Steele, 2013)
	k_{-21}	0.0096	s^{-1}	
(Ang2)4.(Tie2)2 Dimer	k_{22}	0.5	$nM^{-1}s^{-1}$	(Kholodenko *et al.*, 1999) Diffusion limit
	k_{-22}	0.1	s^{-1}	
(Ang2)4.(Tie2)3 Trimer	k_{23}	0.5	$nM^{-1}s^{-1}$	
	k_{-23}	0.1	s^{-1}	
(Ang2)4.(Tie2)4 Tetramer	k_{24}	0.5	$nM^{-1}s^{-1}$	
	k_{-24}	0.1	s^{-1}	
(Ang2)4.Tie2.P phosphorylation	k_{25}	1	$nM^{-1}s^{-1}$	(Kholodenko *et al.*, 1999)
	k_{-25}	0.01	s^{-1}	
(Ang2)4.Tie2.P dephosphorylation	kv_{26}	43	µmol/ min/mg	(Cho *et al.*, 1993) HPTP-β
	k_{-26}	104000	nM	
(Ang2)2 binding to Tie1:Tie2	k_{27}	0.0094	$nM^{-1}s^{-1}$	Same as Ang2 binding to Tie2 Experimental data Dr K. Steele (Steele, 2013)
	k_{-27}	0.0096	s^{-1}	
(Ang2)3 binding to Tie1:Tie2	k_{28}	0.0094	$nM^{-1}s^{-1}$	
	k_{-28}	0.0096	s^{-1}	
(Ang2)4 binding to Tie1:Tie2	k_{29}	0.0094	$nM^{-1}s^{-1}$	
	k_{-29}	0.0096	s^{-1}	
(Ang2)2 binding to sTie2	k_{30}	0.0094	$nM^{-1}s^{-1}$	
	k_{-30}	0.0096	s^{-1}	
(Ang2)3 binding to sTie2	k_{31}	0.0094	$nM^{-1}s^{-1}$	
	k_{-31}	0.0096	s^{-1}	
(Ang2)4 binding to sTie2	k_{32}	0.0094	$nM^{-1}s^{-1}$	
	k_{-32}	0.0096	s^{-1}	

Table 3.7: Reaction constants for Ang2 modelling

Values for each of the reaction constants were taken from the literature. "?" indicates missing data.

The initial main states in the model are; Ang1, Ang2 (dimer, trimer and tetramer), Tie1, Tie2, Tie1:Tie2, nTie2 and sTie2 (Table 3.8). The states which can be changed experimentally are also variable in simulations, therefore the initial concentrations of Ang1, Ang2 (all forms) and sTie2 depend on the simulation and experiment to be performed. The initial concentrations of Tie1, Tie2, Tie1:Tie2 and nTie2 per HUVEC are not available in the literature or databases and will need to be quantified.

State	Concentration (nM)
Ang1	Experimental value
Tie1	?
Tie2	?
Tie1:Tie2	?
nTie2	?
sTie2	Experimental value
(Ang2)2	Experimental value
(Ang2)3	Experimental value
(Ang2)4	Experimental value

Table 3.8: State concentrations to be determined
The initial concentrations for the variable states need to be determined to simulate the model. "?" indicates concentration of states which are not available in the literature and need to be quantified at initial conditions for input into the model.

3.6. Discussion

This chapter aimed to identify the reactions to be modelled and produce a mathematical model which can be simulated by a computer. As the system is very complex many assumptions had to be made to simplify the model. After numerous preliminary attempts to model the system this chapter presents the simplified mathematical model.

To mathematically describe the behaviour of the system a list of kinetic equations was produced, and these equations which are governed by the kinetic reaction rates were fully described by the corresponding list of rate equations. The rate equations identified a list of parameters the values of which many were obtained from various literature data and previous models.

Some of these parameters are not specific to the angiopoietin and Tie system in HUVECs and are therefore used as a guide value for simulations. As these values are not accurate it is possible to change and re-define the parameters in future simulations to fit the simulation results to experimental data.

Furthermore the parameter values and state concentrations which are not available in the literature have been identified and must be quantified before the model can be simulated.

Chapter 4: Experimental quantification and derivation of parameters

In Chapter 3 the mathematical model was constructed and identified a list of rate constants and state concentrations which remain to be quantified before the model can be simulated. This chapter aims to determine and quantify these parameters which are not available in the literature (Tables 3.7 and 3.8) prior to simulating the model.

4.1. Quantification of Tie1 and Tie2 receptors in HUVECs

To quantify the concentration of Tie1 and Tie2 receptors, whole cell lysate samples were compared to a standard calibration curve of recombinant Tie. There are two methods which will be used to detect and quantify the optical densities of the proteins from a western blot. The first method is by using film detection and quantification using Image J software. The second method is by using a cooled charge-coupled device (CCD) camera to capture the chemiluminescent light from the blot and converting this to an electrical signal and finally to a digital signal which can be quantified using MultiGauge ver2.0 software (Young, 2009).

HUVECs were plated at a known amount ($1x10^5$ cells per well) and prepared as described in Chapter 2.21. Five concentrations of recombinant Tie were prepared between the ranges of 0-750 ng/ml. The cell lysates and recombinant Tie (Tie1 or Tie2) were resolved by SDS-PAGE, blotted and probed, with Tie1 or Tie2 primary antibody (R&D Systems) and secondary anti-goat-HRP (Dako) to detect the protein using enhanced chemiluminescence. Figure 4.1 shows the blots for Tie1 and Tie2, and the bands of protein present at their respective sizes of 125 kDa for mature Tie1 (top band) and 150

kDa for Tie2. Chemiluminescence was detected using film or a CCD imager. The bands were quantified by densitometry using ImageJ software for film or MultiGauge ver2.0 software for CCD images.

Probing for Tie1 produces a doublet band consisting of an upper band which is the fully glycosylated surface-expressed Tie1 and the lower band which is the partially glycosylated intracellular Tie1 (Marron *et al.*, 2007). Thus for Tie1 only the top band in the cell lysates samples were quantified as this is the mature form. These results were analysed from 4 experiments using Film (Figure 4.1A), and 5 experiments using the CCD imager (Figure 4.2A).

A graph was plotted of the known concentrations of recombinant Tie against their relative optical densities (Figures 4.1B, 4.2B). The optical densities of Tie1 and Tie2 in the whole cell lysate samples were compared to the standard calibration curve to determine the concentration of protein in the sample analysed per track.

4.1.1. Quantification using ImageJ

A

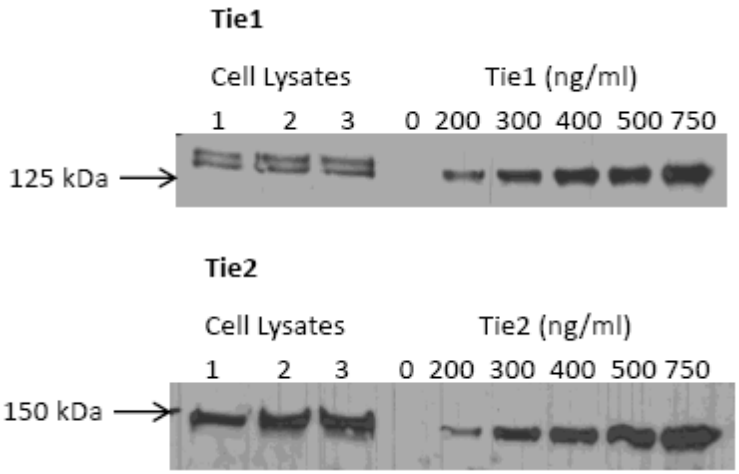

B

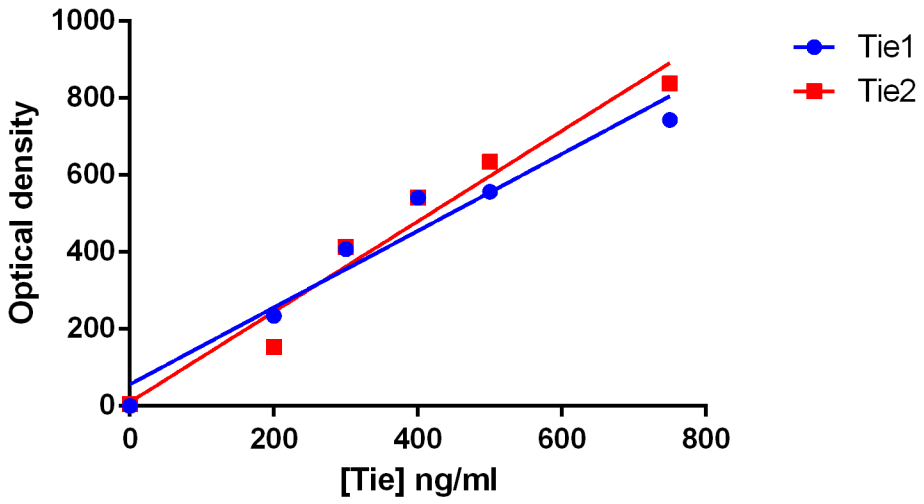

Figure 4.1: Quantification of Tie1 and Tie2 using film detection.
HUVECs were lysed and the proteins from the cell lysates (1-3) and recombinant Tie (0-750 ng/ml) were separated by SDS-PAGE. Tie antibodies were used to detect Tie1 and Tie2 proteins. Bands for mature Tie1 are ~125 kDa (top band for cell lysates) and ~150 kDa for mature Tie2. The bands were quantified by densitometry.
Densitometry was used to quantify the optical densities of bands for Tie1 and Tie2 in the samples of recombinant Tie (of known concentrations) and the cell lysates (unknown concentrations). This graph shows a standard calibration of the recombinant Tie1 (blue) and Tie2 (red) against their relative optical densities. The concentrations of analysed Tie1 and Tie2 in the cell lysates were obtained from the graph using their optical densities. These results are representative of 1 experiment (n = 4).

4.1.2. Quantification using CCD imager

A

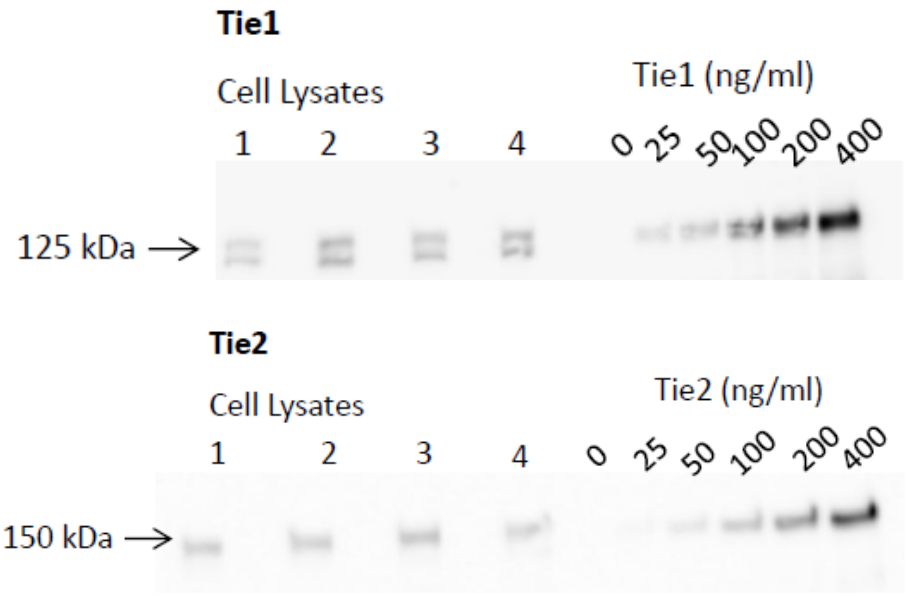

B

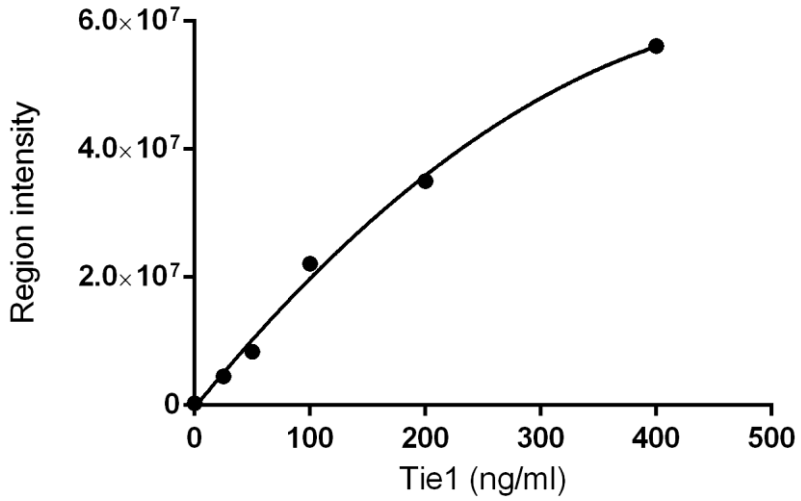

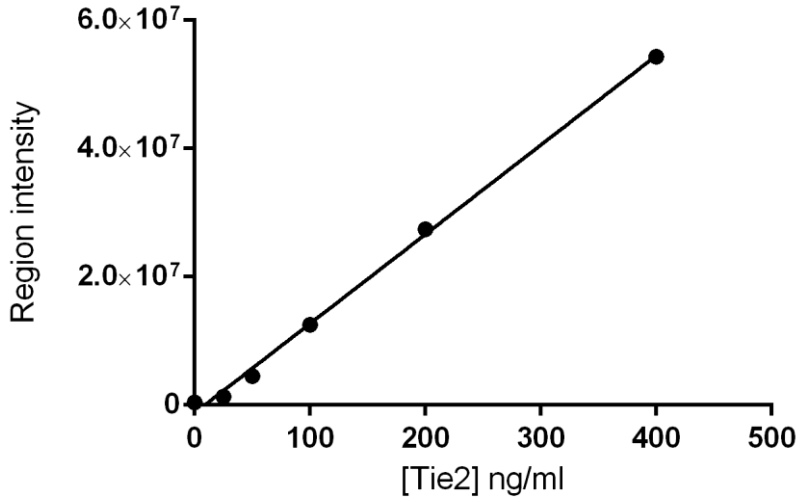

Figure 4.2: Quantification of Tie1 and Tie2 using CCD imaging detection.
A. HUVECs were lysed and the proteins from the cell lysates (1-4) and recombinant Tie1 (0-400 ng/ml) or recombinant Tie2 (0-750 ng/ml) were resolved by SDS-PAGE. Antibodies were used to detect Tie1 or Tie2 protein. Chemiluminescence was detected by the CCD imager and the bands for mature Tie1 (~125 kDa) or Tie2 (~150 kDa) were quantified by densitometry using MultiGauge software.
B. Densitometry using MultiGauge software was performed to quantify the standard region intensities of bands for Tie1 or Tie2 in the samples of recombinant Tie1 or recombinant Tie2 (of known concentrations) and the cell lysates (unknown concentrations). This graph shows a standard calibration of the recombinant Tie1 or Tie2 against the relative standard region intensity. The concentrations of analysed Tie1 or Tie2 in the cell lysates were obtained from the graph using their standard region intensity. These results are representative of 1 experiment (n=5).

4.1.3. Calculation of Tie1 and Tie2 in HUVECs

To analyse Tie protein in HUVECs, the concentrations of analysed Tie for the cell lysates were calculated to find: i) the total concentration in whole cell lysate sample, ii) amount of Tie1 and Tie2 receptors per cell, and iii) their molar concentrations.

i) The concentrations in ng/ml were converted to g/L, multiplied by the amount of recombinant Tie loaded per track, and converted to the total concentration in whole cell lysate sample of $1x10^5$ HUVECs.

ii) The total concentration of Tie per cell was divided by their molecular mass of Tie1 (125 kDa) or Tie2 (150 kDa) to calculate the amount in moles per cell, and multiplied by Avogadro's constant ($6x10^{23}$) to calculate the amount of Tie molecules per cell.

iii) To calculate the molar concentration; the amount of Tie molecules was multiplied by the number of cells per well, then divided by Avogadro's constant ($6x10^{23}$) and multiplied by 1000 to give the molar concentration per litre.

4.1.4. Results of Tie quantification using both methods

Using the Film/ImageJ method for quantification, the results show that per HUVEC it is estimated to have a total of ~300,000 ($5.22*10^{-7}$ nmol/L) Tie1, and ~700,000 ($1.14*10^{-6}$ nmol/L) Tie2 (Table 4.1).

Using the CCD imager/MultiGauge method for quantification, the results show that per HUVEC it is estimated to have a total of ~75,000 ($1.55*10^{-7}$ nmol/L) Tie1 and ~180,000 ($2.99*10^{-7}$ nmol/L) Tie2 (Table 4.2).

Receptor	**Mean no. of Tie per HUVEC**	**SEM**	**Mean [Tie] per HUVEC** (nmol/L)	**SEM** (nmol/L)	**n**
Tie1	314305	83231	$5.22*10^{-7}$	$1.38*10^{-7}$	4
Tie2	684498	138096	$1.14*10^{-6}$	$2.29*10^{-7}$	4

Table 4.1: Quantification of Tie1 and Tie2 in HUVECs using ImageJ.
The mean number of Tie1 and Tie2 per HUVEC and their standard error of the mean (SEM), and the mean concentration of Tie in a HUVEC and SEM were calculated. There are more Tie1 than Tie2 receptors in HUVECs. These results were taken from 4 experiments of Tie1 quantification and 4 experiments of Tie2 quantification.

Receptor	**Mean no. of Tie per HUVEC**	**SEM**	**Mean [Tie] per HUVEC (**nmol/L)	**SEM (**nmol/L)	**n**
Tie1	74774	44674	$1.55*10^{-7}$	$7.42*10^{-8}$	4
Tie2	179880	12202	$2.99*10^{-7}$	$2.03*10^{-8}$	5

Table 4.2: Quantification of Tie1 and Tie2 in HUVECs using CCD imager.
The mean number of Tie1 and Tie2 per HUVEC and their standard error of the mean (SEM), and the mean concentration of Tie in a HUVEC and SEM were calculated. There are more Tie2 than Tie1 receptors in HUVECs. These results were taken from 4 x Tie1, and 5 x Tie2 experiments.

A comparison of the values from the two methods shows that there is a major difference in quantification, although the ratio of Tie1 and Tie2 is similar. Film based detection has many drawbacks due to the threshold level with low levels of signal and saturation effects with high levels of signal. Film only has a dynamic range of $5x10^2$ (500). Therefore film has a smaller limited linear range over which proteins can be quantified. On the other hand CCD detection has a huge dynamic range of 10^3 -10^5 (1000-100,000) and therefore allows accurate quantification.

4.2. Assessing the Film and CCD imaging methods for accuracy in quantification

To determine the most accurate method for quantification, HUVECs were lysed and three cell lysate samples were spiked with a known concentration of recombinant Tie2 (200 ng/ml). Separate gels were loaded with cell lysate samples and the standard calibration of recombinant Tie2; one for detection by film and another for detection by CCD imager. Proteins were resolved by SDS-PAGE, probed for Tie2 and detected using each method. The region intensities (optical densities) of the protein bands were quantified (Figure 4.3).

The concentrations of Tie2 in the cell lysates per track were obtained from the standard calibration curve using their region intensity. The mean average concentration of spiked cell lysate samples was calculated. The expected concentration of the spiked samples was calculated by adding the region intensity of the concentration of cell lysate (control) to the region intensity of the concentration of Tie2 (200 ng/ml) used to spike the samples (Table 4.3). The percentage difference between the average sample value and expected value was calculated as the percentage error.

A

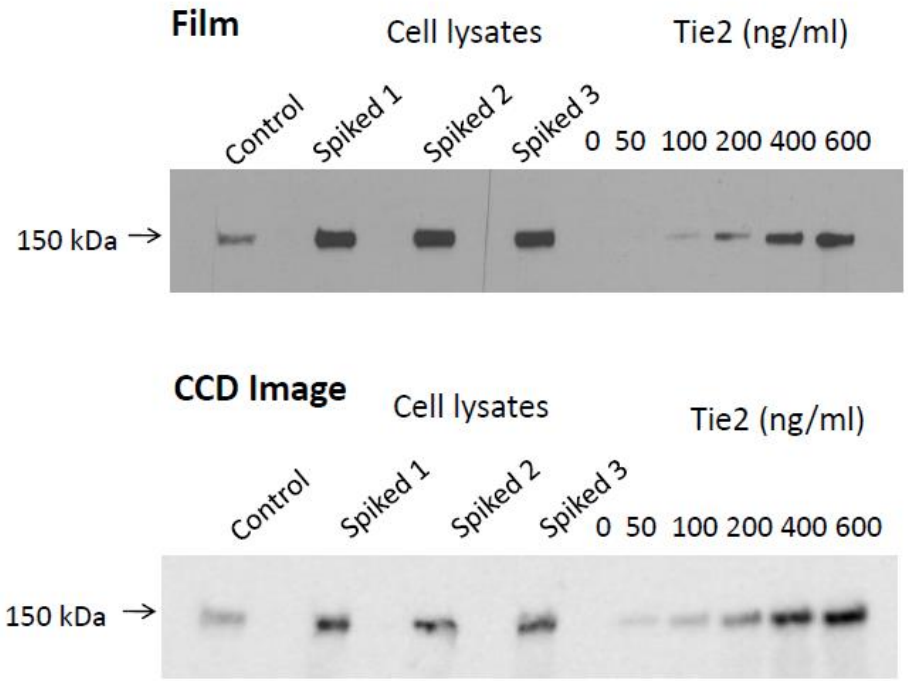
Film
Cell lysates
Tie2 (ng/ml)
Control
Spiked 1
Spiked 2
Spiked 3
0 50 100 200 400 600
150 kDa
CCD Image
Cell lysates
Tie2 (ng/ml)
Control
Spiked 1
Spiked 2
Spiked 3
0 50 100 200 400 600
150 kDa

B

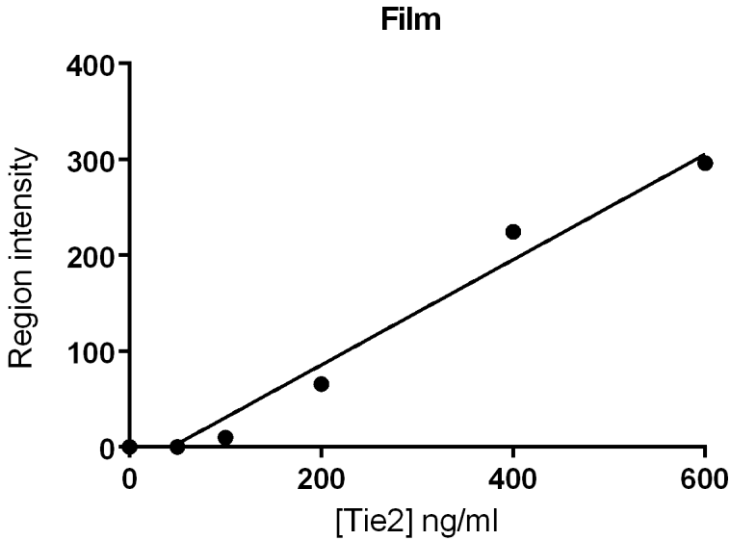
Film
Region intensity
400
300
200
100
0
0
200
400
600
[Tie2] ng/ml

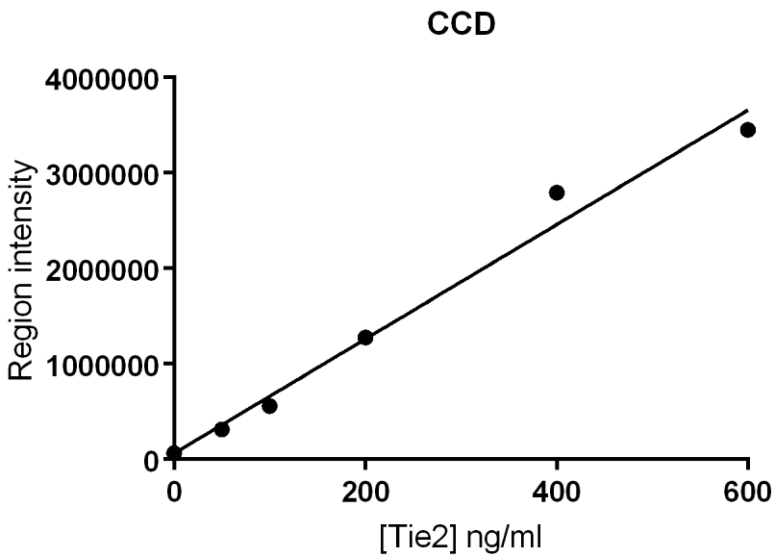

Figure 4.3: Assessing film and CCD imaging methods for accuracy in quantification
A. HUVECs were lysed (cell lysates 1-4) and 3 lysate samples were spiked with 200 ng/ml Tie2. All cell lysate samples and a standard calibration of recombinant Tie2 (0 - 600 ng/ml) were resolved by SDS-PAGE. Tie antibodies were used to detect Tie2 protein. Bands for Tie2 (~150kDa) were quantified by densitometry; ImageJ software for Film and MultiGauge software for CCD images.
B. Densitometry using Film and ImageJ software, or CCD imaging with MultiGauge software was performed to quantify the optical densities of bands for Tie2 in the samples of recombinant Tie2 (of known concentrations) and the cell lysates. This graph shows a standard calibration of the recombinant Tie2 against the optical density. The concentrations of Tie2 in the cell lysates per track were obtained from the graph using their optical density. These results are representative of 1 experiment.

ImageJ

Sample	OD	Tie2 ng/ml
Cell lysate 1	85.19	199.25
200 ng/ml Tie2	65.56	163.47
Spiked cell lysate 2	406.08	784.17
Spiked cell lysate 3	402.54	777.71
Spiked cell lysate 4	369.47	717.44
Average of spiked cell lysates		759.78
Expected spiked concentration		362.72
Standard error of the mean (SEM)		21.25
Percentage difference (error)		109.47

CCD imager

Sample	OD	Tie2 ng/ml
Cell lysate 1	966073	151.11
200 ng/ml Tie2	1276418	202.91
Spiked cell lysate 2	2126975	344.88
Spiked cell lysate 3	1905687	307.94
Spiked cell lysate 4	2178456	353.47
Average of spiked cell lysates		335.43
Expected spiked concentration		354.02
Standard error of the mean (SEM)		13.97
Percentage difference (Error)		-5.25%

Table 4.3: Assessing film and CCD imaging methods for accuracy in quantification. Quantification of Tie2 samples was performed using film detection with ImageJ densitometry, and CCD imaging detection with MultiGauge densitometry. The concentrations of Tie2 in the cell lysates per track were obtained from the graph using their optical density. The mean average concentration of spiked cell lysate samples was calculated. The expected spiked concentration is the concentration of cell lysate plus the concentration of Tie2 used to spike the samples. The standard error of the mean and the percentage difference between the average sample value and expected value (percentage error) was also calculated. These results are representative of 1 experiment.

Overall, this experiment repeated three times independently showed a consistently higher than expected amount of Tie2 (>200 ng/ml) in the spiked samples when using film, whereas the CCD imager detects spiked cell lysate concentrations of Tie2 that are much closer to the actual expected amount. Quantification using film had an average error of 141% whereas the CCD imager had an average error of 10.8%. Therefore this study

suggests that using the CCD imager for quantification is a more accurate and reliable method than using Film. Future experiments for quantification were conducted using CCD imaging detection and MultiGauge Software for densitometry.

4.3. Cell surface concentrations of Tie1, Tie2 and Tie1:Tie2

Preliminary experiments performed by Dr Tariq Tahir show that 90% of total Tie1 and 50% of total Tie2 is on the cell surface of HUVECs. Using the values of total Tie1 and Tie2 per HUVEC this was calculated to be 0.0224 nM for Tie1 and 0.0299 nM for Tie2. A study by Marron and colleagues estimated that 80% of Tie2 exists in complex with Tie1 (Marron *et al.*, 2000). However as the Tie1 concentration is less than 80% of Tie2 it is assumed that 50% of cell surface Tie2 is also in complex with the cell surface Tie1. The cell surface concentrations for Tie1, Tie2 and Tie1:Tie2 are 0.00745, 0.01495, 0.01495 nM respectively (Table 4.4).

4.4. Internal concentration of Tie2

The remaining Tie2 is 50% (0.0299 nM) which is within the cell. The internal new Tie2 (nTie2) is assumed to be transported to the cell surface during ligand stimulation (Table 4.4). As the internal Tie1 (10%) is a very low concentration the replenishment for Tie1 will not be modelled.

4.5. Dephosphorylation of Tie2

The Vmax of HPTP-β is assumed to be 43 μmol/min/mg (as discussed in Chapter 3.3.3). This was recalculated using the concentration of Tie2 to give the Vmax in $nM.s^{-1}$. $kv_6 = 13030.3\ nM.s^{-1}$ (Table 4.5).

4.6. The rate of phosphorylated Tie2 degradation

The process of internalisation to degradation is a complex step to model, and a difficult parameter to quantify. Thus the model assumes that degradation occurs to decrease the internal phosphorylated Tie2 along with dephosphorylation, and thereby down regulating Tie2 activation. However it is assumed to be a slow process, 10 fold slower than internalisation and replenishment, $k_8 = 0.000684\ s^{-1}$ (Table 4.5).

4.7. The rate of Tie1:Tie2 heterodimerisation and dissociation

As the rate of Tie1:Tie2 association and dissociation are difficult to quantify experimentally it is assumed that the dissociation rate is the same as Tie2:Tie2 dissociation ($0.1\ s^{-1}$). To determine the parameter for Tie1 and Tie2 association, the equilibrium of Tie1, Tie2 and Tie1:Tie2 needs to be balanced at initial conditions. Hence the concentrations of the states (scaled to account for the smaller volume of the extracellular space) and dissociation parameter can be substituted into the equation [4.6].

at initial conditions, time = 0

$$K_{14}\,[Tie1].[Tie2] = K_{-14}\,[Tie1{:}Tie2]$$

$$K_{14} = \frac{K_{-14}\,[Tie1{:}Tie2]}{([Tie1] * 2.8x10^{6}) * ([Tie2] * 2.8x10^{6})}$$

[4.6]

The parameter for Tie1:Tie2 heterodimerisation is $1.71x10^{-12}$ $nM^{-1}s^{-1}$ (Table 4.5).

4.8. Quantified parameter values and state concentrations

The quantified state concentrations and calculated parameter values summarised in tables 4.4 and 4.5 were input in to the scripts to prepare the model simulation.

State	Concentration (nM)
Tie1	0.00745
Tie2	0.01495
Tie1:Tie2	0.01495
nTie2	0.0299

Table 4.4: Quantified state concentrations.
The initial concentrations for the variable states were quantified and calculated to give the concentrations of Tie1, Tie2 and Tie1:Tie2 on the cell surface and the concentration of Tie2 within the cell, nTie2.

Reaction	Parameter	Value	Reference
pTie2 dephosphorylation	kv_6	13030.3 $nM.s^{-1}$	Calculated (Cho *et al.*, 1993)
pTie2 degradation	k_8	0.000684 s^{-1}	Estimated from average internalisation value
Tie1:Tie2	k_{14}	$1.71x10^{-12}$ $nM^{-1}s^{-1}$	Calculated from equation [4.6]
	k_{-14}	0.1 s^{-1}	(Kholodenko *et al.*, 1999)

Table 4.5: Calculated parameter values.
The parameter values for phosphorylated Tie2 dephosphorylation and degradation, Tie1 and Tie2 heterodimerisation and Tie1:Tie2 dissociation were calculated.

4.9. Discussion

This chapter presents the quantified parameters; rate constants and state concentrations at initial conditions which are required to complete the model.

The concentration of Tie1 and Tie2 in HUVECs was quantified as accurately as possible using Western blotting and a CCD camera to digitally image the blots and facilitate quantification of region intensities using the MultiGauge quantification software.

From these values and using data provided by Dr Tariq Tahir, the cell surface concentrations of Tie1, Tie2, Tie1:Tie2 and nTie2 were also derived.

The rate constants for degradation of phosphorylated Tie2 and for Tie1:Tie2 heterodimerisation were also determined. However as these values were not directly quantified in HUVECs it is possible to change and re-define the parameters in future simulations to fit the simulation results to experimental data.

In conclusion all the parameters have been quantified and the model is ready to be simulated and validated.

Chapter 5: Model simulations and validation without dephosphorylation

In order to validate the model, *in silico* simulation results need to be compared to experimental results. This model uses the activation of Tie2 as an indicator for the levels of Tie2 signalling thus the levels of Tie2 activation in experiments needs to be measured. Activation of Tie2 signalling can be determined by measuring Y^{992} or Y^{1108} Tie2 phosphorylation, which correlates with receptor activity. Autophosphorylation of the receptor begins with phosphorylation of Y^{992} on the activation loop followed by the phosphorylation of Y^{1108} on the C-terminal tail (Murray *et al.*, 2001).

In preliminary experiments it was difficult to measure the levels of Tie2 phosphorylation stimulated by low levels of Ang1 in the presence of full phosphatase activity. Sodium orthovanadate (vanadate) is a phosphatase inhibitor which has been used as a pre-treatment in many Tie2 studies to reduce phosphatase activity (Kontos *et al.*, 1998; Teichert-Kuliszewska *et al.*, 2001; Jones *et al.*, 2003; Tsai & Lee, 2009; Yacyshyn *et al.*, 2009). Therefore in the following experiments a pre-treatment with vanadate was used for the preservation of phosphorylation and to facilitate the detection of Tie2 phosphorylation in cells stimulated with Ang1. To account for the inhibition of phosphatase activity in the model, the dephosphorylation reaction was removed, and all parts of the model were validated except the dephosphorylation reaction.

Two commonly used procedures to measure phosphorylation are Western blotting and immunofluorescence. The advantages of Western blotting are that the proteins in the cell lysate are resolved and the specific protein can be quantified at its respective mass (kDa).

However the results produce limited information as it cannot be used for individual cells, only the population of cells. Alternatively, fluorescence microscopy can monitor thousands of single cells and therefore generate results of the variation in individual cells, although a specific high quality antibody is needed to discriminate between specific and non-specific protein and produce accurate results. Both techniques allow multiple measuring of state parameters e.g. activated and total receptor.

Preliminary experiments were performed to test whether these techniques can be used to quantify receptor activation for model validation.

5.1. Immunofluorescence detection of Ang1 induced Tie2 activation

Immunofluorescence was performed to quantify the concentration-dependent effect of Ang1 on the levels and localisation of activated Y^{992} Tie2 (phosphorylated Tie2).

HUVECs were grown to 50% confluency on coverslips, serum starved for 4 hours and treated with Ang1 (200 ng/ml) for 30 minutes before fixing, permeablizing with 90% methanol and 0.5% SDS for antigen retrieval, then blocking and staining as described in Chapter 2.3. An antibody for phosphorylated Tie2 (R&D Systems) was used to label the phosphorylated Y^{992} of Tie2. This was detected using the Cy3 fluorochrome and the nuclei were counter-stained with DAPI. Immunofluorescence microscopy was used to visualise and localise phosphorylated Tie2 in HUVECs (Figure 5.1).

The images show an increased fluorescence in Ang1 treated samples, representative of three experiments. The cells are defined and staining is mainly found around the cell membrane with low staining in the nucleus. Attempts to quantify the levels of fluorescence for each cell did not differentiate between phospho-immunofluorescence signal and non-specific signals as the Scan^{R} analysis quantification software provided by Advanced Imaging Facility could not detect the membrane of single cells, and therefore quantify membrane only fluorescence. Despite a number of attempts and due to poor quantification results, immunofluorescence could not be used for further experiments and immunoblotting was used instead.

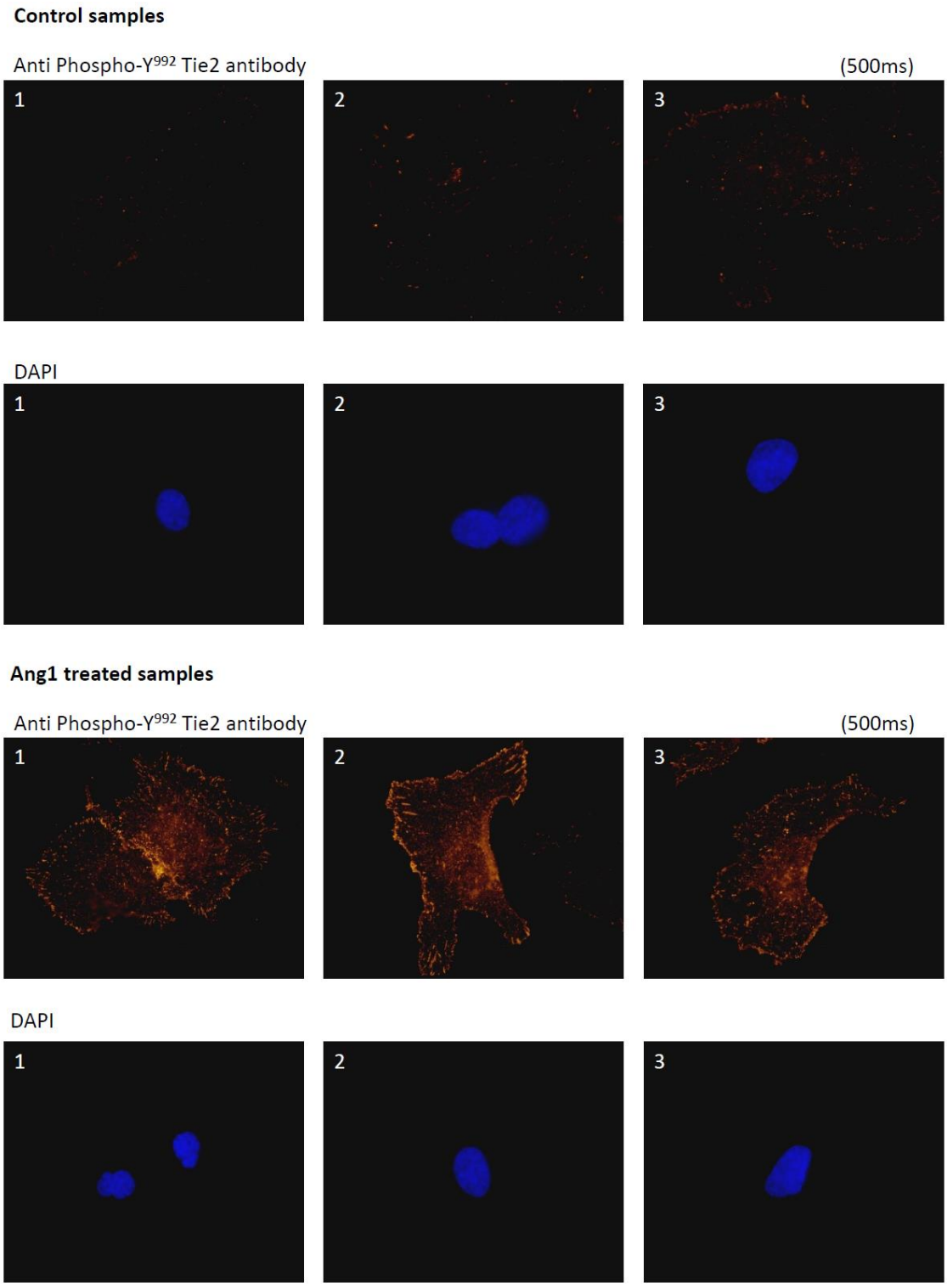

Figure 5.1: Immunofluorescence detection of phospho-Y^{992} Tie2.
HUVECs were serum starved and treated with Ang1. The control and Ang1-treated samples were stained with phospho-Y^{992} Tie2 primary antibody and Cy3 secondary antibody (red fluorescence). All samples were counterstained with DAPI (blue fluorescence). Immunofluorecence was detected using an inverted fluorescence microscope. Results are representative of 3 experiments (100x magnification).

5.2. Immunoblotting of Ang1-induced Tie2 activation

To test whether blotting could be used to quantify Tie2 activation, HUVECs were grown to 50% confluency, serum-starved for one hour and treated with vanadate, followed by the different concentrations of Ang1 for 15 minutes. The samples were prepared (as described in Chapter 2 4.1.2), resolved by SDS-PAGE and blotted. The blots were probed with anti-phospho-Tie2 pY^{992} (figure 5.2A). To quantitatively analyse this blot, the intensities of phospho-Tie2 protein were quantified using a CCD imager and MultiGauge software. The blots were reprobed for Tie2 and also quantified to normalise the results for phosphorylation against Tie2. The results show that Ang1 induced a concentration dependent increase in Tie2 phosphorylation indicated by the increasing intensity of the 145 kDa band of phospho-Tie2 as shown in figure 5.2.

The percentages of maximal phosphorylation calculated using the optical densities of the bands for phospho-Tie2 were plotted against their relative concentrations of Ang1 treatment (Figure 5.2B). The graph in figure 5.2B shows that Ang1 induces an increase in phospho-Tie2 which can be quantified. Hence immunoblotting proved to be an effective method to quantify phosphorylation.

A

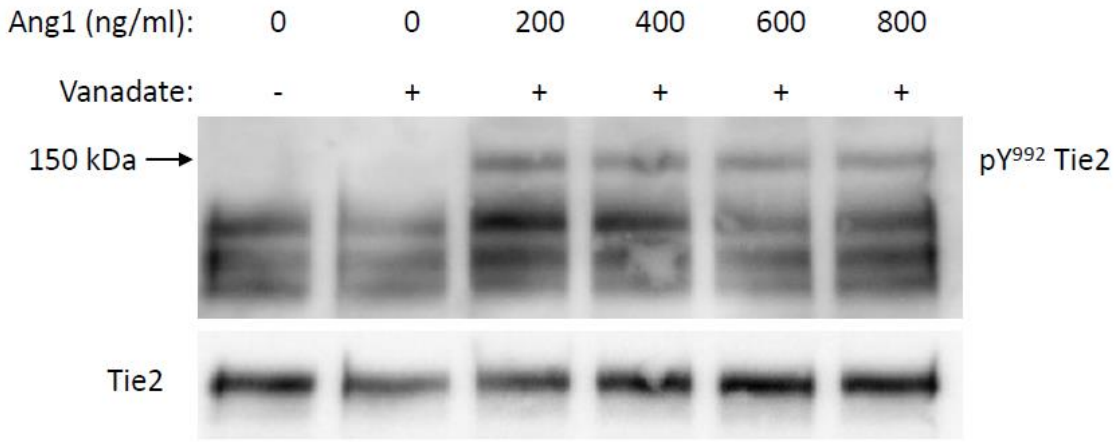

B

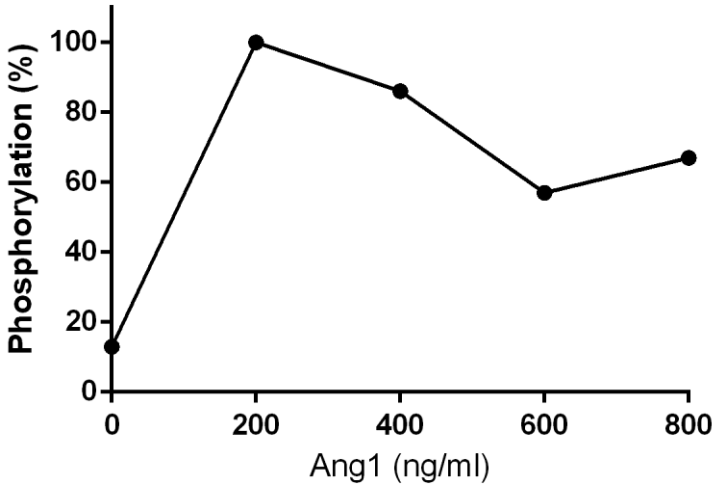

Figure 5.2: Phosphorylation of Y^{992} Tie2 in HUVECs treated with Ang1.
A. Western blotting was used to resolve and identify phospho-Tie2 in HUVECs treated with various concentrations of Ang1. The blots shows that Ang1 induces an increase in phosphorylated Tie2. The blot was reprobed for Tie2 to normalize the results.
B. Phospho-Tie2 protein from the blot was quantified using MultiGauge. The percentage of maximal phosphorylation of Tie2 was calculated and plotted against the respective concentration.

5.3. Conjugation of pY^{992} protein

To quantify the absolute amount of phosphorylated Tie2 in HUVECs, a standard calibration of phospho-Tie2 will be required. The phosphorylation of the Y^{992} tyrosine on Tie2 is the activating tyrosine therefore it will be used to determine the amount of phosphorylated (activated) receptor. Currently no Tie2-pY^{992} protein is available hence a standard protein of pY^{992}, the primary phosphorylated Tyrosine of Tie2 needs to be synthesized (Chapter 2, 5).

The pY^{992} containing peptide for Tie2 is:

GQEVY*VKKTMG Y* = Phosphorylated tyrosine Molecular mass = 1319.438

This peptide sequence for pY^{992} was synthesized and the primary amine (lysine) of pY^{992}-Tie2 was conjugated to the single available sulphydryl (cysteine-34) of bovine serum albumin (BSA) to make it easier to resolve and allow the peptide to bind to the nitrocellulose membrane. The BMPS (N-beta-maleimidopropyl-oxysuccinimide ester) cross-linking reagent which is a non-cleavable short amine-to-sulphydryl cross-linker was used to bind BSA to the synthesized peptide.

Different amounts of the constructed protein were resolved using SDS-PAGE to determine whether the protein has been successfully conjugated to BSA and is present at the correct protein mass. The blots were probed with anti-pY^{992} Tie2 (Figure 5.3).

Figure 5.3 shows that protein is present predominantly at ~69 kDa. The presence of higher bands suggests that the protein may be conjugated to more than one BSA. However mass spectrometry was unable to measure relative amounts of peptide conjugated to BSA and

unconjugated BSA. After using the protein in a series of experiments it was observed that the stability of the conjugated protein was poor. Thus the conjugated pY^{992} Tie2 was not used in future experiments as a standard for calibration, and instead the relative activation was measured.

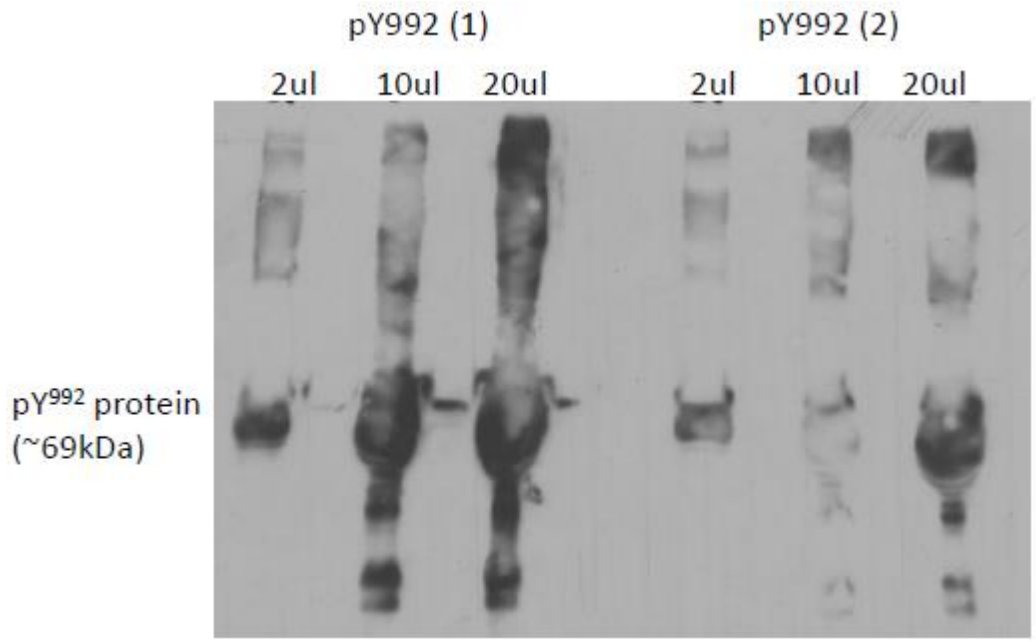

Figure 5.3: Blot of conjugated pY^{992}-Tie2-BSA.
The pY^{992}-Tie2 peptide sequence was synthesized and conjugated to bovine serum albumin using the BMPS crosslinker. Different amounts of the protein were resolved using SDS-PAGE and probed for the new protein. The blot shows that there are concentrated bands present at 69 kDa which corresponds to the conjugated protein. Higher bands suggest that the protein has been conjugated to more than one BSA.

5.4. The effect of vanadate over time

In preliminary experiments to examine Tie2 phosphorylation using Ang1 (below 50 ng/ml) it was difficult to quantify the low levels of phosphorylation. Thus to stop the dephosphorylation of Tie2, vanadate, a phosphatase inhibitor was used to preserve phosphorylation in samples. Conversely it may also induce phosphorylation. To determine whether vanadate has an effect on phosphorylation, an experiment was performed to monitor the effect of vanadate on Y^{992}-Tie2 phosphorylation and the basal activity of phosphatases.

HUVECs were prepared as previously described (Chapter 2.4). Cells were treated with and without vanadate, and without Ang1 stimulation over a time-course. The cells were lysed for each time-point and protein samples were resolved using SDS-PAGE and probed for phospho-Tie2 (Y^{992}). Chemiluminescence was detected using a CCD imager (Figure 5.4A).

The results in figure 5.4 show that in the cells treated with vanadate there is an increase of phosphorylation which is evident at 60 minutes. Whereas cells not treated with vanadate maintain a very low basal level of phosphorylation.

As vanadate has no noticeable effect on phosphorylation in cells stimulated for 30 minutes, all future experiments treated with vanadate were not stimulated for longer than 30 minutes.

However as vanadate inhibits phosphatases the dephosphorylation step must be removed from the model to recreate this effect.

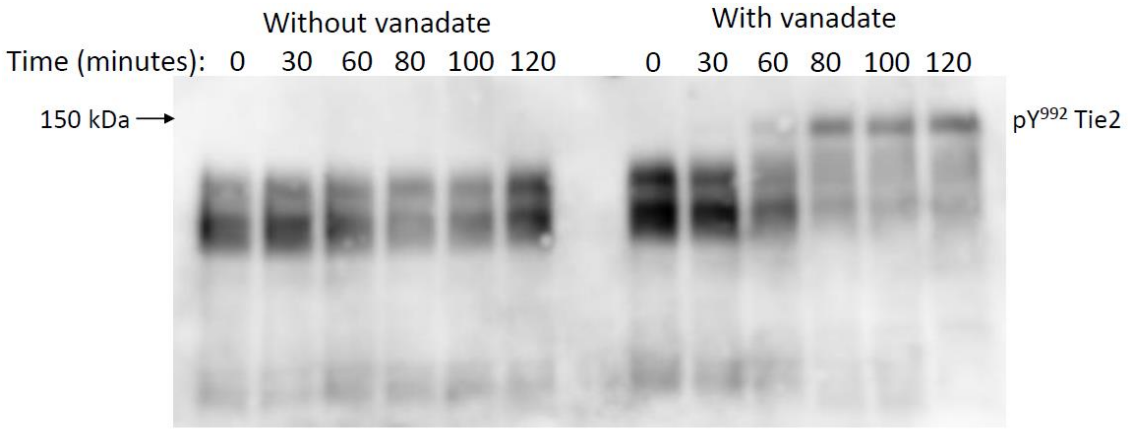

Figure 5.4: Time-course of the effect of vanadate.
Cells were serum-starved and treated with vanadate for different time-points; 0, 30, 60, 80, 100 and 120 minutes. The protein was resolved using SDS-PAGE and probed for phosphorylated Y^{992} Tie2. Chemiluminescence was detected using a CCD imager. The blot shows that in the cells treated with vanadate there is a steady increase of phosphorylation over 120 minutes, whereas cells not treated with vanadate have very low phosphorylation.

Validation of model

5.5. Steady-state analysis

A steady state simulation was performed to determine whether the model is in equilibrium without any angiopoietin stimulation. Any errors in the reactions, initial state concentrations or parameter values will be identified if the model is found not to be in equilibrium. The model was simulated for 5 hours (ten times the length of the usual simulation) without adding initial concentrations of Ang1, Ang2, soluble Tie2 (sTie2) and new Tie2 (nTie2), which is only used to replace Tie2 during Ang1 or Ang2 induced simulations. The simulation plots in Figure 5.5 show that Tie1, Tie2 and Tie1:Tie2 remain at the steady initial concentration throughout the simulation. The other states in the model remained at zero as there was no ligand present in the system to induce the formations of those states. The analysis suggests that the model is in equilibrium.

A

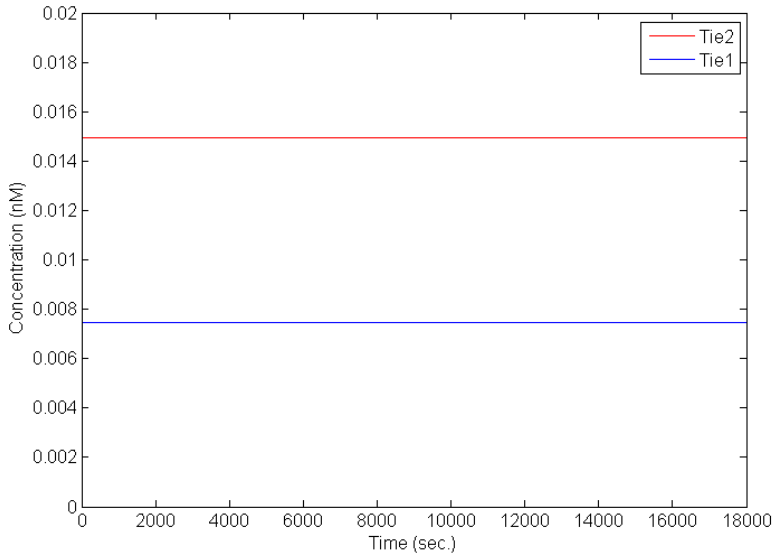

B

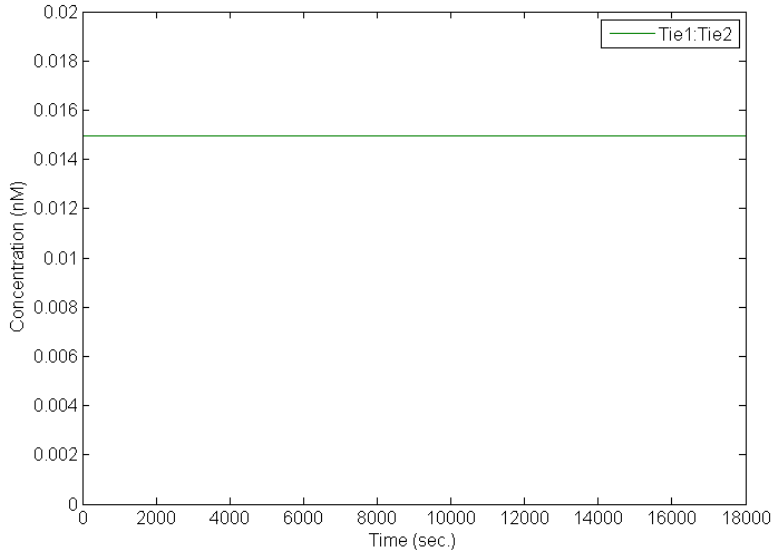

Figure 5.5: Simulation plots at steady-state.
Simulation of the model was performed for 18000 seconds (5 hours) without the addition of Ang1 or new Tie2 (nTie2).
Plot A, shows the concentrations of Tie1 and Tie2 over time.
Plot B, shows the concentration of Tie1:Tie2 over time.

5.6. The effect of Ang1 on Tie1, Tie2 and Tie1:Tie2 equilibrium.

A simulation was performed to examine how the equilibrium between Tie1, Tie2 and Tie1:Tie2 is affected by adding Ang1 and the Tie2 replenishment reaction to the model. The model was simulated for 30 minutes with 50 ng/ml (0.179 nM) Ang1, and the initial concentration of new Tie2. The simulation plots in Figure 5.6 show that Ang1 induces dissociation of the Tie1:Tie2 complex, increases the amount of free Tie1 and decreases the amount of free Tie2. Adding the Tie2 replenishment reaction to the model shows that the concentration of nTie2 gradually decreases over time however the concentration of free Tie2 is not replenished to the initial concentration. This analysis suggests that on the addition of Ang1 the equilibrium between Tie1, Tie2 and Tie1:Tie2 shifts to favour free Tie1 and Tie2 by dissociating the Tie1:Tie2 heterodimer.

A

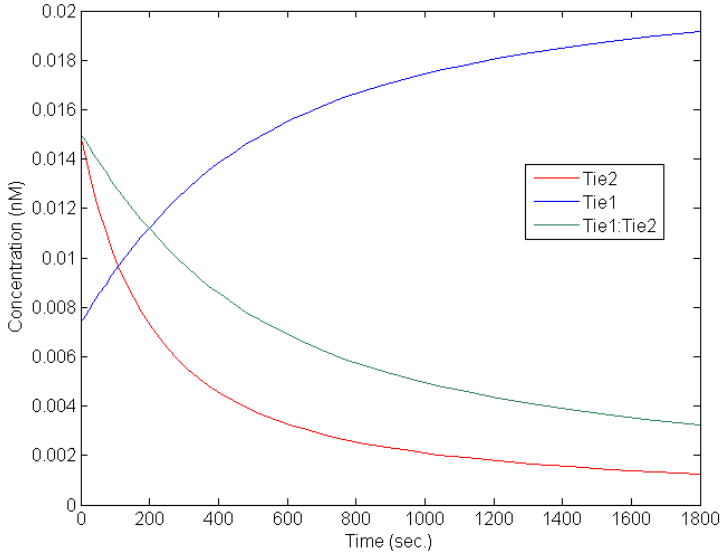

B

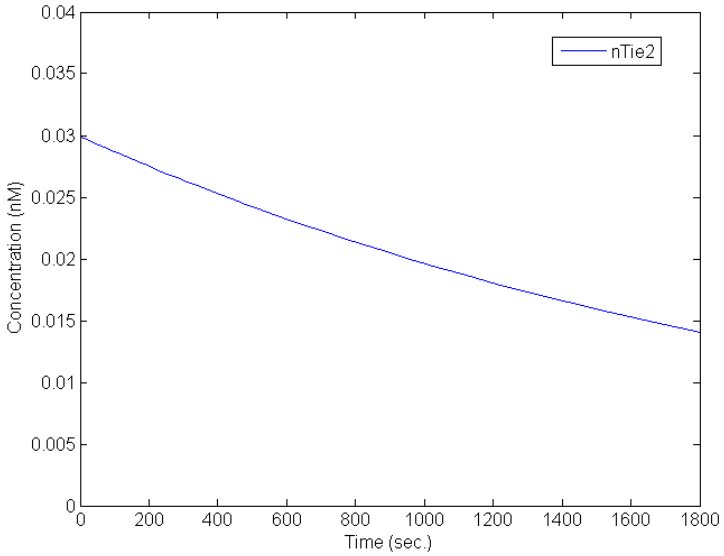

Figure 5.6: Simulation plots of the Ang1-induced effect on the Tie1, Tie2, Tie1:Tie2 equilibrium.

Simulation of the model was performed for 1800 seconds (30 minutes) with the addition of 0.179 nM (50 ng/ml) Ang1 and 0.299 nM new Tie2 (nTie2).

Plot A, shows the concentrations of Tie1 (blue), Tie2 (red) and Tie1:Tie2 (green) over time. The concentrations of Tie1:Tie2 complex and Tie2 decreases while Tie1 increases.

Plot B, shows that the concentration of nTie2 gradually decreases over time.

5.7. The effect of Ang2 on Tie1, Tie2 and Tie1:Tie2 equilibrium.

A simulation was performed to examine how the equilibrium between Tie1, Tie2 and Tie1:Tie2 is affected by adding Ang2 and the Tie2 replenishment reaction to the model. The model was simulated for 30 minutes with 200 ng/ml Ang2, and the initial concentration of new Tie2.

The simulation plots in Figure 5.7 show that similar to Ang1, Ang2 induces dissociation of the Tie1:Tie2 complex, increases the amount of free Tie1 and decreases the amount of free Tie2. Adding the Tie2 replenishment reaction to the model shows that the concentration of nTie2 gradually decreases over time however the concentration of free Tie2 is not replenished to the initial concentration. The concentrations of Ang2 binding to Tie1:Tie2 rapidly increases during the initial 100 seconds of simulation then gradually decreases; furthermore the concentrations of complex formed are low.

This analysis suggests that on the addition of Ang2 the equilibrium between Tie1, Tie2 and Tie1:Tie2 shifts to favour free Tie1 and Tie2 by dissociating the Tie1:Tie2 heterodimer.

A

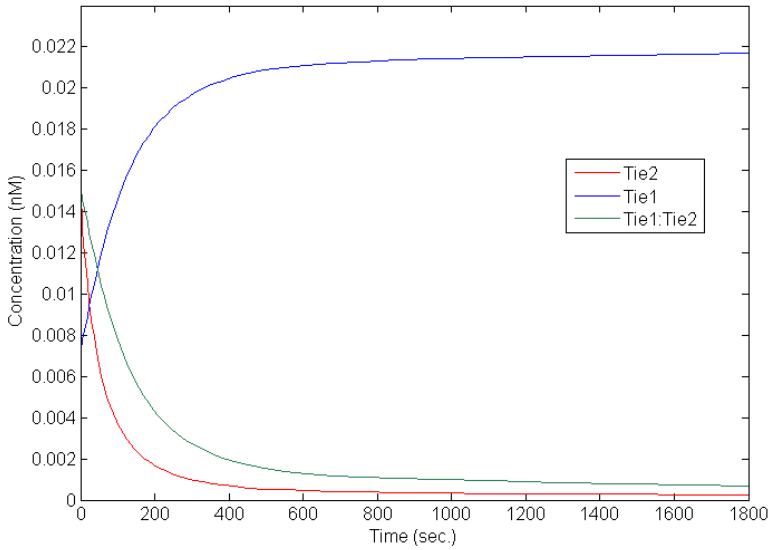
Concentration (nM)
Time (sec.)
Tie2
Tie1
Tie1:Tie2
0
0.002
0.004
0.006
0.008
0.01
0.012
0.014
0.016
0.018
0.02
0.022
0
200
400
600
800
1000
1200
1400
1600
1800

B

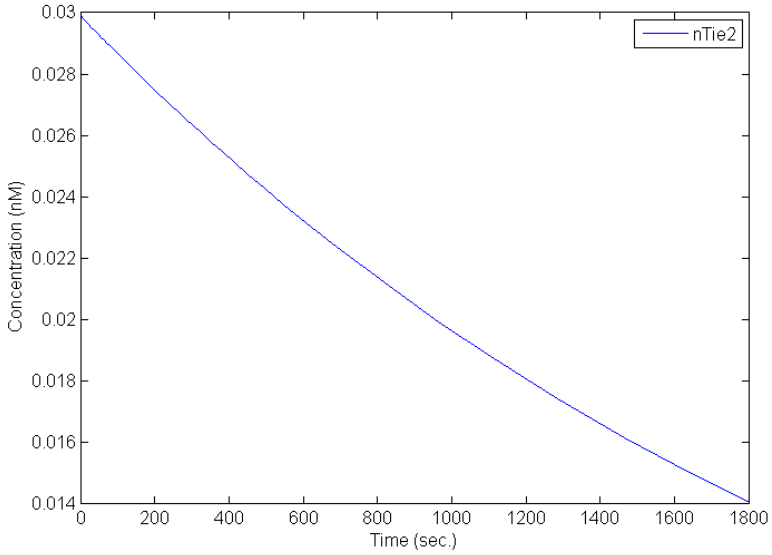
Concentration (nM)
Time (sec.)
nTie2
0.014
0.016
0.018
0.02
0.022
0.024
0.026
0.028
0.03
0
200
400
600
800
1000
1200
1400
1600
1800

C

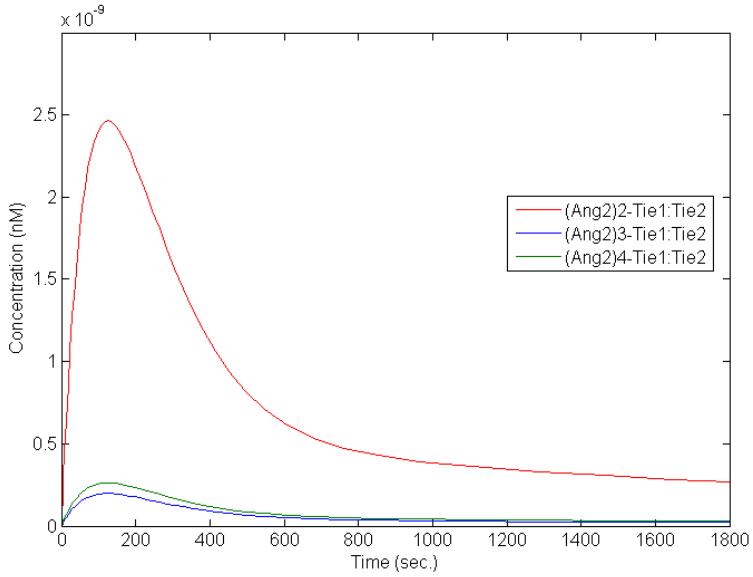

Figure 5.7: Simulation plots of the Ang2-induced effect on the Tie1, Tie2, Tie1:Tie2 equilibrium.

Simulation of the model was performed for 1800 seconds (30 minutes) with the addition of 200 ng/ml Ang2 and 0.299 nM new Tie2 (nTie2).

Plot A, shows the concentrations of Tie1 (blue), Tie2 (red) and Tie1:Tie2 (green) over time. The concentrations of Tie1:Tie2 complex and Tie2 decreases while Tie1 increases.

Plot B, shows that the concentration of nTie2 gradually decreases over time.

Plot C, shows that the concentration of Ang2 (dimeric in red, trimeric in blue and tetrameric in green) bound to Tie1:Tie2. There is a rapid increase in concentration during the initial 100 seconds followed by a gradual decrease over time.

5.8. Validating the effects of Ang1 on Tie2 activation (without dephosphorylation).

In order to validate the model, *in-silico* simulations need to be compared to *in-vitro* experiments. The ways used to validate the model are to compare; 1) the rate of receptor activation for each ligand, and 2) the effect of increasing ligand concentration on receptor activation.

5.8.1. Time-course of Tie2 activation with low Ang1.

5.8.1.1. Simulations

Simulations of the full model were performed by including 50 ng/ml (0.179 nM) of Ang1 and running the model to simulate 1800 seconds (30 minutes) stimulation with Ang1 (Appendix 2). The simulation plot (Figure 5.8A) shows how the concentration of phosphorylated Tie2 changes over time. The different states of phosphorylated Tie2 are shown as; cell surface phosphorylated Tie2 (Ang1-pTie2 in red), internalised phosphorylated Tie2 (i-pTie2 in blue) and degraded phosphorylated Tie2 (d-pTie2 in green).

The model suggests that activated Tie2 on the cell surface peaks at 200 seconds. The amount of phosphorylated Tie2 on the cell surface decreases as the majority of activated Tie2 is internalised into the cell, and is then gradually degraded at a constant rate.

The total amount of phosphorylated Tie2 (cell surface and internalised) at each time-point was calculated as a percentage of maximal phosphorylation. The rate of percentage

change in phosphorylation is shown over time in minutes (Figure 5.8B). Simulation of the model suggests that maximum phosphorylation is reached at 15 minutes with 50 ng/ml Ang1 stimulation.

A

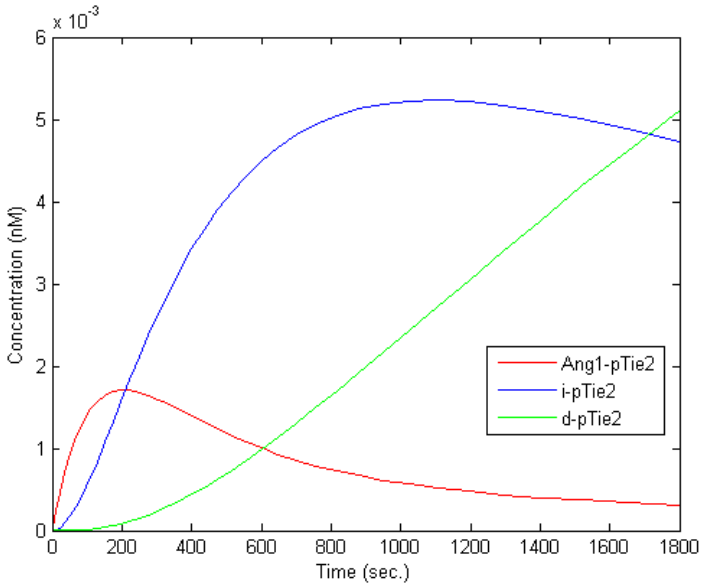

B

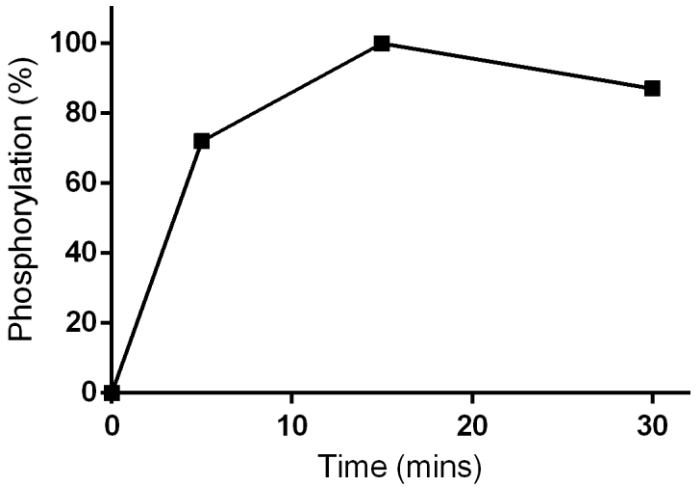

Figure 5.8: Simulation- Time-course for low concentration Ang1-induced Tie2 phosphorylation (excluding the dephosphorylation reaction).
A. The model was simulated with 50 ng/ml Ang1 for 1800 seconds. The plot shows the change in concentrations of cell surface phosphorylated Tie2 (Ang1-pTie2 in red), internalised phosphorylated Tie2 (i-pTie2 in blue) and degraded phosphorylated Tie2 (d-pTie2 in green). The level of Tie2 phosphorylation on the cell surface peaks after 200 seconds stimulation. Most of the phosphorylated Tie2 is internalised into the cell and gradually degraded.
B. Total phosphorylated Tie2 was calculated by adding cell surface pTie2 to internalised pTie. The percentage of maximal phosphorylation was plotted against the time-point in minutes. Maximum phosphorylation of Tie2 is reached at 15 minutes of stimulation.

5.8.1.2. Experiments

Experiments were performed to determine the time-course for Tie2 phosphorylation and the best time-point for stimulation experiments with a low concentration of Ang1.

HUVECs were grown on a 6-well plate to a density of $2x10^5$ cells per well (6 samples). A 30 minute time-course was performed at four different time points; 0, 5, 15 and 30 minutes. Cells were serum-starved for one hour and treated with vanadate (10 mM) for 5 minutes, before stimulation with a low concentration of Ang1 (50 ng/ml). After Ang1 stimulation for each time-point the cells were lysed. Proteins were resolved using SDS-PAGE and probed for phospho-Y^{992} Tie2. Chemiluminescence was detected using a CCD imager (Fujifilm LAS-4000) (Figure 5.9A) and the relevant bands on the image were quantified using the MultiGauge software. The results were normalised to total Tie2 by stripping and reprobing the blots for Tie2.

To monitor how the percentage phosphorylation changes over time, the percentage phosphorylation for each time point was calculated and plotted. The time course plot (Figure 5.9B) shows that cells have 40% basal phosphorylation which rapidly increases after stimulation with Ang1. Maximal phosphorylation occurs at 15 minutes and decreases slowly afterwards. This decrease in phosphorylation may be due to dephosphorylation which was not suppressed by vanadate or the degradation of phosphorylated Tie2.

A

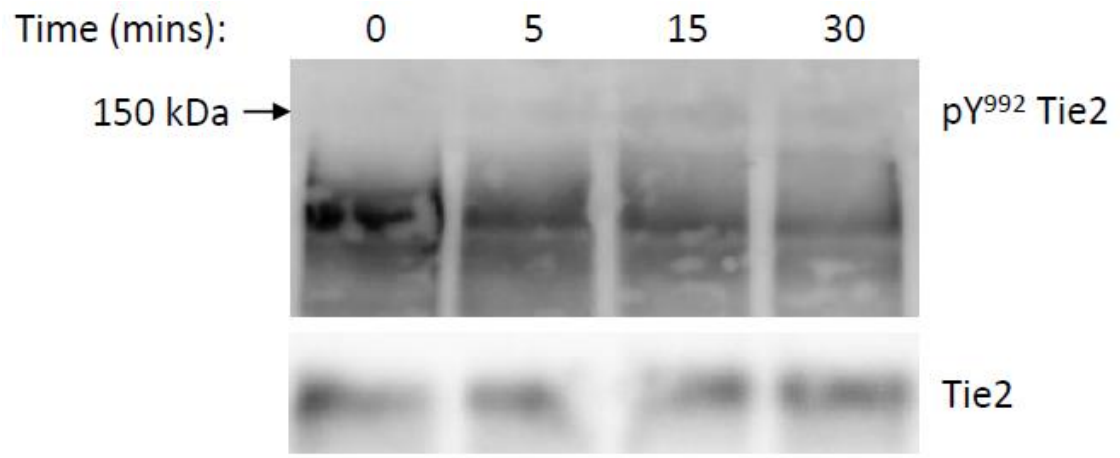

B

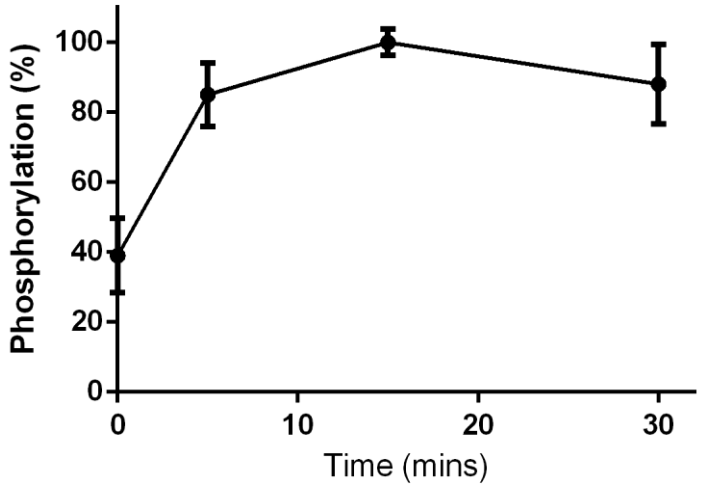

Figure 5.9: Experiment- Time-course for low concentration Ang1-induced Tie2 phosphorylation (with vanadate).

A. Cells were serum-starved, treated with vanadate and the stimulated with 50 ng/ml Ang1 for different time-points; 0, 5, 15 and 30 minutes. The protein was resolved using SDS-PAGE and probed for phosphorylated Y992 Tie2. Chemiluminescence was detected using a CCD imager. The blot shows a steady increase of phosphorylation until 15 minutes then decreases. The blot was reprobed for Tie2 to normalize results.

B. The percentage phosphorylation of Y^{992}-Tie2 was calculated and plotted against the relevant time-point. The plot shows the change of percentage phosphorylation over one hour stimulation with Ang1. There is 40% basal phosphorylation and maximum phosphorylation at 15 minutes, after which the level of phosphorylation decreases. Phosphorylation is normalized to Tie2 and is shown as a percentage of maximal phosphorylation. Data is presented as mean and SEM of relative maximal phosphorylation (n=4). All data is significant to control (p<0.05), One-way ANOVA.

5.8.1.3. Comparison of simulation and experimental time-courses for low Ang1-induced Tie2 phosphorylation (without dephosphorylation).

The total percentage phosphorylation from the normalised experimental data was compared to the simulation data and a graph was plotted of the percentage change in Tie2 phosphorylation over time for both sets of data. Figure 5.10 shows that the simulation data closely resembles the experimental data and maximum phosphorylation in both the experiment and simulation occurs after 15 minutes of stimulation. This suggests that the model is identical to the experiments for the 30 minute time-course of stimulation with a low concentration of Ang1.

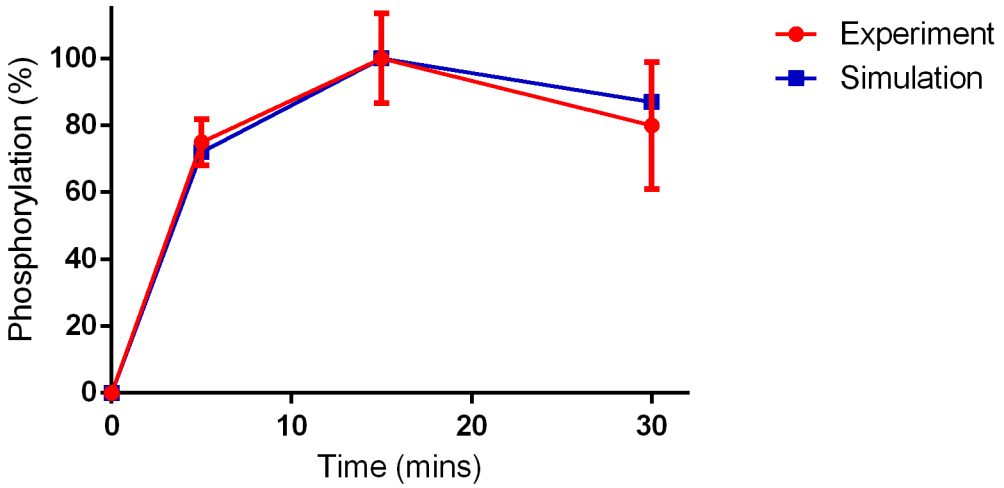

Figure 5.10: Comparison- Time-course for low concentration Ang1-induced Tie2 phosphorylation.
Experimental and simulation data of the time-course for low Ang1 (50 ng/ml) induced Tie2 phosphorylation were compared. The percentages of phosphorylated Tie2 in both the experimental and simulation data are very similar, and both peak at 15 minutes. Experimental data is presented as mean and SEM of relative maximal phosphorylation (n=4). The comparison of experiment to simulation is not significant (p<0.05), Two-way ANOVA.

5.8.2. Time-course of Tie2 activation with high Ang1.

5.8.2.1. Simulations

Simulations of the full model were performed by including 200 ng/ml of Ang1 (0.714 nM) and running the model to simulate 30 minutes (1800 seconds) stimulation with Ang1.

Figure 5.11A shows how the concentration of total phosphorylated Tie2 changes over time. The model suggests that activated Tie2 on the cell surface peaks at 100 seconds, and similar to the previous simulation of low Ang1, the majority of activated Tie2 is internalised and gradually degraded at a constant rate. The amount of phosphorylated Tie2 induced by 200 ng/ml Ang1 stimulation is higher than for 50 ng/ml Ang1 stimulation.

The total amount of phosphorylated Tie2 (cell surface and internalised) at each time-point was calculated as a percentage of maximal phosphorylation. The rate of percentage change in phosphorylation is shown over time in minutes (Figure 5.11B). Simulation of the model suggests that maximum phosphorylation is reached at 5 minutes with 200 ng/ml Ang1 stimulation.

A

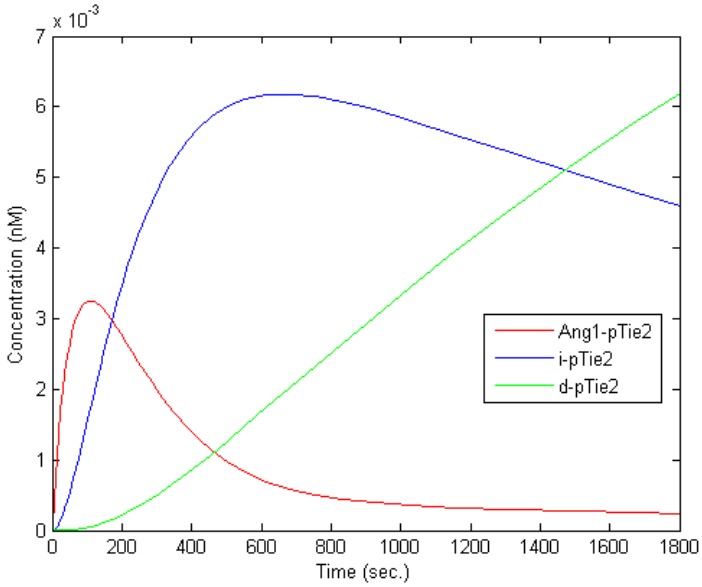

B

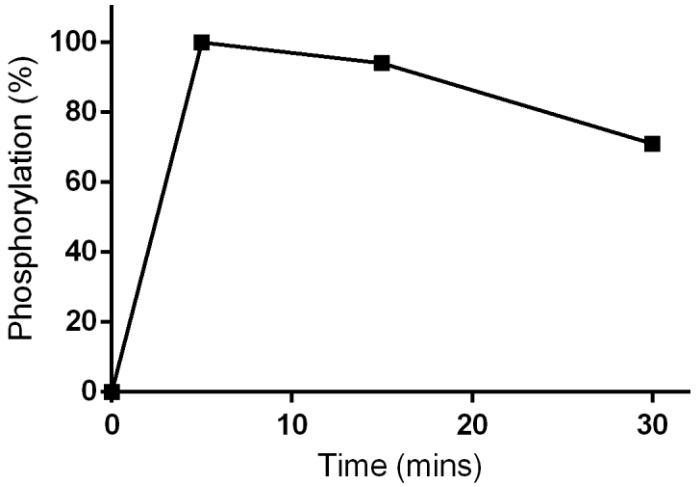

Figure 5.11: Simulation- Time-course for high concentration Ang1-induced Tie2 phosphorylation (excluding the dephosphorylation reaction).
A. The model was simulated with 200 ng/ml Ang1 for 1800 seconds. The time-course plot shows the change in concentrations of phosphorylated Tie2 (Ang1-pTie2), internalised phosphorylated Tie2 (i-pTie2) and degraded phosphorylated Tie2 (d-pTie2). The level of Tie2 phosphorylation on the cell surface peaks after 100 seconds stimulation. Most of the phosphorylated Tie2 is internalised into the cell and gradually degraded.
B. Total phosphorylated Tie2 (cell surface and internalised) was calculated as a percentage of maximal phosphorylation and plotted against the time-point in minutes. Maximum phosphorylation of Tie2 is reached at 5 minutes of stimulation.

5.8.2.2. Experiments

To determine the time-course of Tie2 activation induced by a high concentration of Ang1, cells were prepared as previously described in Chapter 2.4. Cells were serum-starved for thirty minutes at different times and treated with vanadate (10 mM) for 5 minutes before stimulation with a high concentration of Ang1 (200 ng/ml). Subsequently the cells were lysed for each time-point. Proteins were resolved using SDS-PAGE, probed for phospho-Y^{992} Tie2 and detected as before (Figure 5.12A). The phospho-Tie2 results were normalized to total Tie2. The percentage phosphorylation over time was calculated and plotted. The experiment was repeated 5 times.

The time course plot (Figure 5.12B) shows that cells have 35% basal phosphorylation which reaches maximum phosphorylation after 5 minutes stimulation with a high concentration of Ang1.

A

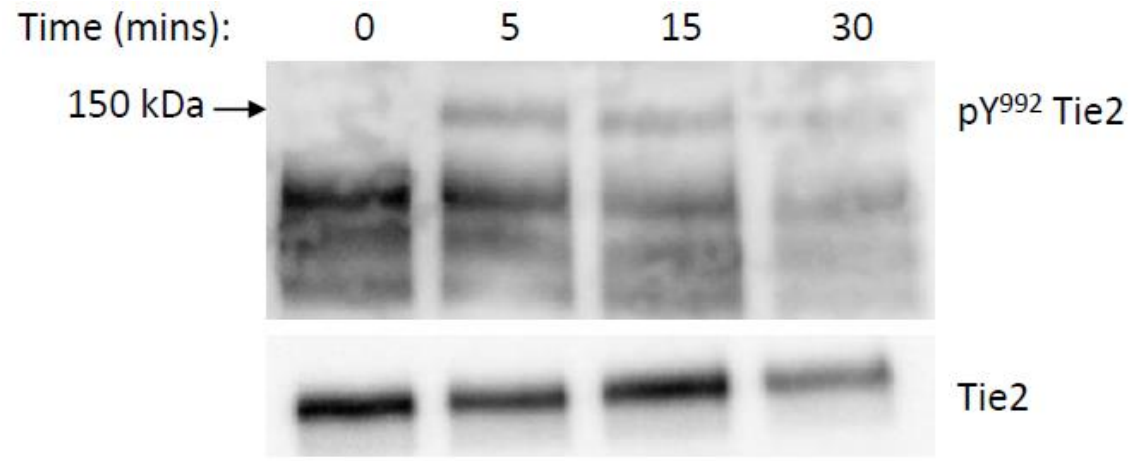

B

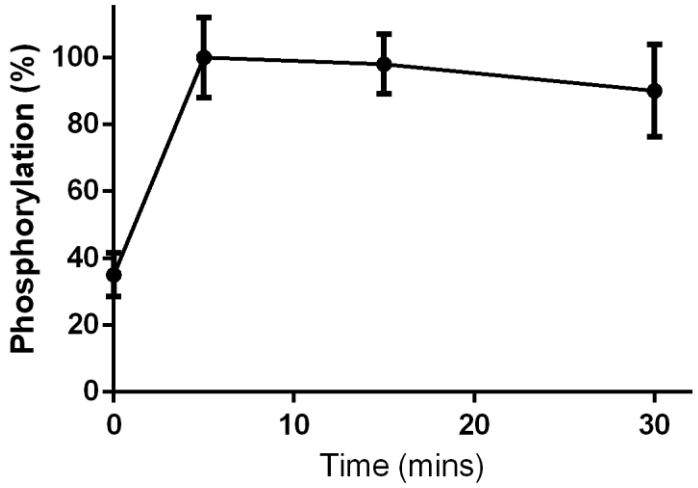

Figure 5.12: Experiment- Time-course for high concentration Ang1-induced Tie2 phosphorylation (with vanadate).

A. Cells were serum-starved, treated with vanadate and stimulated with 200 ng/ml Ang1 for different time-points; 0, 5, 15, 30 minutes. The protein was resolved using SDS-PAGE and probed for phosphorylated Y992 Tie2. Chemiluminescence was detected using a CCD imager. The blot shows a rapid increase of phosphorylation at 5 minutes then slowly decreases. The blot was reprobed for Tie2 to normalize results.

B. The percentage phosphorylation of Y^{992}-Tie2 was calculated and plotted against the relevant time-point. The plot shows the change of percentage phosphorylation over 30 minutes stimulation with Ang1. There is 35% basal phosphorylation, and maximum phosphorylation at 5 minutes, after which the level of phosphorylation slowly decreases. Phosphorylation is normalized to Tie2 and is shown as a percentage of maximal phosphorylation. Data is presented as mean and SEM of relative maximal phosphorylation (n=5). All data is significant to control (p<0.05), One-way ANOVA.

5.8.2.3. Comparison of simulation and experimental time-courses for high Ang1-induced Tie2 phosphorylation (without dephosphorylation).

The total percentage phosphorylation from the normalised experimental data with high Ang1 (200 ng/ml) was compared to the simulation data and a graph was plotted of the percentage change in Tie2 phosphorylation over time for both sets of data. Figure 5.13 shows the simulation data closely resembles the experimental data and maximum phosphorylation occurs after 5 minutes of stimulation. This suggests that the model is identical to the experiments and is valid for the 30 minute time-course with a high concentration of Ang1.

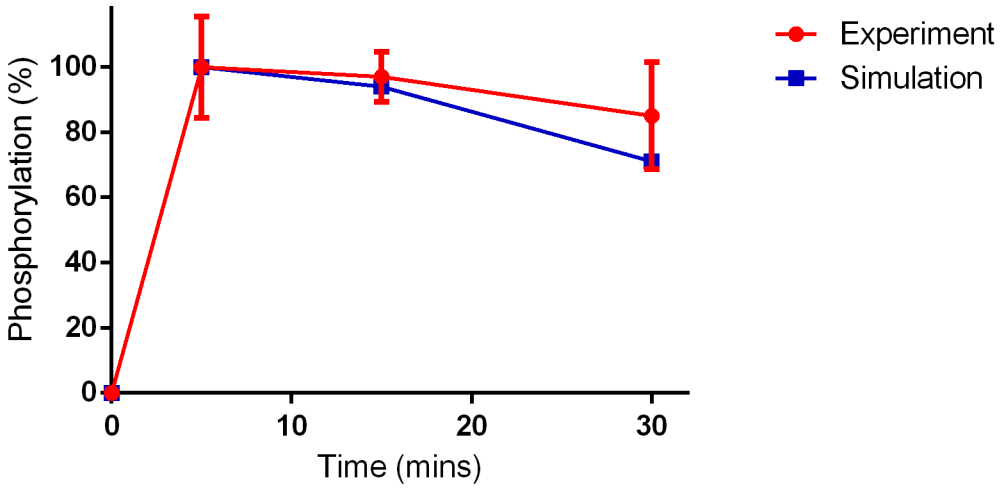

Figure 5.13: Comparison- Time-course for high concentration Ang1-induced Tie2 phosphorylation.
Experimental and simulation data of the time-course for high Ang1 (200 ng/ml) induced Tie2 phosphorylation were compared. The percentages of phosphorylated Tie2 in both the experimental and simulation data are very similar, and both peak at 5 minutes. Experimental data is presented as mean and SEM of relative maximal phosphorylation (n=5). The comparison of experiment to simulation is not significant (p<0.05), Two-way ANOVA.

5.8.3. The concentration dependent effect of Ang1 on Tie2 activation.

5.8.3.1. Simulations

The effect of increasing concentrations of Ang1 on the levels of Tie2 phosphorylation is the second approach used to validate the Ang1 model. The model was simulated for 30 minutes each time with an increasing concentration of Ang1; 0.0357 nM (10 ng/ml), 0.0893 nM (25 ng/ml), 0.179 nM (50 ng/ml), 0.357 nM (100 ng/ml), 0.714 nM (200 ng/ml). The total concentration of phosphorylated Tie2 (surface and internalised) was quantified after 15 minutes. This time-point was previously determined to give maximum phosphorylation with low and high concentrations of Ang1 (Figures 5.9, 5.10, 5.11, 5.12, 5.13).

The percentage of maximal Tie2 phosphorylation was calculated for each Ang1 concentration with 200 ng/ml Ang1 being 100% phosphorylation. The total percentage phosphorylation was plotted against the Ang1 concentration to produce the concentration-dependent curve (Figure 5.14). The simulation results suggest that phosphorylation increases with up to 50 ng/ml Ang1 treatment and then plateaus after 100 ng/ml Ang1.

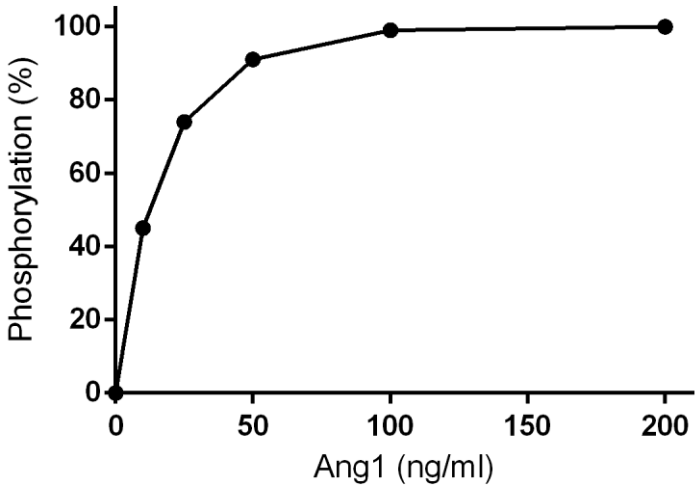

Figure 5.14: Simulation- The concentration dependent effect of Ang1 on Tie2 phosphorylation (excluding the dephosphorylation reaction).
The model was simulated with various concentrations of Ang1 and the concentration of Tie2 phosphorylated was quantified after 15 minutes of stimulation. The percentage of maximal Tie2 phosphorylation was calculated for each Ang1 concentration. The graph shows that the percentage of Tie2 phosphorylation increases with Ang1 and plateaus after stimulation with 100 ng/ml Ang1.

5.8.3.2. Experiments

To determine the relative effect of Ang1 concentration on Tie2 activation, HUVECs were prepared as described in Chapter 2.2.4. serum-starved for one hour and treated with the different concentrations of Ang1 for 15 minutes. The samples were prepared (as described in Chapter 2.2.1), resolved by SDS-PAGE and blotted. The blots were probed for phospho-Tie2 (pY^{992}). To quantitatively analyse this blot, the intensities of phospho-Tie2 protein were quantified by densitometry using a CCD imager and MultiGauge software. The results show that Ang1 induced a concentration dependent increase in Tie2 phosphorylation indicated by the increasing intensity of the 145 kDa band of phosphorylated Tie2 as shown in figure 5.15A.

The intensities of the phospho-Tie2 bands were expressed as a percentage of maximal phosphorylation and were plotted against their relative concentrations of Ang1 treatment (Figure 5.15B). The graph in Figure 5.15 shows that there is an increase in phosphorylated Tie2 in samples treated up to 50 ng/ml Ang1 and then the level of phosphorylation begins to plateau.

A

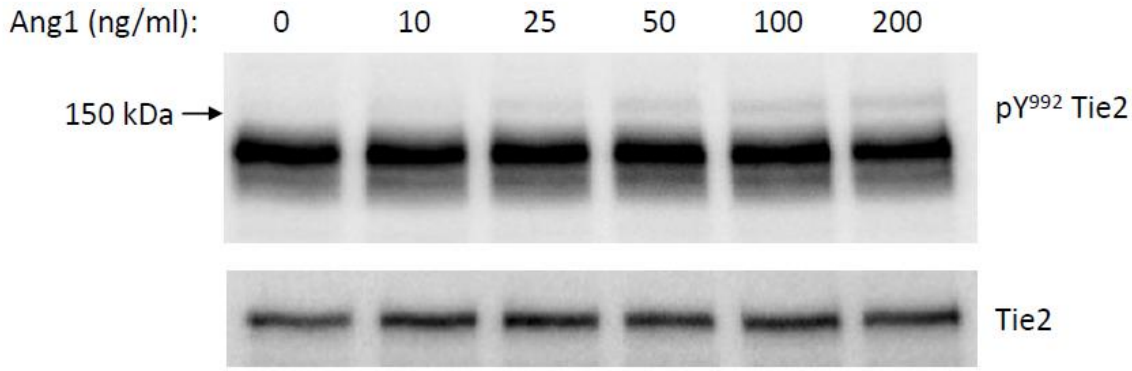

B

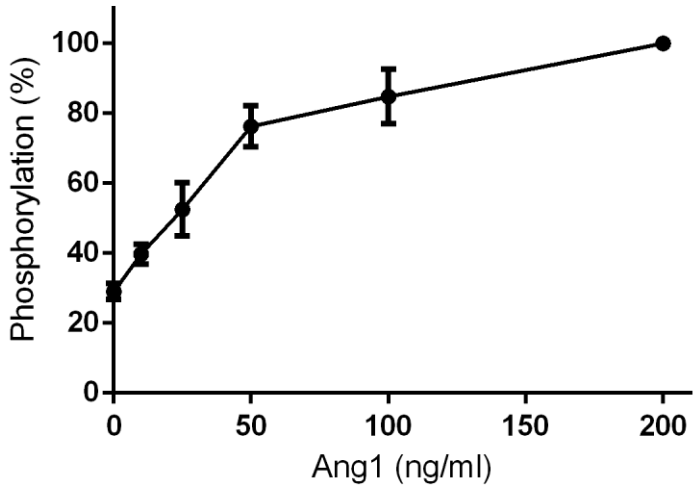

Figure 5.15: Experiment- The concentration dependent effect of Ang1 on Tie2 phosphorylation (with vanadate).

A. Western blotting was used to resolve and identify phosphorylated Y^{992} Tie2 in HUVECs treated vanadate and various concentrations of Ang1; 10, 25, 50, 100 and 200 ng/ml. Tie2 phosphorylation increases as the concentration of Ang1 treatment increases. The blot was reprobed for Tie2 to normalize the results.

B. Phospho-Tie2 protein from the blot was quantified using MultiGauge. The percentage of maximal Tie2 phosphorylation (200 ng/ml is 100% phosphorylation) was calculated and plotted against the respective concentration. There is an increase of activated receptors in samples treated with 0-200 ng/ml. Phosphorylation is normalized to Tie2 and is shown as a percentage of maximal phosphorylation. Data is presented as mean and SEM of relative maximal phosphorylation (n=3). Data is significant for 25, 50, 100 and 200 ng/ml Ang1 in comparison to no Ang1 ($p<0.05$), One-way ANOVA.

5.8.3.3. Comparison of simulation and experimental concentration dependence curves of Ang1-induced Tie2 phosphorylation (without dephosphorylation).

The percentage change in Tie2 phosphorylation over the concentration of Ang1 from the simulation data and experimental data were compared. Figure 5.16 shows that both data sets have a concentration dependent increase in Tie2 phosphorylation until 50 ng/ml, where the levels begin to plateau. However the percentage of phosphorylation is different. Overall both concentration-dependence curves are similar however there is a difference in the percentages of phosphorylation. This discrepancy may be due to the initial concentration of Tie2 phosphorylation which is higher for the experiment because of the basal level phosphorylation; this is not accounted for in the simulation. Another reason may be the effect of vanadate treatment. The statistical analysis suggests that the difference between the experiments and simulation is significant.

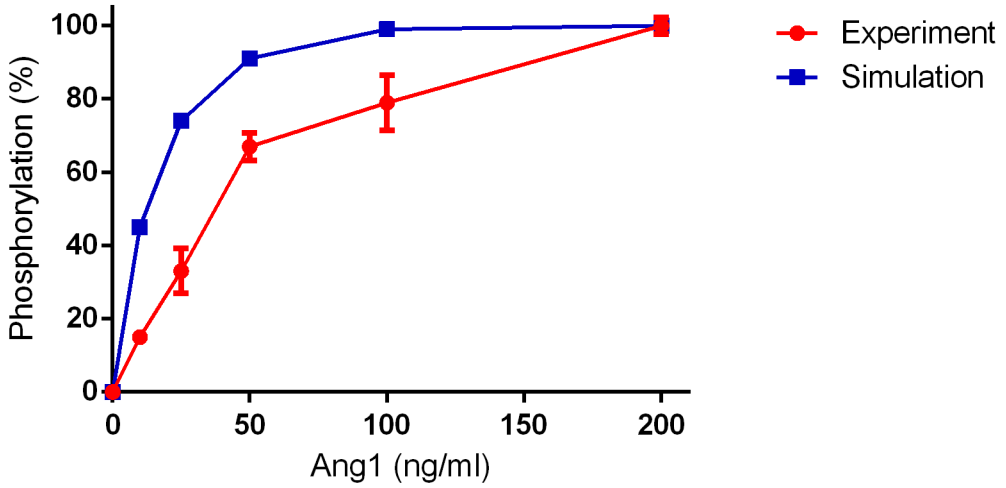

Figure 5.16: Comparison- The concentration dependent effect of Ang1 on Tie2 phosphorylation.
Experimental (red) and simulation (blue) data of the Ang1 concentration-dependent effect on Tie2 phosphorylation were compared. Both methods show an increase in phosphorylation which is not as pronounced after 50ng/ml. However the percentages of phosphorylated Tie2 are different. Experimental data is presented as mean and SEM of relative maximal phosphorylation (n=3). The comparison of experiment to simulation is significant (p<0.05), Two-way ANOVA.

5.9. Validating the effect of soluble Tie2 on Ang1-induced Tie2 activation (without dephosphorylation).

To validate the sTie2 interactions in the model, the effect of increasing sTie2 concentrations on the levels of 50 ng/ml Ang1-induced Tie2 phosphorylation was performed *in-silico* and by experiments.

5.9.1. Simulations

The model was simulated for 30 minutes with 50 ng/ml Ang1 for each simulation with an increasing concentration of sTie2 (100, 200, 500 and 1000 ng/ml). The total concentration of phosphorylated Tie2 (surface and internalised) was quantified after 15 minutes.

The total percentage phosphorylation for each concentration of sTie2 added was calculated with Ang1-only induced Tie2 activation being 100% phosphorylation. Figure 5.17 shows the concentration-dependent curve of percentage phosphorylation for each concentration of sTie2. The simulation predicts that sTie2 has an inhibitory effect on Ang1-induced Tie2 phosphorylation.

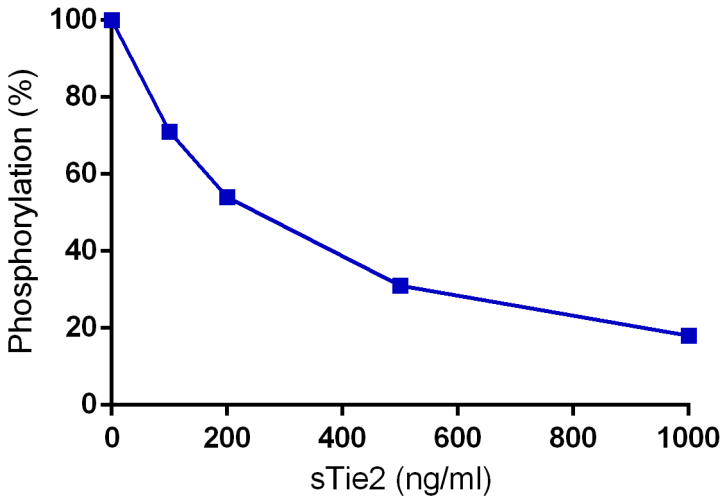

Figure 5.17: Simulation- The concentration dependent effect of sTie2 on Tie2 phosphorylation (excluding the dephosphorylation reaction).
The model was simulated with 50 ng/ml Ang1 and various concentrations of sTie2; 100, 200, 500, 1000 ng/ml. The concentrations of total Tie2 phosphorylation (cell surface and internalised) were quantified after 15 minutes of stimulation. The results show that sTie2 has a concentration dependent inhibitory effect on Ang1-induced Tie2 phosphorylation.

5.9.2. Experiments

The wild-type ectodomain of Tie2 was produced by Professor Nicholas Brindle and Teonchit Nuamchit, and used in further experiments as soluble Tie2.

The HUVECs were setup as previously described, serum-starved for one hour and treated with vanadate for 5 minutes. During this period different concentrations of sTie2 wild-type and Ang1 (50 ng/ml) were incubated together for 15 minutes (at room temperature). The solutions were added to the cells and incubated for 15 minutes at 37^{o}C. The blots were probed for pY^{992}-Tie2 and chemiluminescence was detected using a CCD imager. Following this the blot was stripped and reprobed for ectodomain Tie2 chemiluminescence and detected with a CCD imager to normalize results as in previous experiments. This experiment was repeated 4 times.

The results (Figure 5.18A), show that there is a decrease in phosphorylated Tie2 when soluble Tie2 is increased. The reprobed blot for Tie2 shows full length cellular Tie2 at ~150 kDa and residual sTie2 wild-type at ~100 kDa.

Quantification and normalisation of phosphorylated Tie2 to total Tie2 shows an obvious decrease in phosphorylation when the sTie2 concentration is increased. The overall effect of sTie2 on Ang1-induced phosphorylation from 4 independent experiments show that phosphorylation is inhibited to 50% with 200 ng/ml sTie2, and maximal inhibition with 1000 ng/ml sTie2 (Figure 5.18C).

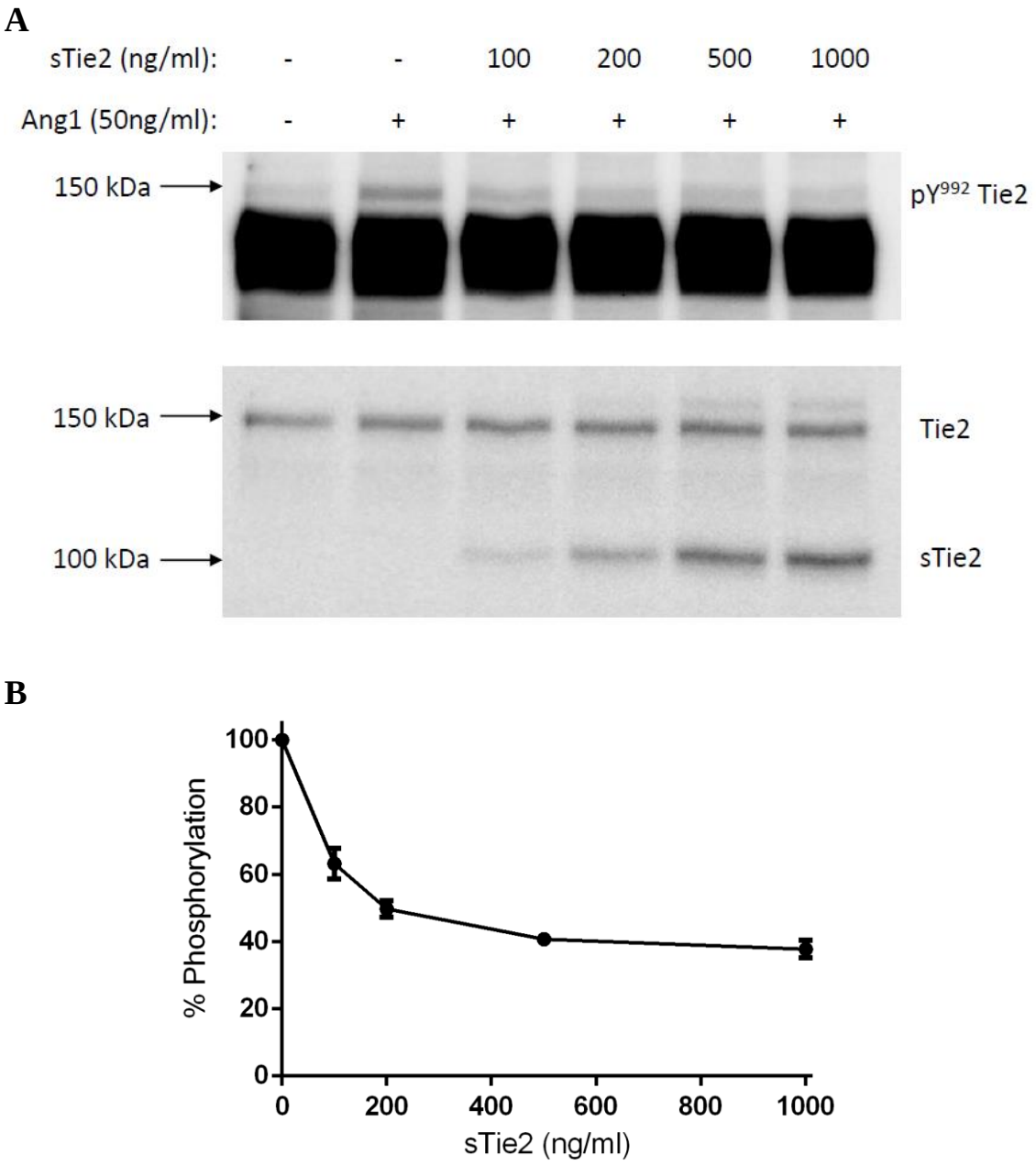

Figure 5.18: Experiment- The concentration dependent effect of sTie2 on Tie2 phosphorylation (with vanadate).

A. HUVECs were serum starved for 1 hour after which vanadate was added for 5 minutes. sTie2 was incubated with Ang1 together for 15 minutes then added to the cells for a further 15 minutes. Cell lysates were collected and protein was resolved by SDS-PAGE. The blot was probed for pY992 Tie2 then stripped and reprobed for Tie2 for normalisation. Chemiluminescence was detected using a CCD imager. The blots show that increasing the concentration of sTie2 decreases Ang1-induced Tie2 phosphorylation.

B. Quantification of chemiluminescence for pY992 was normalised to Tie2 and is shown as a percentage of maximal phosphorylation. The percentage change of Tie2 phosphorylation shows that phosphorylation decreases as sTie2 is increased. Phosphorylation is inhibited to 50% with 200 ng/ml sTie2. Maximum inhibition occurs with 1000 ng/ml sTie2. The data is presented as mean and SEM of relative maximal phosphorylation (n=4). All data is significant to Ang1 (p<0.05), One-way ANOVA.

5.9.3. Comparison of simulation and experimental concentration dependence curves of sTie2 on Ang1-induced Tie2 phosphorylation (without dephosphoryation).

The percentage change in total Tie2 phosphorylation over the concentration of sTie2 from the simulation data and experimental data were compared. Figure 5.19 shows that the simulation results are close to the results from experiments for the lower values for sTie2. However there is a difference between both data when treated with over 200 ng/ml sTie2. In the experiments the levels of total phosphorylation plateaus whilst the level in the simulation gradually decreases. 50% inhibition of phosphorylation is achieved with 200 ng/ml sTie2 in experiments and 240 ng/ml sTie2 in the simulation. However the comparison using the two-way ANOVA statistical analysis suggests that there is no significant difference between the experiments and simulation.

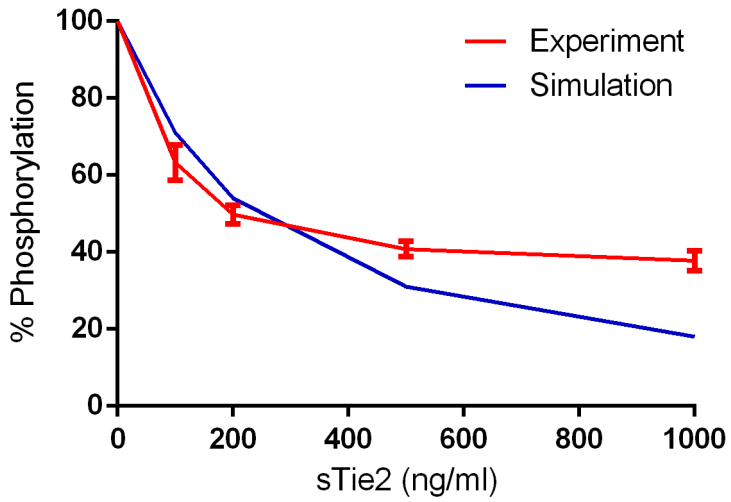

Figure 5.19: Comparison- The concentration dependent effect of sTie2 on Tie2 phosphorylation.
Experimental and simulation data of the sTie2 concentration-dependent effect on Ang1-induced Tie2 phosphorylation were compared. The percentages of phosphorylated Tie2 are similar for sTie2 treatment below 200 ng/ml, and the levels are very different with higher concentrations of sTie2. Experimental data is presented as mean and SEM of relative maximal phosphorylation (n=4). The comparison of experiment to simulation is not significant (p<0.05), Two-way ANOVA.

5.10. Validating the effect of Ang2 on Tie2 activation (without dephosphorylation).

Ang2 has been shown to be a partial agonist for Tie2 (Bogdanovic *et al.*, 2006; Yuan *et al.*, 2009). The effect of Ang2 on Tie2 phosphorylation in a concentration-dependent manner was simulated and compared to experimental results.

5.10.1. Simulations

The model was simulated with increasing concentrations of Ang2; 50, 100, 200, 500, 800 and 1000 ng/ml (Appendix 1). The amount of Ang2-induced phosphorylation was quantified after 15 minutes of stimulation. The percentage change in total phosphorylated Tie2 was calculated and plotted.

The graph of percentage change of phosphorylated Tie2 over increasing Ang2 (Figure 5.20A) suggests that Ang2 induces Tie2 phosphorylation. Half maximum phosphorylation is reached with 30 ng/ml of Ang2 and maximum phosphorylation with 400 ng/ml of Ang2

To examine the agonist activity of Ang2 in comparison to the agonist activity of Ang1 the levels of Ang1-induced and Ang2-induced Tie2 phosphorylation from both Ang1 and Ang2-induced simulations (in Figures 5.14 and 5.20A) were compared. Figure 5.20B shows the percentage Tie2 phosphorylation induced by increasing concentrations of Ang1 and Ang2. The percentages of phosphorylation are shown as a percentage of maximal Ang1-induced phosphorylation. The comparison with Ang1 shows that Ang2

has a partial agonist effect which is 25% of the maximum Ang1-induced Tie2 phosphorylation.

A

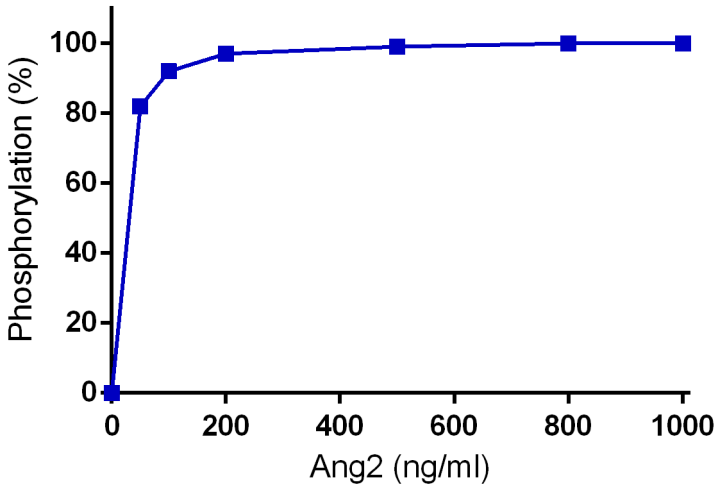

B

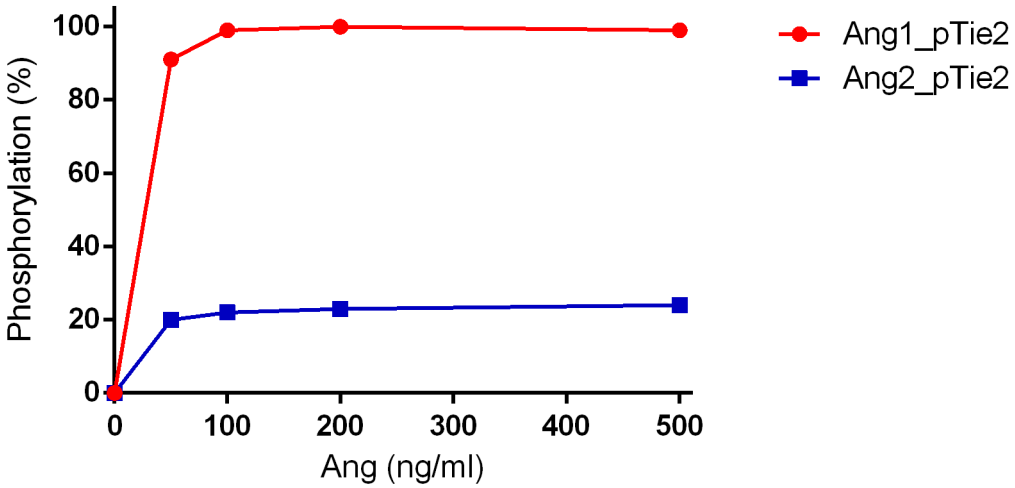

Figure 5.20: Simulation- The concentration dependent effect of Ang2 on Tie2 phosphorylation (excluding the dephosphorylation reaction).
A. The model was simulated for various concentrations of Ang2; 50, 100, 200, 500, 800 and 1000 ng/ml, and the effects on Tie2 phosphorylation at 15 minutes were quantified. The simulations show an increase in phosphorylation, and maximum phosphorylation being reached with 400 ng/ml Ang2. With higher concentrations of Ang2 the levels of phosphorylation remains at maximum suggesting saturation of Tie2.
B. The percentage Tie2 phosphorylation induced by increasing concentrations of Ang1 (from previous simulations) and Ang2 were compared. The percentages of phosphorylation are shown as a percentage of maximal Ang1-induced phosphorylation. Ang2 has a partial agonist effect which is 25% of maximum Ang1-induced Tie2 phosphorylation.

5.10.2. Experiments

To determine the relative effect of Ang2 concentration on Tie2 activation *in vitro*, HUVECs were prepared as described (Chapter 2.4), serum-starved for one hour, treated with 10mM vanadate for 5 minutes, and stimulated with different concentrations of Ang2 for 15 minutes. In some experiments an additional sample was treated with 50 ng/ml Ang1 for 15 minutes to observe the difference between Ang1 and Ang2 induced Tie2 phosphorylation (three independent experiments). The samples were prepared (as described in Chapter 2.2.1), resolved by SDS-PAGE and blotted. The blots were probed for phospho-Tie2 (pY^{992}) and reprobed for Tie2 to normalize the results (Figure 5.21A). To quantitatively analyse this blot, the intensities of phospho-Tie2 protein were quantified by densitometry using a CCD imager and MultiGauge software. The results show that Ang2 induced an increase in Tie2 phosphorylation as shown in Figure 5.21A.

The percentages of maximal phosphorylation calculated using the region intensities of the bands for phospho-Tie2 were plotted against their relative concentrations of Ang1 treatment. The graph in Figure 5.21B shows that there is an increase in Tie2 phosphorylation in samples, which reaches maximum phosphorylation with 100 ng/ml before slightly decreasing. Half maximal phosphorylation of Tie2 is reached with a treatment of 25 ng/ml Ang2.

To examine the agonist activity of Ang2 in experiments in comparison to the agonist activity of Ang1 the percentage phosphorylation from both Ang1 and Ang2-induced samples were compared. Figure 5.21C shows the percentage Tie2 phosphorylation induced by Ang1 and Ang2. The percentages of Ang2-induced phosphorylation are shown as a percentage of maximal Ang1-induced phosphorylation. The results show that

Ang2 has a partial agonist effect which is 35% of the Ang1-induced Tie2 phosphorylation.

A

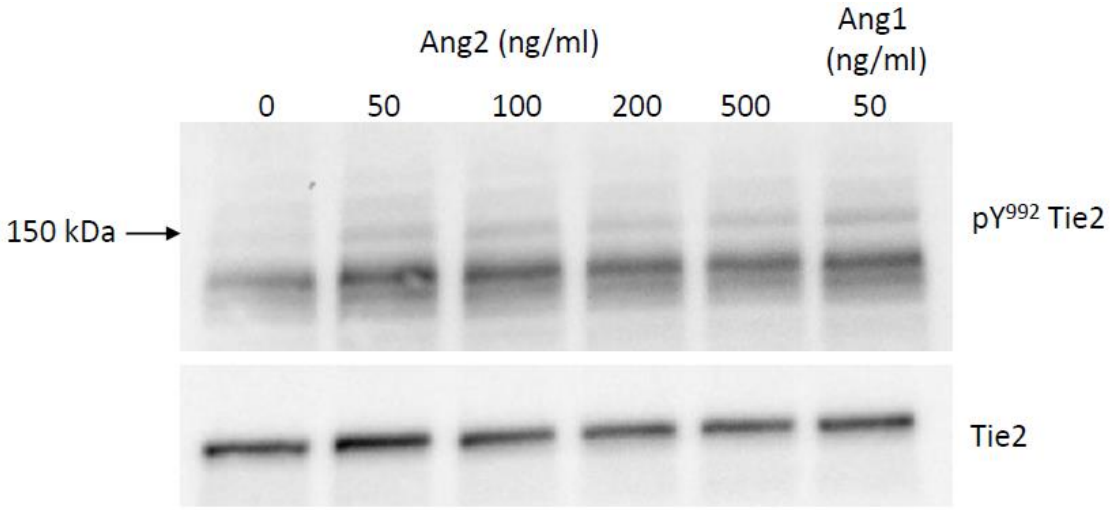

B

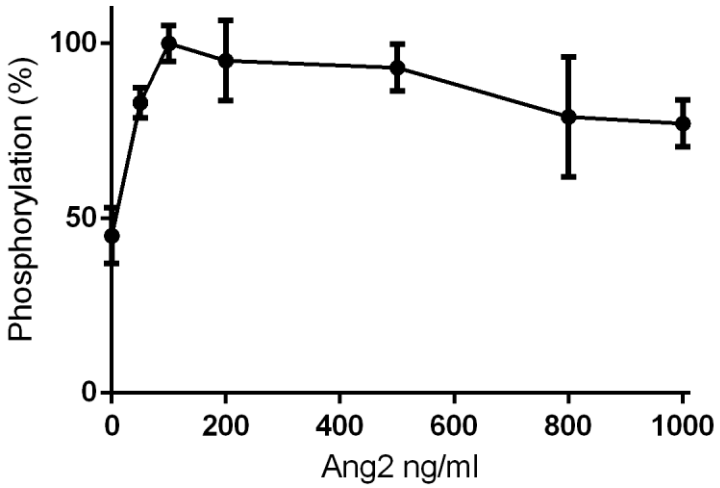

C

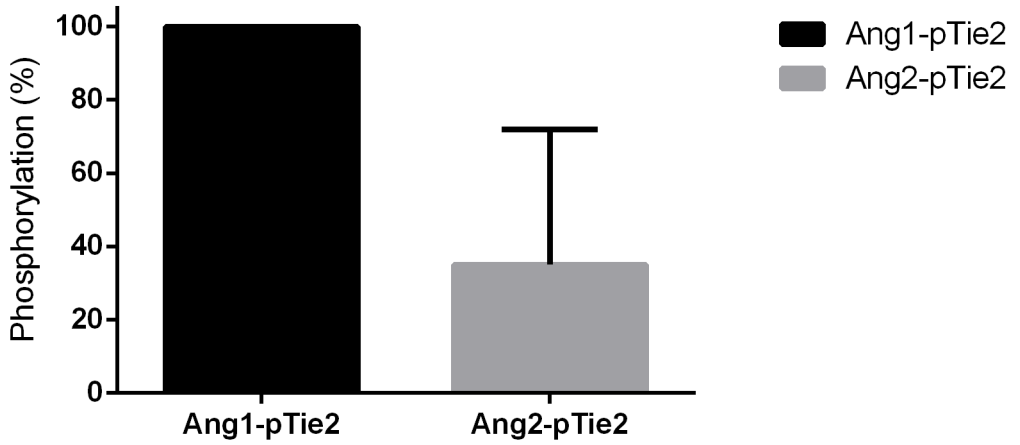

Figure 5.21: Experiment- The concentration dependent effect of Ang2 on Tie2 phosphorylation (with vanadate).

A. Cells were serum-starved, treated with vanadate, and stimulated with Ang1 or increasing concentrations of Ang2 for 15 minutes. The protein was resolved using SDS-PAGE and probed for phosphorylated Y^{992} Tie2. Chemiluminescence was detected using a CCD imager. The blot shows an increase of phosphorylation with low concentrations of Ang2. The blot was reprobed for Tie2 to normalize results.

B. The percentage phosphorylation of Y^{992}-Tie2 was calculated and normalized to Tie2. The results are shown as a percentage of maximal phosphorylation (induced by 100 ng/ml Ang2). The plot shows the change of percentage phosphorylation over increasing Ang2. The cells initially have 45% basal phosphorylation, and reaches maximum phosphorylation with 100ng/ml Ang2, after which the level of phosphorylation plateaus and slightly decreases. Data is presented as the mean and SEM of relative maximal phosphorylation (n=5). Data is significant for 100, 200 and 500 ng/ml Ang2 in comparison to no Ang2 ($p<0.05$), One-way ANOVA.

C. The percentage Tie2 phosphorylation induced by 50 ng/ml Ang1 and 50 ng/ml Ang2 were compared. The percentages of Ang2-induced phosphorylation are shown as a percentage of Ang1-induced phosphorylation. Ang2 has a partial agonist effect which is 35% of Ang1-induced Tie2 phosphorylation. Data is presented as the mean and SEM (n=3) and is significant, $p<0.05$, Students *t* test.

5.10.3. Comparison of simulation and experimental concentration dependence curves of Ang2-induced Tie2 phosphorylation (without dephosphorylation).

The simulation results of increasing Ang2 were compared to the normalised experimental results (Figure 5.22). Both methods show that Ang2 induces Tie2 phosphorylation with similar concentrations of Ang2 (30 ng/ml in simulations and 25 ng/ml in HUVECs) for half maximum phosphorylation. In simulations the maximum phosphorylation is reached with 200 ng/ml Ang2 as opposed to 100 ng/ml Ang2 in experiments. Furthermore after maximum phosphorylation is reached the model suggests a saturation and plateau effect with higher concentrations of Ang2, and does not predict the actual lower level of phosphorylation as shown in HUVECs. However the comparison using the two-way ANOVA statistical analysis suggests that there is no significant difference between the experiments and simulation.

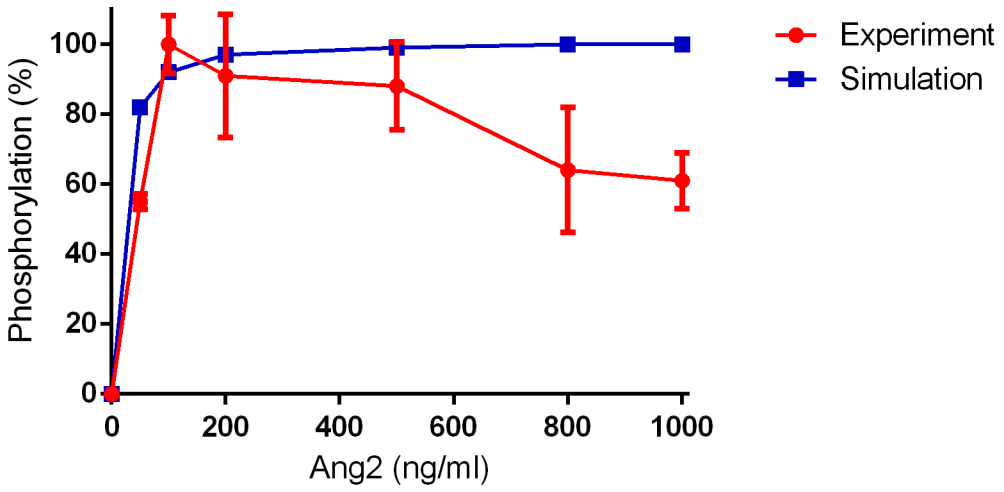

Figure 5.22: Comparison- The concentration dependent effect of Ang2 on Tie2 phosphorylation.
The simulation effect of increasing Ang2 on Tie2 phosphorylation was compared to the effect in HUVEC experiments. Both methods show an increase in phosphorylation however maximum phosphorylation is reached at different Ang2 concentrations; 200 ng/ml in simulations and 100 ng/ml in experiments. After maximum phosphorylation is achieved the model suggests that Tie2 phosphorylation is saturated with higher concentrations of Ang2 and therefore plateaus, whereas the experimental data shows that Tie2 phosphorylation decreases. Experimental data is presented as mean and SEM of relative maximal phosphorylation (n=5). The comparison of experiment to simulation is not significant (p<0.05), Two-way ANOVA.

5.11. The effect of vanadate on Ang2-induced Tie2 phosphorylation.

Experiments monitoring the effect of Ang2 on Ang1-induced Tie2 activation using vanadate produced inconsistent results showing the effects of Ang2 being both an agonist and antagonist of Tie2 for different concentrations. This may be because phosphorylated Tie2 only produces two- to threefold changes when stimulated (Yu *et al.*, 2013), and the pY992-Tie2 antibody may not be sensitive enough to detect the subtle changes of Tie2 phosphorylation in response to Ang2. As vanadate is well known to increase the levels of phosphorylation by inhibiting phosphatases (thus stopping dephosphorylation) the use of vanadate may be a problem as any slight changes in phosphorylation due to Ang2 may not be detected (Yacyshyn *et al.*, 2009).

Experiments were performed to determine the effect of Ang2 on Tie2 phosphorylation with and without the presence of vanadate. HUVECs were prepared and serum-starved as in previous experiments. Cells were treated with or without vanadate for 5 minutes and challenged with either 50 ng/ml Ang1 or 200 ng/ml Ang2 for 15 minutes. Figure 5.23A shows that vanadate increases the levels of Ang1 and Ang2-induced Tie2 phosphorylation. The blot was stripped and reprobed for Tie2 to normalise the amount of phosphorylation. Tie2 phosphorylation was calculated as a percentage of maximal Ang1-induced Tie2 phosphorylation for samples with and without vanadate. Samples treated with vanadate show an 11% difference in Ang1 and Ang2-induced Tie2 phosphorylation whereas samples without vanadate show a 48% difference (Figure 5.23B). This may suggest that the use of vanadate may mask the true effect of Ang2 on Tie2 phosphorylation.

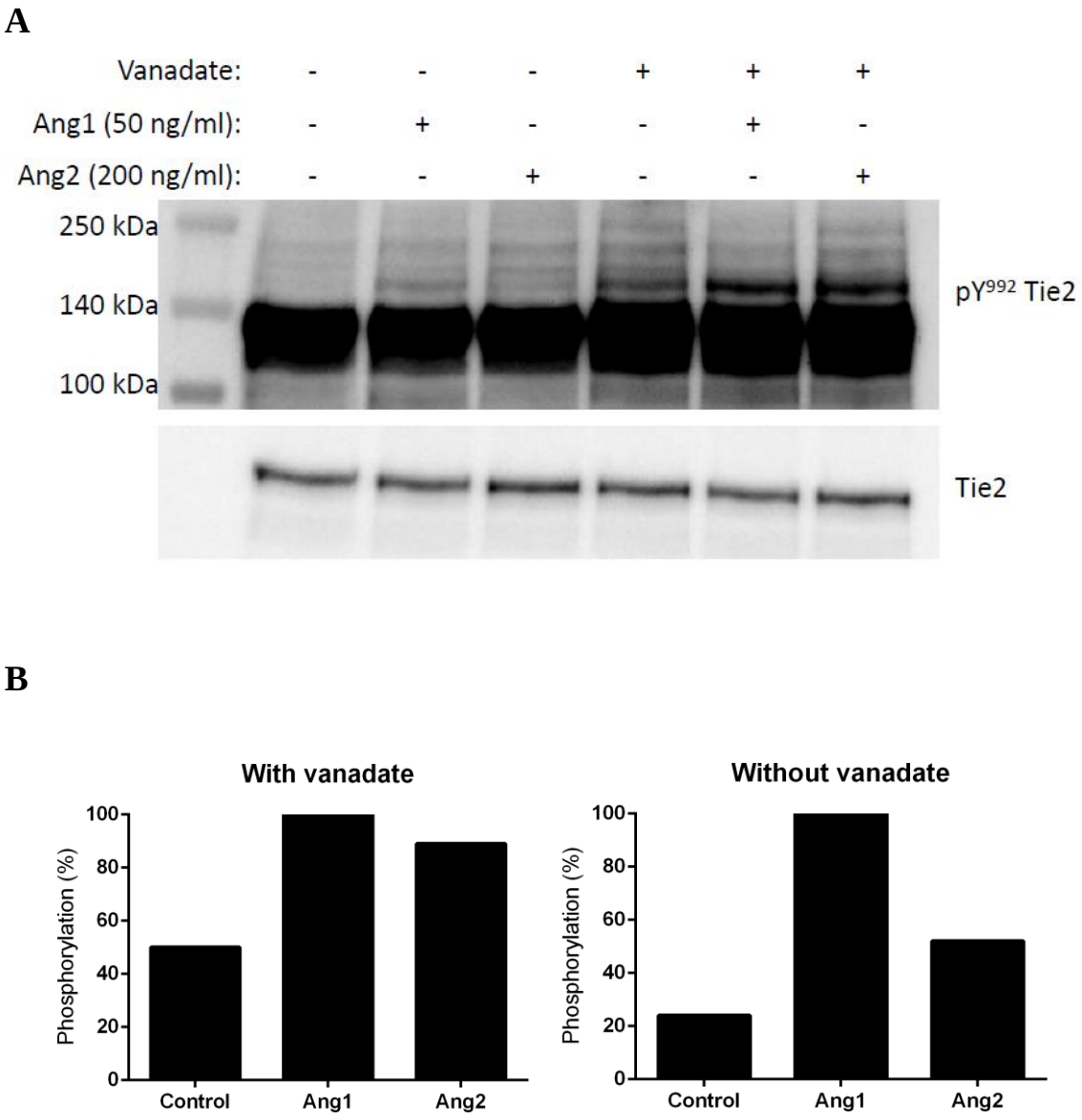

Figure 5.23: The effect of vanadate on Ang1 and Ang2-induced Tie2 phosphorylation.
A. Cells were serum-starved, treated with or without vanadate, and stimulated with Ang1 or Ang2 for 15 minutes. The protein was resolved using SDS-PAGE and probed for phosphorylated Y^{992} Tie2. Chemiluminescence was detected using a CCD imager. The blot shows that vanadate treated samples increase the levels of phosphorylation.
B. The percentage Tie2 phosphorylation was calculated for samples with and without vanadate. Samples with vanadate treatment show an 11% difference between Ang1 and Ang2 induced Tie2 phosphorylation. Samples without vanadate treatment show a 48% difference between Ang1 and Ang2 induced Tie2 phosphorylation. The results show that the difference between Ang1-induced phosphorylation and Ang2-induced phosphorylation is greater in samples without vanadate. Phosphorylation is normalized to Tie2 and is shown as a percentage of maximal Ang1-induced Tie2 phosphorylation.

5.12. Discussion

This chapter aimed to simulate and validate the model by comparing the simulation results to experimental results.

Prior to the model simulation and validation a suitable method to measure receptor activation was required for the accurate experimental detection and quantification of phosphorylated Tie2. Immunofluorescence was the first method of choice as it can generate results on the variation in individual cells. However the phospho-Tie2 antibody used could not discriminate between specific and non-specific protein and furthermore the levels of phosphorylation on the cell membrane could not be quantified. Therefore Western blotting was shown to be the more effective method when coupled with a CCD imager and quantification software.

Conversely the method used for quantitative Western blotting in this study is not completely accurate. Aside from the general problem of potential protein loss during the transfer step and non-specific protein detection, the stripping of the membrane to reprobe for Tie2 is a greater problem in regards to the accuracy of protein quantification. It is inevitable that some protein is lost from the membrane during the stripping process and may not be evenly stripped across the membrane. An alternative to this process could be the use of a quantitative imagining scanner such as the LI-COR Odyssey infrared imaging system which allows for highly sensitive two-colour fluorescence detection and quantification (Schutz-Geschwender *et al.*, 2004). Hence the feature of dual staining will remove the need for stripping and reprobing membranes.

Another problem with the quantification method in experiments is that the actual concentration of phosphorylated Tie2 cannot be obtained from experiments as there is no standard Tie2 tyrosine 992 protein available to produce a standard calibration curve. Thus the validation is only focussed on the relative levels of phosphorylation changes in respect to maximum phosphorylation.

Simulations of the model were performed to assess the equilibrium between Tie1, Tie2 and Tie1:Tie2. At steady state without the addition of ligand the model showed that the concentrations of states remain constant over an extended time and hence suggests that the model is valid for the steady-state equilibrium.

The addition of Ang1 to the system induces the dissociation of the Tie1:Tie2 heterodimer favouring free Tie1 and Tie2. This has also been demonstrated by Seegar and colleagues (2010) who used an *in vivo* fluorescence resonance energy transfer-based proximity assay with confocal microscopy to monitor the association of Tie1 and Tie2 (Seegar *et al.*, 2010). Conversely the addition of Ang2 in the system was shown by Seegar and colleagues (2010) not to have any effect on the Tie1:Tie2 heterodimer. However the simulation of the model suggests that the Tie1:Tie2 heterodimer also dissociates in the presence of Ang2. A reason for this discrepancy could be that Ang2 has a different binding affinity between Tie2 and Tie2 in complex with Tie1. The model assumes that Ang2 can bind to either Tie2 or Tie1:Tie2 with similar affinities. As the concentrations of free Tie2 and Tie1:Tie2 on the cell surface are the same, the free Tie2 will be recruited to form oligomeric Tie2 complexes, and as a consequence could shift the equilibrium to favour Tie1:Tie2 dissociation to free more Tie2 for binding and oligomerisation. This could suggest that the model is not valid for Tie1:Tie2 initial concentrations or the

parameters for Ang2 binding to Tie2/Tie1:Tie2. However it is difficult to experimentally measure the concentrations of Tie1:Tie2 on the cell surface due to dissociation (even when crosslinked) and the differences in Ang2 binding have not been reported in the literature.

Validation of the model for Ang1 simulations suggest that the model is valid for time-courses as the simulations match the experimental data for both low and high concentrations of Ang1. However the model does not produce similar results to experiments for the concentration dependent effect on Tie2 phosphorylation. This may be due to the high concentration of basal phosphorylation and the use of vanadate which reduces dephosphorylation of Tie2. On the other hand as the level of phosphorylation in experiments does not plateau after 50 ng/ml Ang1 treatment as shown in the simulation this could suggest that the vanadate may not be fully effective at blocking dephosphorylation, thus allowing a low level of dephosphorylation to occur and not saturate Tie2 with lower concentrations of Ang1.

Validation of model for sTie2 effects on Ang1-induced Tie2 phosphorylation suggests that the model is valid. However the model seems to be sensitive to high concentrations of sTie2 and thus inhibits Tie2 phosphorylation more than as demonstrated in the experiments. The reason for this could also be related to the concentration dependent effect on Ang1 which may be due to the binding parameters, although this is not the case for the time-course.

Furthermore a comparison of the Ang2 concentration dependent effect on Tie2 phosphorylation suggested that the model is possibly valid for concentrations below 400

ng/ml, however experiments suggest a decrease in phosphorylation with higher concentrations of Ang2. Further experiments would be necessary to confirm the validity of Ang2 modelling e.g. Ang2 concentration dependent effect on phosphorylation in the presence of Ang1.

The reason for lower levels of phosphorylation with higher concentrations of Ang2 in experiments could be a result of Ang2 binding to integrins; $\alpha_v\beta_3$, $\alpha_v\beta_5$, $\alpha_5\beta_1$. Although Ang2 binds to integrins with a lower affinity than to Tie2 (Felcht *et al.*, 2012).

Another reason could be that Ang2 binding association and or dissociation parameters may be different for the various oligomeric Ang2 forms. Although there is no data available to suggest that dimeric Ang2 binds faster to Tie2 than tetrameric Ang2.

The experiment with Ang2 produced fluctuating levels of phosphorylation as shown by the large error bars in Figure 5.21. After many months of optimising the experiments for Ang2 the problem was found to be the poor state and batch of the cells and the presence of vanadate. The examination of the effect of vanadate on Ang2 suggests that the use of vanadate may disguise the true effect of Ang2 on Tie2 phosphorylation by reducing the receptors sensitivity to changes in Tie2 phosphorylation.

In a study by Bogdanovic and colleagues, the treatment of cells with pervanadate was shown to increase the levels of tyrosine phosphorylation and also enhance the release of Ang1 and Ang2 from Tie2 (Bogdanovic *et al.*, 2006). Although this study used pervanadate which is an irreversible inhibitor of phosphatases and formed in the presence

of hydrogen peroxide, it could be possible that sodium orthovanadate used in the experiments produces a similar effect (Huyer *et al.*, 1997).

Overall this chapter proposes that the modelling of high concentrations of Ang1 and Ang2 is not valid as the results do not represent the experiments. This could possibly be due to the usage of vanadate in experiments. Hence the validation will need to be repeated in experiment with a stable batch of HUVECs without the presence of vanadate, and with the dephosphorylation reaction included in the simulations.

Chapter 6: Model simulations and validation with dephosphorylation

The use of vanadate in experiments and excluding dephosphorylation from the model does not produce a model which is similar to physiological conditions. Furthermore data in Chapter 5 suggests that vanadate may have an effect on Ang2 in experiments. It is important to establish and validate a model closer to physiological conditions. Therefore simulations were performed again including the dephosphorylation reaction. Due to the time constraints of the project, the experiments for the Ang1 validation were performed by Dr Tariq Tahir who used a new batch of HUVECs and was able to detect Tie2 phosphorylation in the absence of vanadate.

6.1. Validating the effects of Ang1 on Tie2 activation (with dephosphorylation)

6.1.1. Time-course of Tie2 activation with low Ang1

6.1.1.1. Simulations

Simulations of the full model including the dephosphorylation reaction were performed by running the model to simulate 1800 seconds (30 minutes) stimulation with 50 ng/ml of Ang1 (0.179 nM) (Appendix 3). The simulation plot (Figure 6.1A) shows how the concentration of total phosphorylated Tie2 changes over time.

The model suggests that activated Tie2 on the cell surface peaks at 200 seconds. The majority of activated Tie2 is internalised into the cell (decreasing the amount of pTie2 on

the cell surface) and is gradually degraded at a constant rate. Maximum total phosphorylation occurs at 900 seconds (15 minutes).

The total amount of phosphorylated Tie2 (cell surface and internalised) at each time-point was calculated as a percentage of maximal phosphorylation. The rate of percentage change in phosphorylation is shown over time in minutes (Figure 6.1B). Simulation of the model suggests that maximum phosphorylation is reached at 15 minutes with 50 ng/ml Ang1 stimulation.

A

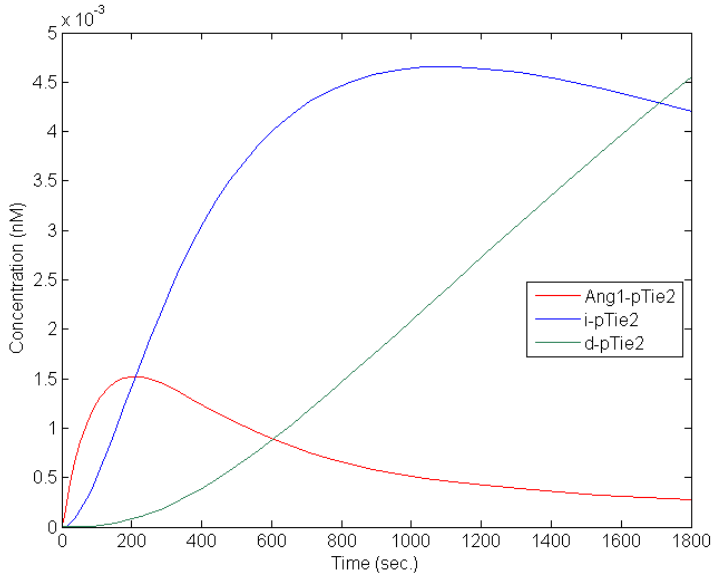

B

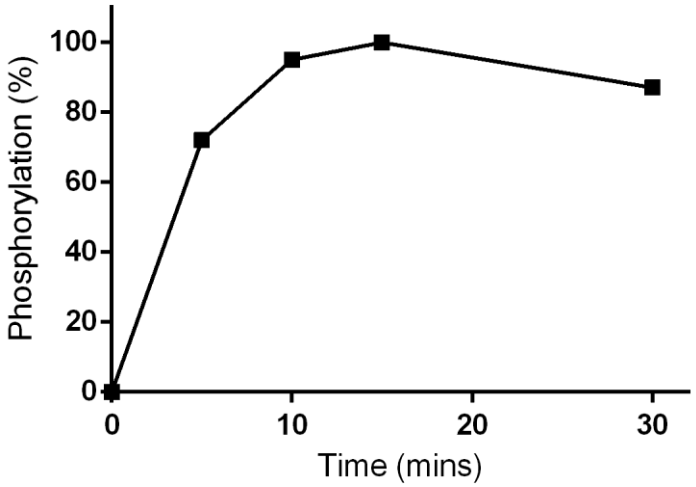

Figure 6.1: Simulation- Time-course for low concentration Ang1-induced Tie2 phosphorylation (including the dephosphorylation reaction).

A. The model including the dephosphorylation reaction was simulated with 50 ng/ml (0.179 nM) Ang1 for 1800 seconds. The plot shows the change in concentrations of cell surface phosphorylated Tie2 (Ang1-pTie2), internalised phosphorylated Tie2 (i-pTie2) and degraded phosphorylated Tie2 (d-pTie2). The level of Tie2 phosphorylation on the cell surface peaks at 200 seconds of stimulation with maximum total phosphorylation at 900 seconds. Most of the phosphorylated Tie2 is internalised into the cell and gradually degraded.

B. Total phosphorylated Tie2 (cell surface and internalised) was calculated as a percentage of maximal phosphorylation and plotted against the time-point in minutes. Maximum phosphorylation of Tie2 is reached at 15 minutes of stimulation.

6.1.1.2. Experiments

The rate of Tie2 activation with a low Ang1 concentration (50 ng/ml Ang1) was repeated again as described in Chapter 5.6.1.2 only this time without the addition of vanadate. Due to the time constraints of the project, the experiments were performed by Dr Tariq Tahir. The percentage Tie2 phosphorylation (normalized to Tie2 and as a percentage of maximal phosphorylation) at each time point was plotted to show the change of percentage phosphorylation over 30 minutes stimulation (Figure 6.2). Tie2 phosphorylation reaches a maximum at 10 minutes then slightly decreases.

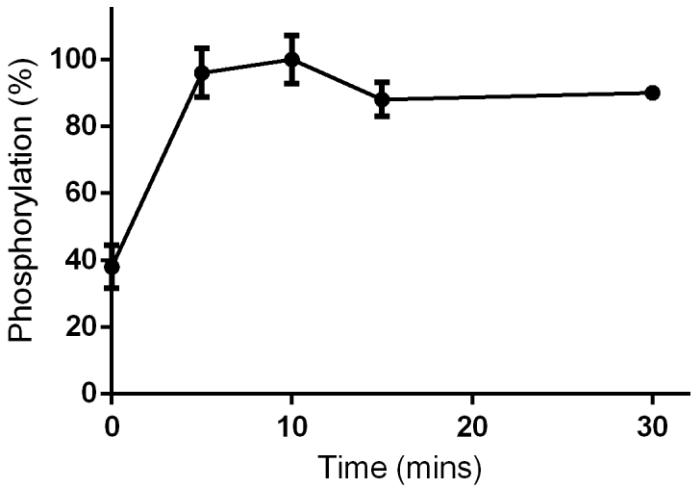

Figure 6.2: Experiment- Time-course for low concentration Ang1-induced Tie2 phosphorylation (without vanadate).
A. The time-course for 50 ng/ml Ang1 induced Tie2 phosphorylation without vanadate was performed in HUVECs (by Dr Tariq Tahir). The plot shows the change of percentage phosphorylation over 30 minutes stimulation. Maximum phosphorylation is reached at 10 minutes and then decreases. Phosphorylation is normalized to Tie2 and is shown as a percentage of maximal phosphorylation. Data is presented as mean and SEM of relative maximal phosphorylation (n=4). All data is significant to control (p<0.05), One-way ANOVA.

6.1.1.3. Comparison of simulation and experimental time-courses for low Ang1-induced Tie2 phosphorylation (with dephosphorylation).

The total percentage phosphorylation from the normalised experimental data was compared to the simulation data and a graph was plotted of the percentage change in Tie2 phosphorylation over time for both sets of data. Figure 6.3 shows that maximum phosphorylation is reached at 10 minutes in experiments and at 15 minutes in the simulation. Following this both levels of phosphorylation decrease and at 30 minutes both methods have similar percentages of phosphorylation. This suggests that the model has similar percentages of phosphorylation to the experiments at 10 minutes and at 30 minutes after stimulation with a low concentration of Ang1.

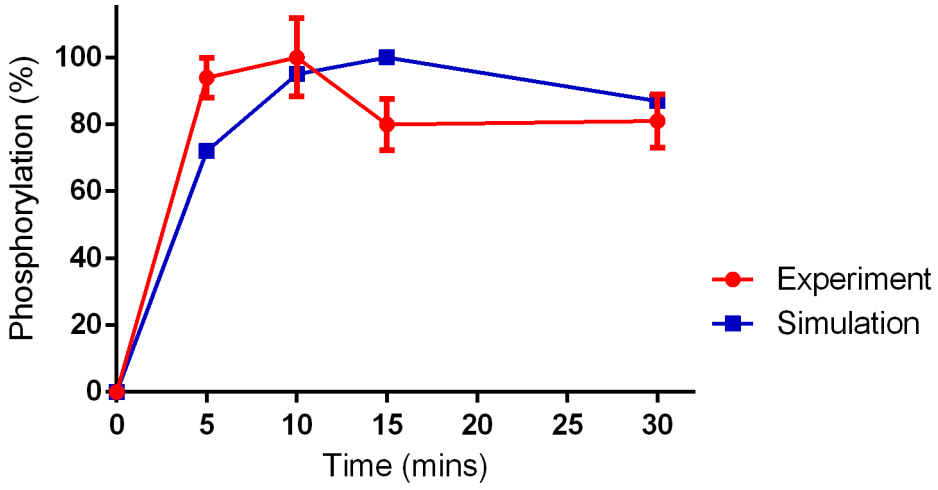

Figure 6.3: Comparison- Time-course for low concentration Ang1-induced Tie2 phosphorylation (including the dephosphorylation reaction).
Normalised experimental and simulation data of the time-course for low Ang1 (50ng/ml) induced Tie2 phosphorylation were compared. Initially the percentages of phosphorylated Tie2 are different, however they are similar at 10 and 30 minutes. Maximum phosphorylation is reached at 10 minutes in the experiment and at 15 minutes in the simulation. Experimental data is presented as mean and SEM of relative maximal phosphorylation (n=4). The comparison of experiment to simulation is not significant (p<0.05), Two-way ANOVA.

6.1.2. Time-course of Tie2 activation with high Ang1.

6.1.2.1. Simulations

Simulations of the full model including the dephosphorylation reaction were performed by running the model to simulate 30 minutes (1800 seconds) stimulation with 200 ng/ml of Ang1 (0.714 nM).

Figure 6.4A shows how the concentration of total phosphorylated Tie2 changes over time. The model suggests that activated Tie2 on the cell surface peaks at 100 seconds, and total phosphorylation reaches maximum at 600 seconds. The majority of activated Tie2 is internalised and is gradually degraded at a constant rate. The concentration of phosphorylated Tie2 induced by 200 ng/ml Ang1 stimulation is higher than for 50 ng/ml Ang1 stimulation.

The total amount of phosphorylated Tie2 (cell surface and internalised) at each time-point was calculated as a percentage of maximal phosphorylation. The rate of percentage change in phosphorylation is shown over time in minutes (Figure 6.4B). Simulation of the model suggests that maximum phosphorylation is reached at 10 minutes with 200 ng/ml Ang1 stimulation.

A

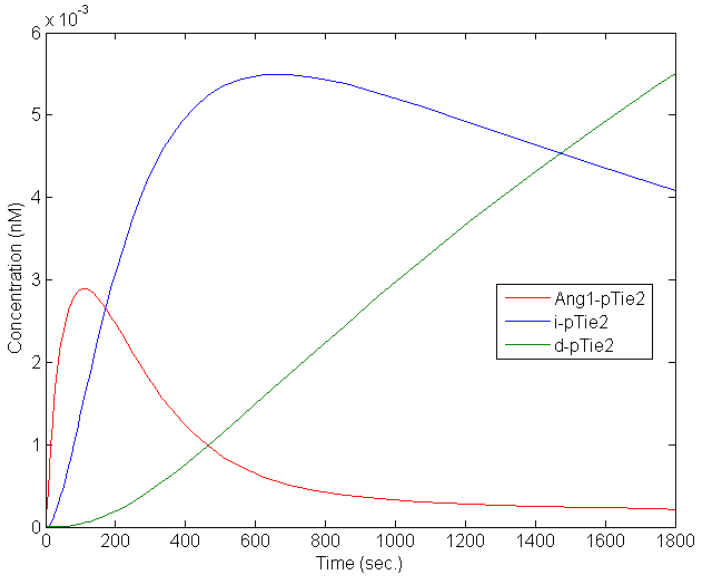

B

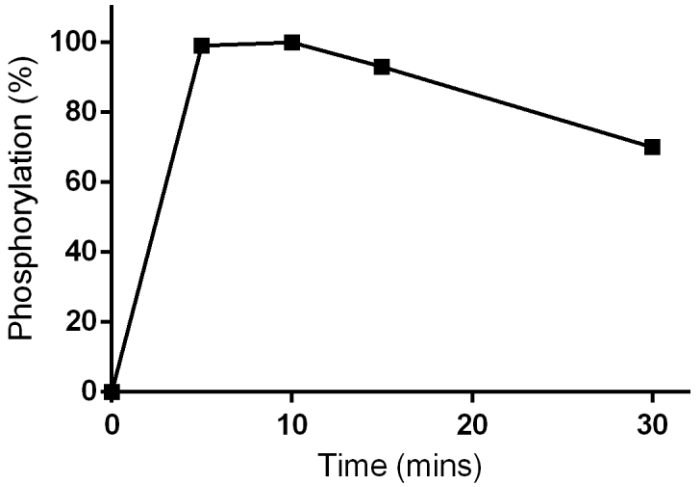

Figure 6.4: Simulation- Time-course for high concentration Ang1-induced Tie2 phosphorylation (including the dephosphorylation reaction).

A. The model including the dephosphorylation reaction was simulated with 200 ng/ml Ang1 for 1800 seconds. The time-course plot shows the change in concentrations of phosphorylated Tie2 (Ang1-pTie2), internalised phosphorylated Tie2 (i-pTie2) and degraded phosphorylated Tie2 (d-pTie2). The level of Tie2 phosphorylation on the cell surface peaks after 100 seconds stimulation with maximum total phosphorylation at 600 seconds. Most of the phosphorylated Tie2 is internalised into the cell and gradually degraded.

B. Total phosphorylated Tie2 (cell surface and internalised) was calculated as a percentage of maximal phosphorylation and plotted against the time-point in minutes. Maximum phosphorylation of Tie2 is reached at 10 minutes of stimulation.

6.1.2.2. Experiments

The rate of Tie2 activation with a high Ang1 concentration (200 ng/ml Ang1) was repeated again as described in Chapter 5.6.2.2 only this time without the addition of vanadate. Due to the time constraints of the project, the experiments were performed by Dr Tariq Tahir. Tie2 phosphorylation was normalized to Tie2 and the percentage phosphorylation was calculated as a percentage of maximal phosphorylation at each time point. Figure 6.5 shows the change of percentage phosphorylation over 30 minutes stimulation. Tie2 phosphorylation reaches a maximum at 15 minutes and plateaus.

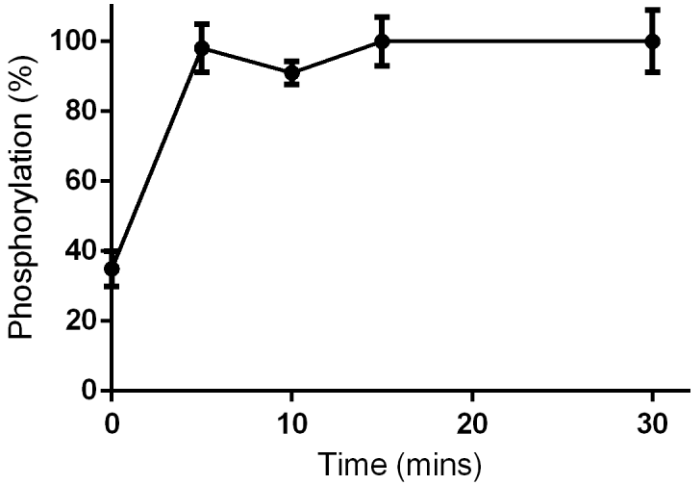

Figure 6.5: Experiment- Time-course for high concentration Ang1-induced Tie2 phosphorylation (without vanadate reaction).
A. The time-course for 200 ng/ml Ang1 induced Tie2 phosphorylation without vanadate was performed in HUVECs (by Dr Tariq Tahir). The plot shows the change of percentage phosphorylation over 30 minutes stimulation. A plateau is reached at 5 minutes with maximum phosphorylation at 15 minutes. Phosphorylation is normalized to Tie2 and is shown as a percentage of maximal phosphorylation. Data is presented as mean and SEM of relative maximal phosphorylation (n=4). All data is significant to control (p<0.05), One-way ANOVA.

6.1.2.3. Comparison of simulation and experimental time-courses for high Ang1-induced Tie2 phosphorylation (with dephosphorylation)

The total percentage phosphorylation from the experimental data was compared to the simulation data and a graph was plotted of the percentage change in Tie2 phosphorylation over time for both sets of data. Figure 6.6 shows that maximum phosphorylation is reached at 15 minutes in experiments and at 10 minutes in the simulation. After 10 minutes the level of phosphorylation in experiments remains the same while the levels in the simulation begin to decrease. However at 15 minutes the level of phosphorylation in the simulation is within the SEM range of the experiment. This suggests that the model is similar to the experiments for the first 15 minutes of stimulation with a high concentration of Ang1. Although there is a slight decrease in phosphorylation at 10 minutes in experiments.

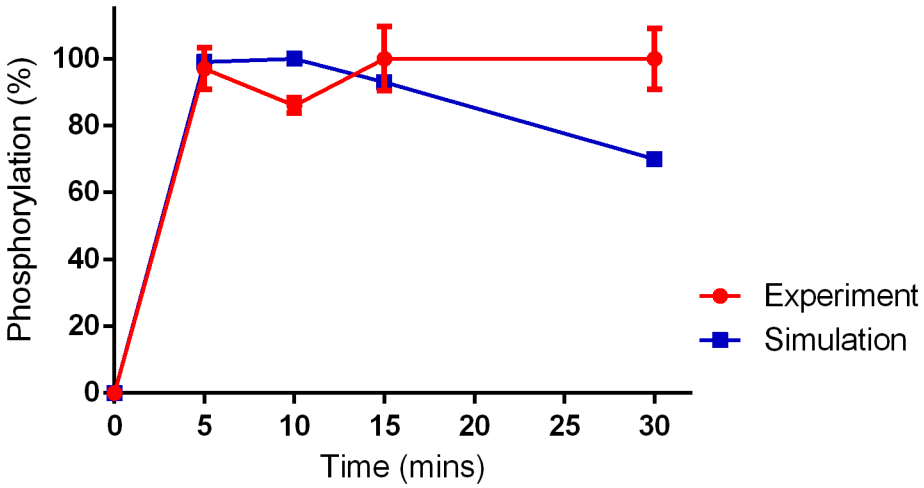

Figure 6.6: Comparison- Time-course for high concentration Ang1-induced Tie2 phosphorylation (including the dephosphorylation reaction).
Experimental and simulation data of the time-course for high Ang1 (200 ng/ml) induced Tie2 phosphorylation were compared. Initially the percentages of phosphorylated Tie2 are similar, however maximum phosphorylation is reached at 15 minutes in the experiment and at 10 minutes in the simulation. After 15 minutes the level of phosphorylation in experiments remains the same while the levels in the simulation begin to decrease. However at 15 minutes the level of phosphorylation in the simulation is within the SEM of the experiment. Phosphorylation is normalized to Tie2 and is shown as a percentage of maximal phosphorylation. Experimental data is presented as mean and SEM of relative maximal phosphorylation (n=4). The comparison of experiment to simulation is not significant (p<0.05), Two-way ANOVA.

6.1.3. The concentration-dependent effect of Ang1 on Tie2 activation

6.1.3.1. Simulation

The model was simulated for 30 minutes each time with an increasing concentration of Ang1; 0.0357 nM (10 ng/ml), 0.0893 nM (25 ng/ml), 0.179 nM (50 ng/ml), 0.357 nM (100 ng/ml), 0.714 nM (200 ng/ml). The total concentration of phosphorylated Tie2 (surface and internalised) was quantified after 15 minutes.

The percentage of maximal Tie2 phosphorylation was calculated for each Ang1 concentration with 200 ng/ml Ang1 being 100% phosphorylation. The total percentage phosphorylation was plotted against the Ang1 concentration to produce the concentration-dependent curve (Figure 6.7). The simulation results suggest that phosphorylation increases with up to 50 ng/ml Ang1 treatment and then plateaus after 100 ng/ml Ang1.

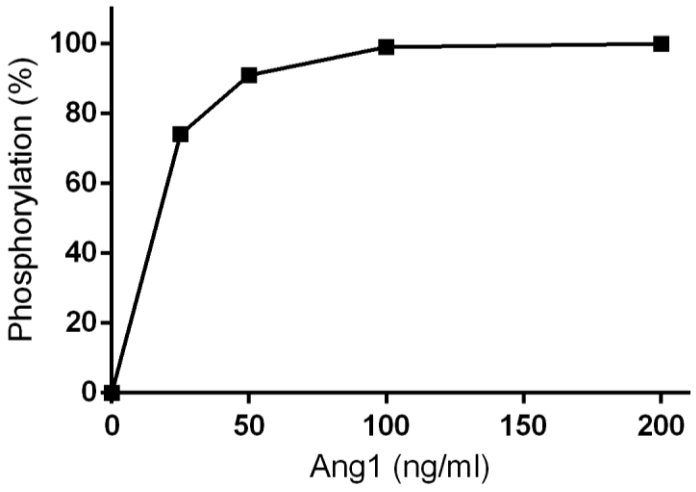

Figure 6.7: Simulation- The concentration dependent effect of Ang1 on Tie2 phosphorylation (including the dephosphorylation reaction).
The model was simulated with various concentrations of Ang1 and the concentration of Tie2 phosphorylated was quantified after 15 minutes of stimulation. The percentage of maximal Tie2 phosphorylation was calculated for each Ang1 concentration. The graph shows that the percentage of Tie2 phosphorylation increases with Ang1 and plateaus after stimulation with 100 ng/ml Ang1.

6.1.3.2. Experiments

The experiments to determine the concentration dependent effect of Ang1 on Tie2 activation was repeated again. The experiments were performed as described in Chapter 5.6.3.2 (without the addition of vanadate) by Dr Tariq Tahir.

Tie2 phosphorylation in samples was expressed as a percentage of maximal phosphorylation and were plotted against the relative concentrations of Ang1 treatment (Figure 6.8). The graph in Figure 6.8 shows that there is an increase in phosphorylated Tie2 in samples treated up to 25 ng/ml Ang1 and then the level of phosphorylation plateaus. There is a second increase in phosphorylation after 50 ng/ml Ang1 which plateaus at 100 ng/ml Ang1.

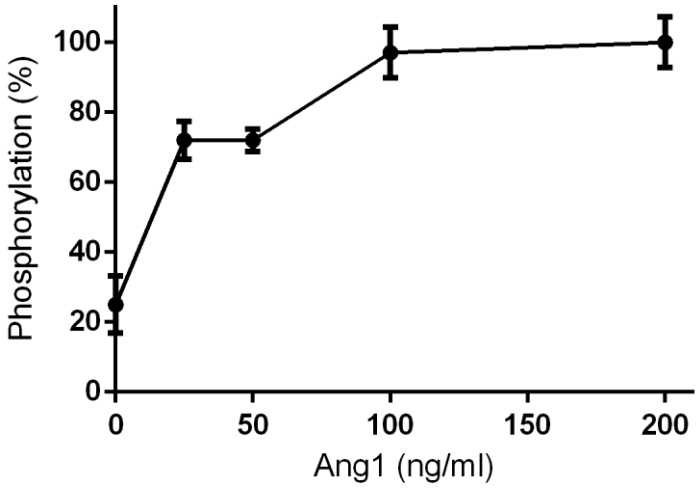

Figure 6.8: Experiment- The concentration dependent effect of Ang1 on Tie2 phosphorylation (without vanadate).
The concentration dependent effect of Ang1 on Tie2 phosphorylation without vanadate was performed in HUVECs (by Dr Tariq Tahir). The percentage of maximal Tie2 phosphorylation (200 ng/ml is 100% phosphorylation) was calculated and plotted against the respective concentration. There is an increase of phosphorylated Tie2 in samples treated with 0 - 200 ng/ml. However there is a plateau at 50 ng/ml Ang1. Phosphorylation is normalized to Tie2 and is shown as a percentage of maximal phosphorylation. Data is presented as mean and SEM of relative maximal phosphorylation (n=3). All data is significant to no Ang1 (p<0.05), One-way ANOVA.

6.1.3.3. Comparison of simulation and experimental concentration dependence curves of Ang1-induced Tie2 phosphorylation (with dephosphorylation).

The relative effect of Ang1 concentration on Tie2 activation without the addition of vanadate in experiments (normalised data) and simulations was compared. The percentage change of Tie2 phosphorylation over the concentration of Ang1 from the simulation data and experimental data are shown in Figure 6.9. Both methods show a concentration dependent increase in Tie2 phosphorylation with maximum phosphorylation being achieved with 200 ng/ml Ang1. The levels of phosphorylation are similar for 25, 100 and 200 ng/ml Ang1 stimulation.

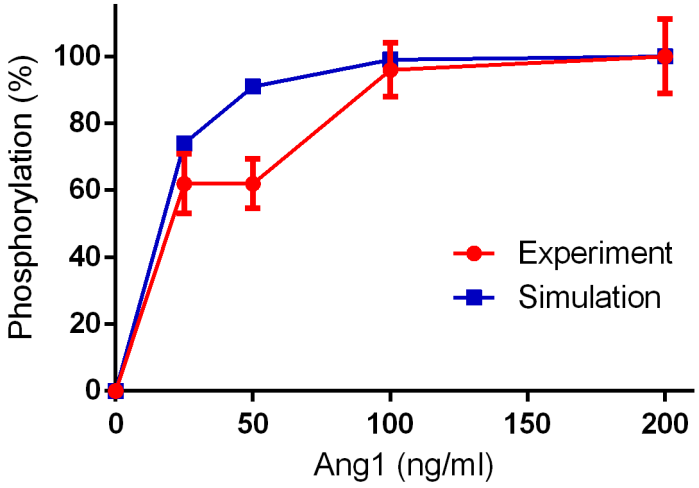

Figure 6.9: Comparison- The concentration dependent effect of Ang1 on Tie2 phosphorylation (including the dephosphorylation reaction).
Experimental and simulation data of the Ang1 concentration dependent curve of Tie2 phosphorylation with dephosphorylation was compared. The plot shows the change of percentage phosphorylation with increasing Ang1 stimulation. The percentage phosphorylation in both methods is similar for 25, 100 and 200 ng/ml Ang1. Maximum phosphorylation is attained with 200 ng/ml Ang1 in both the experiment and simulation Phosphorylation is normalized to Tie2 and is shown as a percentage of maximal phosphorylation. Experimental data is presented as mean and SEM of relative maximal phosphorylation (n=3). The comparison of experiment to simulation is not significant (p<0.05), Two-way ANOVA.

6.2. Validating the effects of Ang2 on Tie2 activation (with dephosphorylation)

6.2.1. The concentration-dependent effect of Ang2 on Tie2 phosphorylation

6.2.1.1. Simulation

A simulation of the model was performed to validate the concentration-dependent effect of Ang2 on Tie2 phosphorylation. The model was simulated (including the dephosphorylation reaction) each time with various concentrations of Ang2; 50, 100, 200, 500, 800 and 1000 ng/ml. The percentage change of Tie2 phosphorylation was calculated and plotted (Figure 6.10). The simulation shows an increase in phosphorylation and a plateau after reaching maximum phosphorylation with 200 ng/ml Ang2.

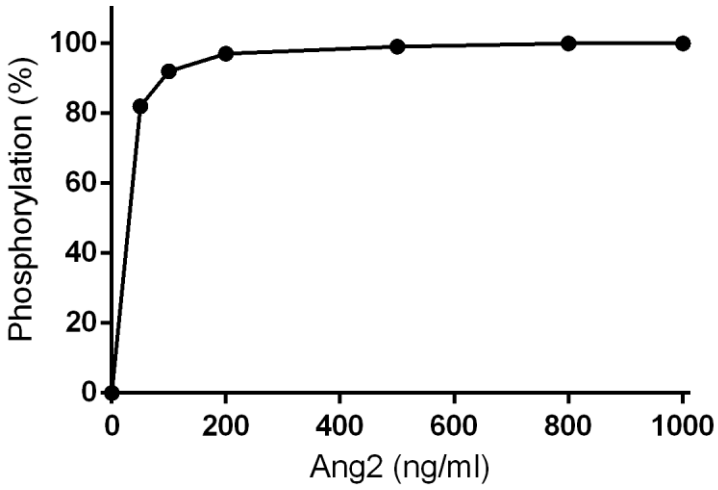

Figure 6.10: Simulation- The concentration dependent effect of Ang2 on Tie2 phosphorylation (including the dephosphorylation reaction).
The model was simulated each time with various concentrations of Ang2; 50, 100, 200, 500, 800 and 1000 ng/ml. The amount of Tie2 phosphorylated at 15 minutes was quantified and the percentage of maximal phosphorylation was calculated. The simulations show an increase in phosphorylation with a plateau in phosphorylation being reached with 200ng/ml Ang2. With higher concentrations of Ang2 the levels of phosphorylation remains at maximum suggesting saturation of Tie2. Phosphorylation is shown as a percentage of maximal phosphorylation.

6.2.1.2. Experiment

The experiments to determine the relative effect of Ang2 concentration on Tie2 activation was repeated again. The experiments were performed as described in Chapter 5.8.1.2 (without the addition of vanadate). In this experiment the Supersignal ECL solution (Pierce) was used to detect picomolar levels of protein. The CCD imager failed to detect phospho-Tie2 specific bands. This may be due to the low levels of Ang2-induced phosphorylation and rapid dephosphorylation as no vanadate was used to inhibit dephosphorylation and preserve phosphorylation. Thus validation of the concentration-dependent effect of Ang2 on Tie2 phosphorylation and the time-course of Ang2 on Tie2 phosphorylation could not be performed.

Alternatively a study by Bogdanovic and colleagues has demonstrated that Ang2 phosphorylates Tie2 in a concentration dependent manner with maximal phosphorylation being observed at 800 ng/ml (Bogdanovic *et al.*, 2006). However this study was performed using a different method and will be discussed further in section 6.4.2.

6.3. Validating the effect of Ang2 on Ang1-induced Tie2 activation (with dephosphorylation)

6.3.1. Simulation

To validate the effect of Ang2 on Ang1-induced Tie2 phosphorylation the model was simulated with 50 ng/ml Ang1 and increasing concentrations of Ang2.

Figure 6.11 shows the change in total Tie2 phosphorylation over the concentration of Ang2 for each simulation. The model simulation suggests that Ang1-induced Tie2 phosphorylation is reduced by over 50% with 200 ng/ml Ang2 treatment. This effect plateaus after treatment with 500 ng/ml Ang2.

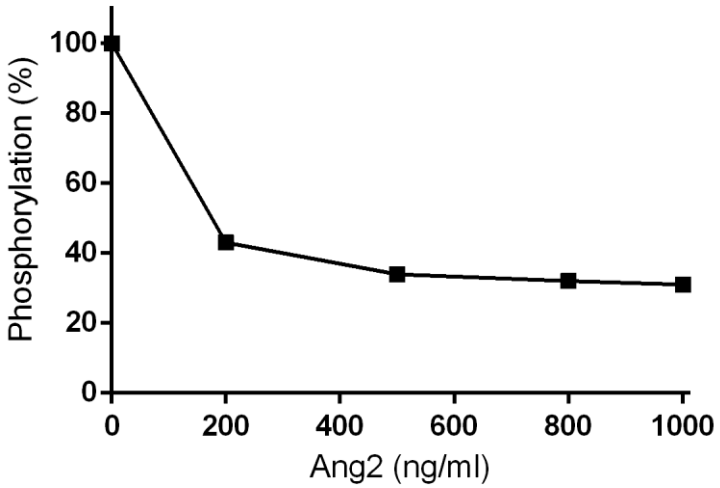

Figure 6.11: Simulation- The concentration dependent effect of Ang2 on Ang1-induced Tie2 phosphorylation (including the dephosphorylation reaction).
The model was simulated for 1800 seconds with 50 ng/ml and increasing concentrations of Ang2. The total concentration of Tie2 phosphorylation was calculated after 15 minutes of simulation. The graph shows that treatment with 200 ng/ml Ang2 decreases Tie2 phosphorylation by over 50%. The inhibitory effect of Ang2 plateaus with concentrations greater than 500 ng/ml Ang2.

6.3.2. Experiments

As shown in previous experiments Ang1 stimulation produces quantifiable levels of Tie2 phosphorylation in HUVECs. Hence if Ang1 is used to increase Tie2 phosphorylation the levels of phosphorylation should be high enough to detect the effects of Ang2. This effect of Ang2 on Ang-induced Tie2 phosphorylation in experiments can be used to validate the model.

Experiments were performed to determine the effect of Ang2 on Ang1-induced Tie2 phosphorylation, and also to validate this in the model. HUVECs were prepared (as described in Chapter 2.4), serum-starved for one hour, treated with increasing concentrations of Ang2 for 5 minutes (no vanadate treatment), and followed by stimulation with a low concentration of Ang1 for 15 minutes. Samples were collected and proteins were resolved and blotted as described previously. The membrane was probed for phosphorylated Y^{992}-Tie2 and reprobed for Tie2. As Ang1 is present in the samples the levels of phosphorylated Tie2 was high enough to detect.

The results in Figure 6.12 show that Ang2 has a slight antagonist effect on Ang1 induced phosphorylation.

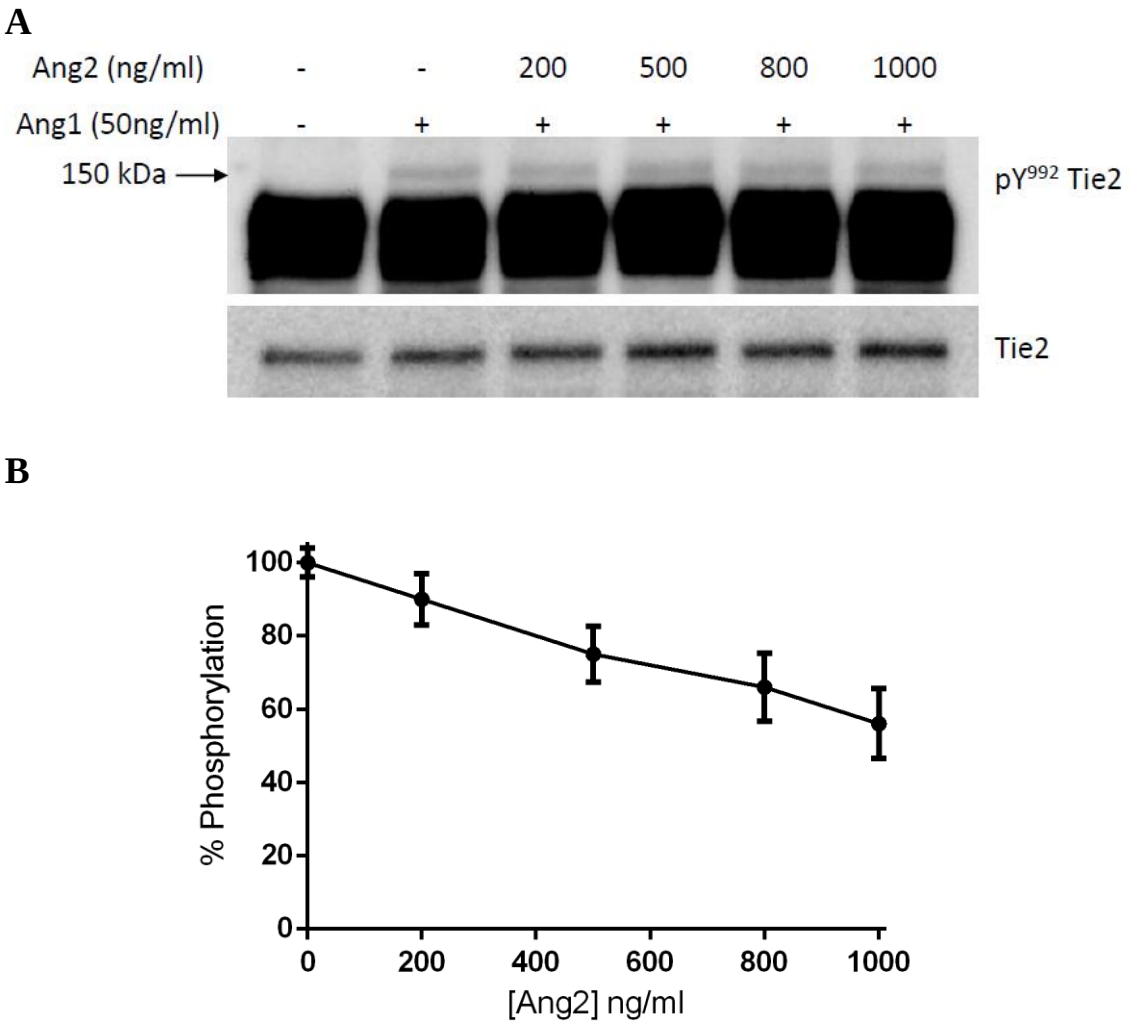

Figure 6.12: Experiment- The concentration dependent effect of Ang2 on Ang1-induced Tie2 phosphorylation (without vanadate).

A. Cells were serum-starved, treated with vanadate, and stimulated with Ang1 and increasing concentrations of Ang2 for 15 minutes. The protein was resolved using SDS-PAGE and probed for phosphorylated Y^{992} Tie2. Chemiluminescence was detected using a CCD imager. The blot shows a slight decrease in phosphorylation with increasing concentrations of Ang2. The blot was reprobed for Tie2 to normalize results.

B. The percentage phosphorylation of Y^{992}-Tie2 was calculated and plotted to show the change of percentage phosphorylation over increasing Ang2 for 4 experiments. The graph shows that the level of phosphorylation gradually decreases. Phosphorylation is normalized to Tie2 and is shown as a percentage of maximal phosphorylation. Data is presented as mean and SEM of relative maximal phosphorylation (n=4). Data is significant for 800 and 1000 ng/ml in comparison to Ang1 only (p<0.05), One-way ANOVA.

6.3.3. Comparison of simulation and experimental effects of Ang2 on Ang1-induced Tie2 phosphorylation (with dephosphorylation).

The experimental results (normalised) were compared to the simulation results to determine whether the model is valid for effects of combined Ang1 and Ang2 treatment on Tie2 phosphorylation. Figure 6.13 shows that the levels of phosphorylation in both methods are different. Although both methods show that Ang2 plays an inhibitory role, Ang2 in experiments does not have a major inhibitory effect on Tie2 phosphorylation unlike Ang2 in the model, which inhibits phosphorylation by over 50% with 200ng/ml treatment.

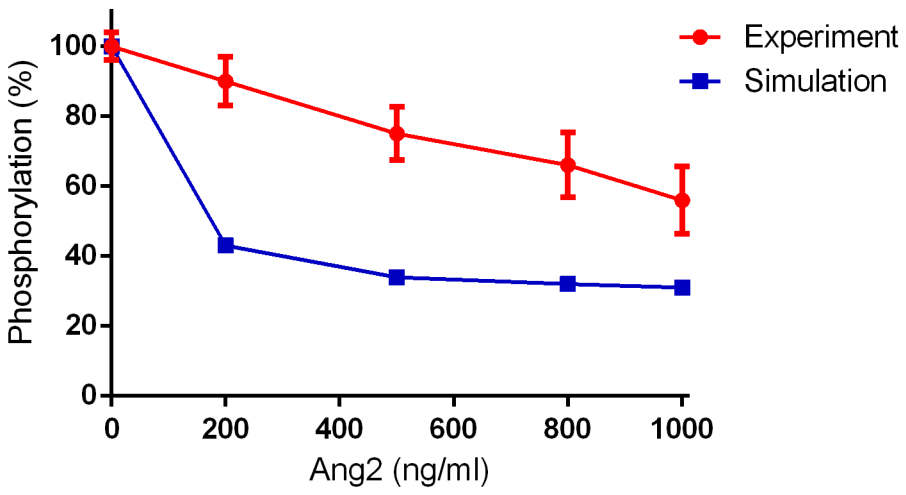

Figure 6.13: Comparison- The concentration dependent effect of Ang2 on Ang1-induced Tie2 phosphorylation (including the dephosphorylation reaction).
The simulation effect of increasing Ang2 on Ang1 and Ang2-induced Tie2 phosphorylation (blue) was compared to the effect in experiments (red). The simulation and experiments show that Ang2 inhibits Tie2 phosphorylation however the model simulations suggest that Ang2 has a bigger effect than shown in experiments. Experimental data is presented as mean and SEM of relative maximal phosphorylation and normalized to Tie2 (n=4). The comparison of experiment to simulation is significant (p<0.05), Two-way ANOVA.

The simulation shows that Ang2 has a greater effect on Tie2 phosphorylation than in experiments. This suggests that the binding of Ang2 to Tie2 is too high and therefore binds more Tie2 which decreases the amount of free Tie2 required for Ang1-induced Tie2 phosphorylation. Hence the binding affinity and binding association parameters used in the model produces simulation results which do not fit the experimental data.

To address this the value for Ang2 k_{on} was changed and used in simulations until the simulation plot matched the experimental data (Figure 6.14). The k_{off} remained at 0.0096 s^{-1} as this is an experimentally measured value (Steele, 2013). The values substituted for k_{on} were; 0.0094 (original value), 0.006, 0.00094, 0.0006 $nM^{-1}s^{-1}$.

Figure 6.4 shows that the results produce a near perfect fit when k_{on} is 0.0006 $nM^{-1}s^{-1}$ and k_{off} is 0.0096 s^{-1}. However using these values increases the K_D to 16 nM which is higher than the measured values; 1.026 ± 0.22 nM (Steele, 2013) and 3 nM (Maisonpierre *et al.*, 1997). Moreover as the measured values were determined *in vitro* from DT40 cells with the over expression of Tie2 these values may differ from the actual *in vivo* values.

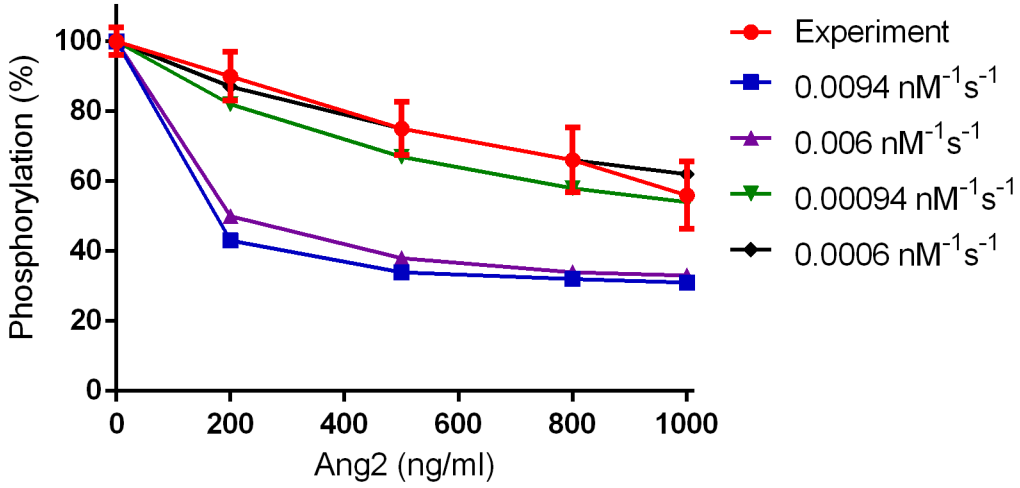

Figure 6.14: Comparison- The concentration dependent effect of Ang2 on Ang1-induced Tie2 phosphorylation (including the dephosphorylation reaction, using various parameters).
The model was simulated for 30 minutes with 50 ng/ml Ang1 and increasing concentrations of Ang2. The Ang2 k_{on} binding parameters for Ang2 was changed each time; 0.0094 $nM^{-1}s^{-1}$ (blue), 0.006 $nM^{-1}s^{-1}$ (purple), 0.00094 $nM^{-1}s^{-1}$ (green) and 0.0006 $nM^{-1}s^{-1}$ (black). The k_{off} parameter remained at 0.0096 s^{-1}. The percentage phosphorylation was compared to the experiments (red). The plot shows that decreasing the k_{on} parameter decreases the effect of Ang2 on Tie2 phosphorylation. The 0.0006 $nM^{-1}s^{-1}$ k_{on} parameter produces the best fit with the experimental data. Experimental data is presented as mean and SEM of relative maximal phosphorylation and normalized to Tie2 (n=3).

The parameters were modified again using the K_D of 3 nM and k_{on} as 0.0006 $nM^{-1}s^{-1}$. From these values the k_{off} was calculated to be 0.0018 s^{-1}. This k_{off} parameter has a 2-fold difference to that of Ang1 (k_{off} is 0.0043 s^{-1}). Furthermore this parameter is suitable to use as it has been shown that Ang2 is released faster than Ang1 after binding (Bogdanovic *et al.*, 2006).

The model was simulated with the new parameter values and the results were compared to the experimental data (Figure 6.15). The simulation results are similar to the experimental results even though the K_D and k_{off} have changed.

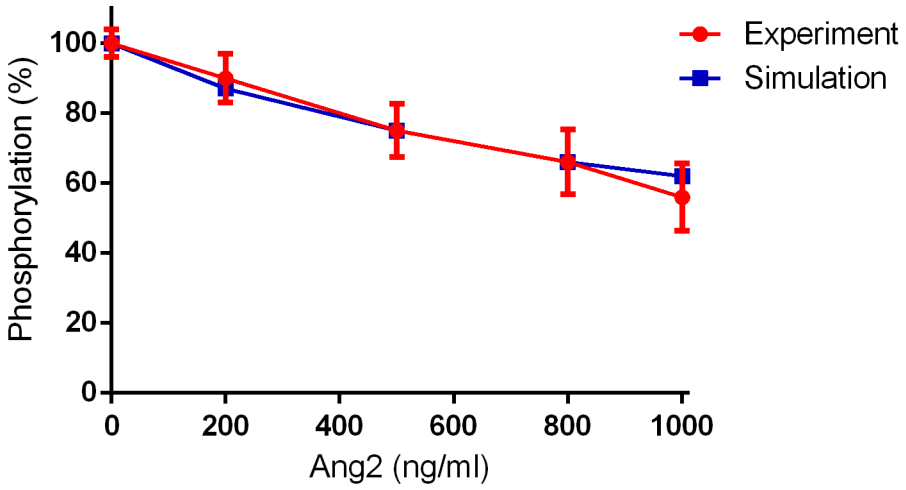

Figure 6.15: Comparison- The concentration dependent effect of Ang2 on Ang1-induced Tie2 phosphorylation (including the dephosphorylation reaction, with new parameters). The model was simulated using the new parameters for Ang2 binding; K_D is 3 nM, k_{on} is 0.0006 $nM^{-1}s^{-1}$, k_{off} is 0.0018 s^{-1}. The simulation effect of increasing Ang2 on Ang1-induced Tie2 phosphorylation (blue) was compared to the effect in HUVEC experiments (red). The model and experiment are very similar and show that Ang2 inhibits Tie2 phosphorylation in a concentration dependent manner. Phosphorylation is shown as a percentage of maximal phosphorylation. Experimental data is presented as mean and SEM of relative maximal phosphorylation and normalized to Tie2 (n=3). The comparison of experiment to simulation is not significant (p<0.05), Two-way ANOVA.

6.4. The re-analysed concentration-dependent effect of Ang2 on Tie2 activation (with dephosphorylation).

In order to redefine the model and test whether the new binding parameter values are correct the Ang2 section of the model was reanalysed for validation.

6.4.1. Simulation using new binding parameter values.

The model was simulated including the dephosphorylation reaction as previously described in section 6.2.1.1., and also using new binding parameter values. The concentrations of Ang2 used in each simulation were; 50, 100, 200, 500, 800 and 1000 ng/ml. The percentage change of Tie2 phosphorylation was calculated and plotted (Figure 6.16). The simulation shows a concentration dependent increase in phosphorylation.

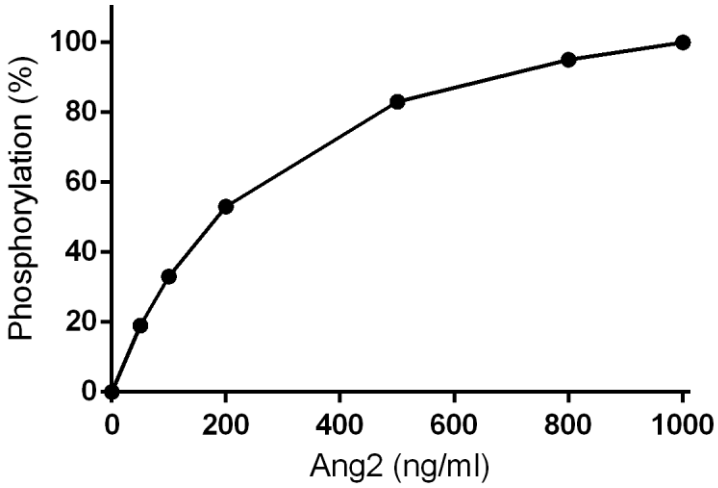

Figure 6.16: Simulation- The concentration dependent effect of Ang2 on Tie2 phosphorylation (including the dephosphorylation reaction and new binding parameters). The model was simulated each time with various concentrations of Ang2; 50, 100, 200, 500, 800 and 1000 ng/ml. The amount of Tie2 phosphorylated at 15 minutes was quantified and the percentage of maximal phosphorylation was calculated. The simulations show an increase in phosphorylation with increasing concentrations of Ang2.

6.4.2. Comparison of simulation and literature data on Ang2 –induced Tie2 activation (with dephosphorylation).

As mentioned in section 6.2.1.2, a study on the Ang2 concentration dependent effect on Tie2 activation has been published by Bogdanovic and colleagues (Bogdanovic *et al.*, 2006). This study also used HUVECs stimulated for 15 minutes with increasing concentrations of Ang2. Although the cells were lysed with radio immunoprecipitation lysis buffer and samples were immunoprecipitated for Tie2 before resolving the proteins by SDS-PAGE. The blot was probed for anti-phosphotyrosine antibody 4G10 (Upstate) and not the specific phosphorylated tyrosine 992 (Bogdanovic *et al.*, 2006).

The simulation results were compared to the data in the study by Bogdanovic and colleagues to determine whether the model could potentially be valid for effects of Ang2 treatment on Tie2 phosphorylation. Figure 6.17 shows Ang2 phosphorylates Tie2 in a concentration dependent manner. Furthermore the levels of phosphorylation for each simulated Ang2 concentration is close to the percentage phosphorylation demonstrated by Bogdanovic and colleagues.

However as this study was performed using a different method, this comparison does not fully confirm the validity of the model. It can only imply that the model could potentially be valid for the Ang2 concentration dependent effect on Tie2 activation.

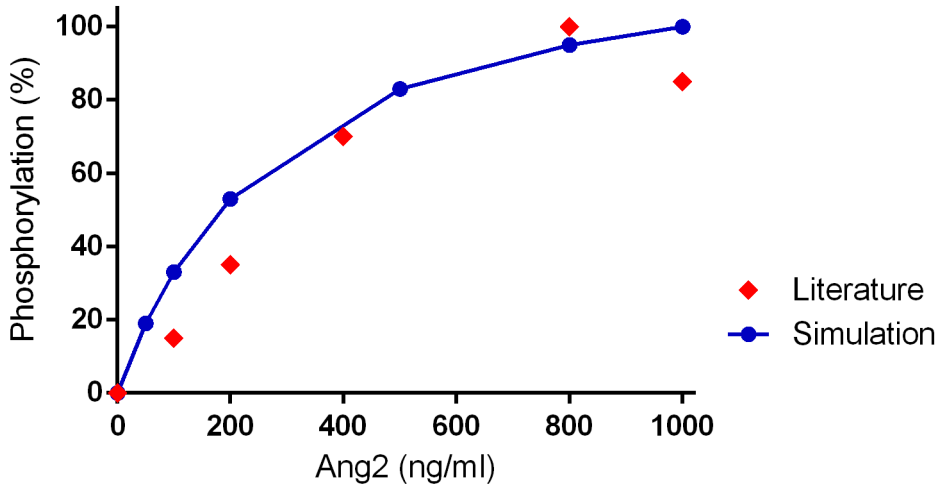

Figure 6.17: Comparison of simulation and literature on the concentration dependent effect of Ang2 on Tie2 phosphorylation (including the dephosphorylation reaction and new binding parameters).

The effect of increasing Ang2 on Tie2 phosphorylation in the simulation (blue) was compared to the effect demonstrated in a study by (Bogdanovic *et al.*, 2006) (red). The model simulation results show that the percentage of maximum phosphorylation for each Ang2 concentration is close to the percentage phosphorylation demonstrated by Bogdanovic and colleagues. Phosphorylation is shown as a percentage of maximal phosphorylation. The comparison of literature to simulation is not significant ($p<0.05$), Two-way ANOVA.

6.5. The re-analysed concentration-dependent effect of Ang2 on Tie2 activation (without dephosphorylation).

6.5.1. Simulation using new binding parameter values.

To determine whether the new binding parameter values produce valid simulations for the model without dephosphorylation, the model simulation as described in Chapter 5.8.1.1 was repeated. This simulation was without the dephosphorylation reaction, and used the new binding parameter values and varying concentrations of Ang2; 50, 100, 200, 500, 800 and 1000 ng/ml. The percentage change in total phosphorylated Tie2 was calculated and plotted.

The graph of percentage change of phosphorylated Tie2 over increasing Ang2 (Figure 6.18A) suggests that Ang2 induces Tie2 phosphorylation in a concentration dependent manner.

The agonist activity of Ang2 was also compared to the agonist activity of Ang1. The levels of Ang1-induced and Ang2-induced Tie2 phosphorylation from both Ang1 and Ang2-induced simulations (in Figures 5.14 and 6.18A) were compared. Figure 6.18B shows the percentage Tie2 phosphorylation induced by increasing concentrations of Ang1 and Ang2. The percentages of phosphorylation are shown as a percentage of maximal Ang1-induced phosphorylation. The comparison with Ang1 shows that Ang2 has a partial agonist effect which is around 10% of the maximum Ang1-induced Tie2 phosphorylation.

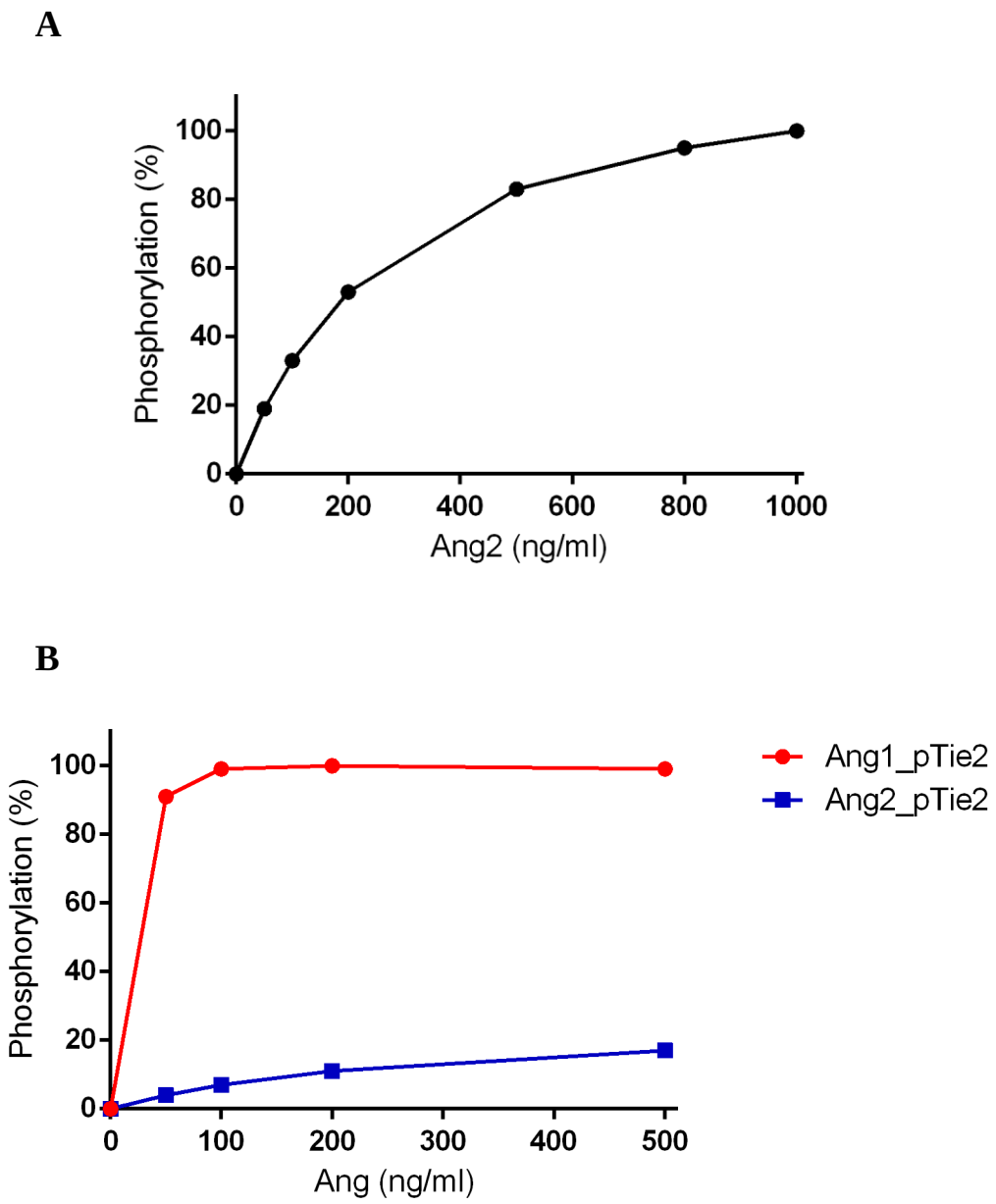

Figure 6.18: Simulation- The concentration dependent effect of Ang2 on Tie2 phosphorylation (no dephosphorylation reaction and with new binding parameters).
A. The model using the new parameter values and without the dephosphorylation reaction was simulated for various concentrations of Ang2; 50, 100, 200, 500, 800 and 1000 ng/ml. The effect on Tie2 phosphorylation at 15 minutes was quantified and the percentage phosphorylation for each concentration was plotted. The simulations show an increase in phosphorylation.
B. The percentage Tie2 phosphorylation induced by increasing concentrations of Ang1 (from previous simulations) and Ang2 were compared. The percentages of phosphorylation are shown as a percentage of maximal Ang1-induced phosphorylation. Ang2 has a partial agonist effect which is around 10% of maximum Ang1-induced Tie2 phosphorylation.

6.5.2. Comparison of simulation and experimental concentration dependence curves of Ang2-induced Tie2 phosphorylation (without dephosphorylation).

The simulation results of increasing Ang2 concentration on Tie2 activation were compared to the experimental results from Chapter 5.8.1.2. Figure 6.19 shows that both methods have different percentages of Tie2 phosphorylation for all concentrations of Ang2, apart from 500 ng/ml Ang2 which for the simulation is within the standard error range for the mean value in experiments. This comparison suggests that using the new binding parameter values for simulating the model without the dephosphorylation reaction is not valid for the Ang2 effects on Tie2 phosphorylation. However the statistical analysis suggests that the comparison is not significant.

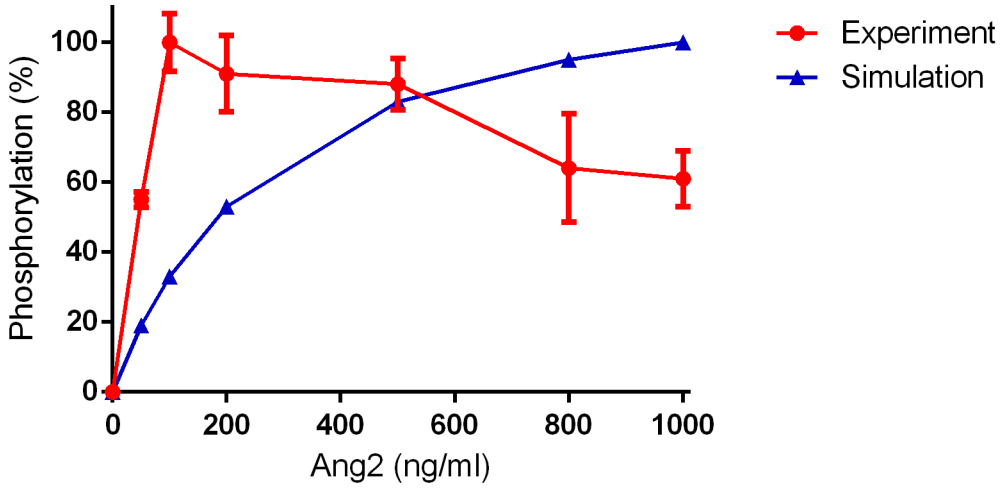

Figure 6.19: Comparison- The concentration dependent effect of Ang2 on Tie2 phosphorylation (no dephosphorylation reaction and new binding parameters).
The simulation effect of increasing Ang2 on Tie2 phosphorylation was compared to the effect in HUVEC experiments. Both methods show an increase in phosphorylation however the percentage phosphorylation is only similar for 500 ng/ml Ang2. Phosphorylation is shown as a percentage of maximal phosphorylation. Experimental data is presented as mean and SEM of relative maximal phosphorylation (n=5). The comparisons of the experiment to simulation and between concentrations is not significant (p<0.05), Two-way ANOVA.

6.6. The re-analysed effect of Ang2 on Tie1, Tie2 and Tie1:Tie2 equilibrium.

The simulation from Chapter 5.5 was repeated to examine how the equilibrium between Tie1, Tie2 and Tie1:Tie2 is affected by adding Ang2 using the new parameter values for Ang2 binding. The model was simulated for 30 minutes with 200 ng/ml Ang2, and the initial concentration of new Tie2.

The simulation plots in Figure 6.20 show that unlike the effect of Ang1 and the previous analysis for Ang2 (Figure 5.7), Ang2 induces a lower amount of Tie1:Tie2 dissociation. 32% of the initial Tie1:Tie2 concentration has been dissociated. The amount of free Tie1 increases whilst the amount of free Tie2 decreases. Adding the Tie2 replenishment reaction to the model shows that the concentration of nTie2 gradually decreases over time however the concentration of free Tie2 is not replenished to the initial concentration. The concentrations of Ang2 binding to Tie1:Tie2 gradually increases and reaches a plateau around 900 seconds although the concentrations of complex formed are very low.

This analysis suggests that on the addition of Ang2 the equilibrium between Tie1, Tie2 and Tie1:Tie2 shifts to favour free Tie1 and Tie2 by dissociating the Tie1:Tie2 heterodimer.

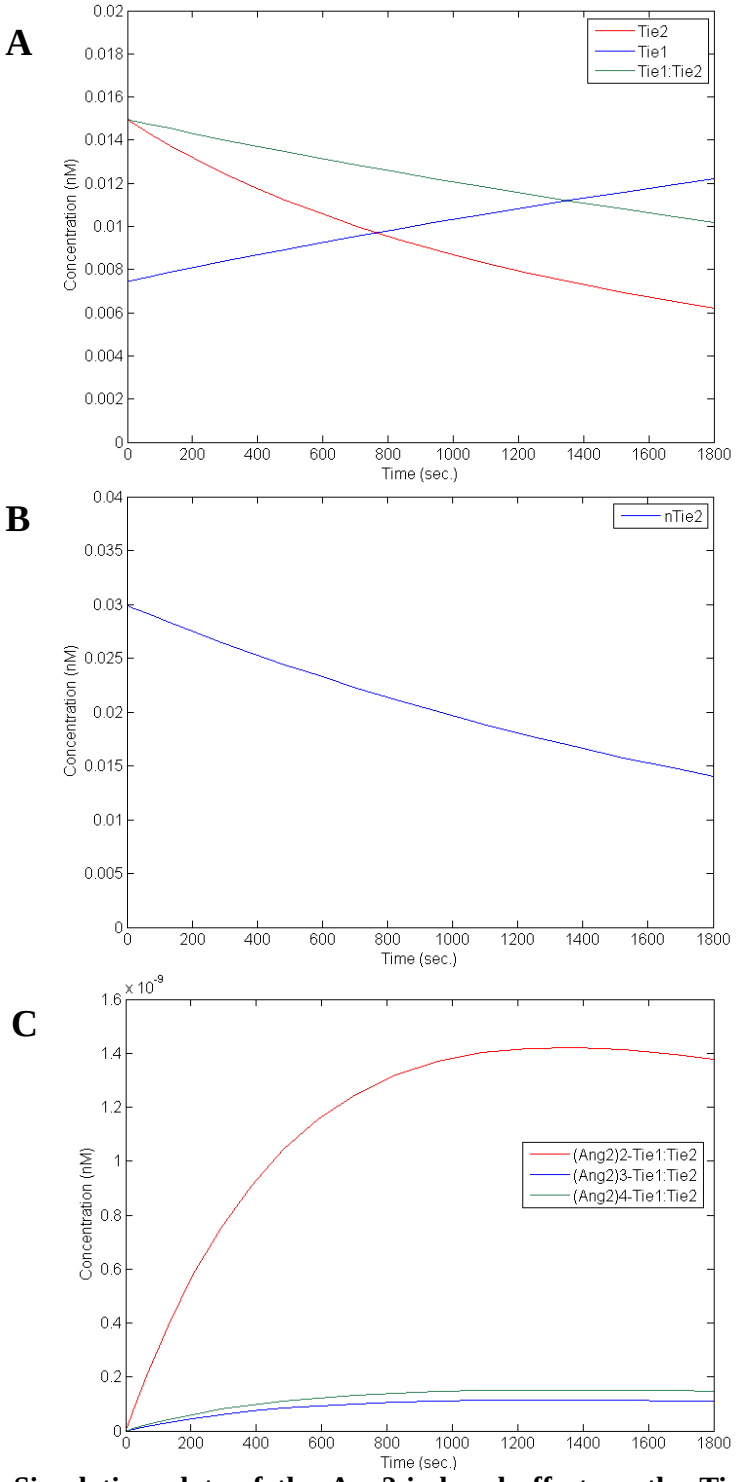

Figure 6.20: Simulation plots of the Ang2-induced effect on the Tie1, Tie2, Tie1:Tie2 equilibrium (including the dephosphorylation reaction and new binding parameters).
Simulation of the model was performed for 1800 seconds (30 minutes) with the addition of 200 ng/ml Ang2 and 0.299 nM new Tie2 (nTie2).
Plot A, shows the concentrations of Tie1 (blue), Tie2 (red) and Tie1:Tie2 (green) over time. The concentrations of Tie1:Tie2 complex and Tie2 decreases while Tie1 increases.
Plot B, shows that the concentration of nTie2 gradually decreases over time.
Plot C, shows Ang2 (dimeric in red, trimeric in blue and tetrameric in green) bound to Tie1:Tie2. There is an increase in concentration which reaches a plateau around 900 seconds. The change in concentration is very small.

6.7. Discussion

The aim of this chapter was to simulate the model with the dephosphorylation reaction included and validate the model by comparing the simulation results to experiments without the use of vanadate.

The validation of the rate of Ang1-induced Tie2 activation suggests that for the low concentration of Ang1 the simulation does not match the experiments for 5 or 15 minutes. However if the experiments showed a gradual decrease between the 10 and 30 minute time-points the model would be valid at 15 minutes.

For the high concentration of Ang1, both methods confirm a similar rapid increase in phosphorylation during the first 5 minutes although the maximal levels of phosphorylation are reached at different times. Moreover the simulation shows a decrease in phosphorylation after 10 minutes whilst the experiments show a plateau in phosphorylation. The plateau shown in experiments could be due to the release of Ang1 which occurs after binding prior to Tie2 internalisation. This allows for the recycling of Ang1 in new binding to free Tie2 which has been proposed to occur (Bogdanovic *et al.*, 2006). Hence this could maintain the level of phosphorylation shown in experiments. The mechanisms which regulate angiopoietin ligand release are unknown and a separate reaction for ligand release prior to Tie2 internalisation is not accounted for in the model. Though it has been suggested that the release of angiopoietins could be a result of changes in receptor affinity after binding to Tie2 (Bogdanovic *et al.*, 2006).

The simulation for the effects of Ang1 concentration on Tie2 phosphorylation was also examined. From the results only the percentage phosphorylation for 50 ng/ml does not

correspond to the experimental data which could be due to experimental error. The experiments suggest that the increase in Ang1 from 25 ng/ml to 50 ng/ml has little to no effect on phosphorylation. However previous experiments (Chapter 5.6.3.2) and many studies have shown that Ang1 increases phosphorylation in a concentration dependent manner (Bogdanovic *et al.*, 2006; Yuan *et al.*, 2007; Yuan *et al.*, 2009). Thus it is possible that the percentage phosphorylation for 50 ng/ml Ang1 is increased and higher than shown for 25 ng/ml, which would make the simulation valid for this part of the model.

The next part of the model for validation was the effect of Ang2 on Tie2 phosphorylation. There were difficulties in detecting Tie2 phosphorylation in samples treated with Ang2 thus the modelling of Ang2 was validated by comparing the effects of Ang2 on Ang1-induced Tie2 phosphorylation. The comparison of the simulation and experimental data showed that the model was not valid and suggested that the model was sensitive to Ang2. This could be due to the Ang2 binding parameters for Tie2 which promotes a high affinity for binding. Hence simulations were conducted to determine a set of parameters which when simulated produced a concentration dependent curve that corresponded to the experimental data.

The K_D proposed was higher than the measured value (Steele, 2013) however as the measured K_D is too low (causing high binding affinity) this was replace with the K_D measured by Maisonpierre and colleagues (Maisonpierre *et al.*, 1997). The method used by Dr Steele over-expressed Tie2 on DT40 cells and combined with the different charges from the cell surface glycoproteins (not similar to HUVECs) could influence the avidity of the ligand-receptor binding. Conversely the surface plasmon resonance method used by Maisonpierre and colleagues isolates the Tie2 on a chip and is probably more relevant

to the cellular experiments used for validation (Maisonpierre *et al.*, 1997). Nevertheless the K_D measured by surface plasmon resonance is comparable to the K_D measured by Dr Steele.

The k_{off} proposed from the simulation is a few fold lower than the original measured value and the k_{off} for Ang1. Hence the proposed value is practical and can also be justified by Ang2 having a faster release rate than Ang1 after binding to Tie2 (Bogdanovic *et al.*, 2006). The k_{on} proposed from the simulation is 15-fold lower than the original calculated value and can only be justified by validating the model using this value.

Therefore the new Ang2 binding parameters were used in simulations for the concentration dependent effect of Ang2 on Tie2 phosphorylation. As this could not be compared to experimental data (for reasons described previously) it was compared to a study by Bogdanovic and colleagues who were able to show that Ang2 increases Tie2 phosphorylation in a concentration dependent manner (Bogdanovic *et al.*, 2006). This comparison only suggests a possibility that the model is valid as this study was performed by using a different method with a phosphotyrosine antibody not specific to Y^{992} Tie2 phosphorylation.

A further simulation of the new values was performed using the model without the dephosphorylation reaction. As the experimental effects of increasing Ang2 concentration on Tie2 phosphorylation were quantified in the presence of vanadate (Chapter 5.8.1.2) this could be compared to the simulated data with new Ang2 binding parameters. The comparison shows that the new parameters values are not suitable for use in this model as the comparison suggests that the model is no longer valid. Although

the simulation with new values does show that Ang2 has a partial agonist effect on Tie2 phosphorylation when compared to Ang1.

The analysis on the effect of Ang2 on the Tie1, Tie2, Tie1:Tie2 equilibrium was repeated using the new values. The simulation results suggest that Ang2 induces the dissociation of Tie1:Tie2, although on the contrary the *in vivo* study monitoring the association of Tie1 and Tie2 has suggested that Ang2 is unable to dissociate the Tie1:Tie2 complex (Seegar *et al.*, 2010). However the simulations with the new parameter values have resulted in a lower amount of Tie1:Tie2 dissociation when compared to the original simulation. This discrepancy with the literature could still be caused by the binding parameters for Ang2 binding to Tie1:Tie2 although the Ang2 effect has been validated against experiments. Another cause could be the structural residues on Ang2 which have recently been discovered to influence Tie1:Tie2 interactions (Yu *et al.*, 2013). The simulations also show that a low amount of Ang2 binds to Tie1:Tie2 although another study has shown that Ang2 can bind to Tie2 just as well in the presence or absence of Tie1 (Hansen *et al.*, 2010). Hence if the amount of Ang2 bound to Tie1:Tie2 is higher this should theoretically reduce the amount of Tie1:Tie2 complexes dissociated. Furthermore it has been suggested that the binding of Ang2 may electrostatically stabilize the Tie1:Tie2 complex (Yu *et al.*, 2013). This indicates that the discrepancy for this analysis may be due to the Ang2 molecular structural issues which are beyond the scope of the kinetic model.

Overall this chapter has established a model which is close to physiological conditions and is valid for Ang1 interactions and also potentially valid for Ang2 interactions.

Chapter 7: Conclusion and future work

Angiopoietins are ligands of the receptor tyrosine kinase, Tie2, whose activation by Ang1 stimulation results in vascular quiescence and angiogenesis (Davis *et al.*, 1996; Fukuhara *et al.*, 2010). This vascular effect makes the Tie2 signalling pathway a therapeutic target for many diseases such as; heart disease, stroke and cancer. However, Tie2 regulation is under tight control and has many complex factors which regulate its activation. Computational modelling can be used to model this receptor and ligand interactions, and the complex regulatory features to help understand the behaviour of this system.

The main aim of this project was to produce a quantitative computer model of the Ang-Tie interactions and its various regulatory features at the endothelial cell surface. A schematic representation of Ang-Tie interactions was produced in CellDesigner™ to identify the reactions required for modelling. Mathematical kinetic equations were formulated to describe the system and change of states over time. These equations identified a set of parameters required for input before the model could be simulated. Most of these parameters were obtained from the literature or quantified and determined experimentally.

This model uses the relative change in Tie2 phosphorylation as an indicator for the levels of activated Tie2 and signalling, thus the levels of Tie2 phosphorylation in experiments need to be determined for comparing both methods. Quantitative Western blotting was determined to be a suitable quantitative method for detecting the amounts of proteins in cell samples. However this method is not fully accurate as some protein is inevitably lost while stripping the membrane for reprobing. Hence a more accurate method that could

be used is the LI-COR Odyssey infrared imaging system which eliminates the need for stripping due to its dual staining features. Another limitation to this method is that only the relative levels can be quantified and not the actual concentrations of protein.

There were initial difficulties in detecting Tie2 phosphorylation using low concentrations of Ang1 hence a phosphatase inhibitor (vanadate) was used to inhibit dephosphorylation. Consequently the dephosphorylation reaction had to be removed from the model to mimic experiments for validation of the simulations. However the use of vanadate in experiments and excluding dephosphorylation from the model does not produce a model similar to physiological conditions. Unfortunately the use of this chemical was responsible for some inconsistencies in experiments and invalidations of the model.

After many months of optimising the culture and maintenance of HUVECs for use in experiments the levels of Tie2 phosphorylation were able to be consistently detected and quantified. The validations for the model were repeated again with simulations including the dephosphorylation reaction. There was a discrepancy between the simulation results and experimental results on the effect of Ang2 on Ang1-induced Tie2 phosphorylation. This was thought to be due to the high binding affinity of Ang2 for Tie2. The parameters were changed until a set of appropriate Ang2 binding parameters were identified to produce simulation results corresponding to experimental data. The validations for Ang2 were repeated and were proven to be valid for the model including the dephosphorylation reaction by comparisons with experiments and studies from the literature.

The model suggests that Ang1 phosphorylation peaks between 10 and 15 minutes after stimulation and that Ang1 and Ang2 both induce Tie2 in a concentration dependent

manner, and is in agreement with many studies (Bogdanovic *et al.*, 2006; Yuan *et al.*, 2007; Yuan *et al.*, 2009). The model has also demonstrated that Ang2 has a partial agonist effect on Tie2 phosphorylation however in the presence of Ang1 it reduces the levels of phosphorylation, which is also consistent with the literature (Bogdanovic *et al.*, 2006; Yuan *et al.*, 2009). The model also suggests that Ang1 induces the dissociation of the Tie1:Tie2 complex which is consistent with a recent study (Seegar *et al.*, 2010). Conversely the addition of Ang2 also dissociated the Tie1:Tie2 complex in simulations which is not in accordance with the literature (Seegar *et al.*, 2010) .

There are many factors that contribute to the complexity of Ang1 and Ang2 and their function on Tie2 activation which the model has tried to incorporate. However the effect of binding parameters on Tie2 is only a small part of the greater problem which could possibly be highly influenced by the β6-β7 loop in the P domain of the Ang2 molecular structure (Yu *et al.*, 2013). This loop may be responsible for the differences in functional activity between Ang1 and Ang2, and as this cannot be mathematically modelled, the model is restricted to kinetic interactions and can therefore only be defined to a limit.

In conclusion this project has established a model similar to physiological conditions which is valid for Ang1 and potentially for Ang2 interactions. This simplified model of Ang1 and Ang2 interactions with Tie2 on the endothelial cell surface provides a foundation on which further analysis, hypotheses, and additional receptor modelling can be performed and expanded. The initial intention of the project was to identify the main regulatory states or parameters of the model and use synthetic biology to manipulate and modify these states. However this was not accomplished due to the length of model

development and the time constraints; the project is now being continued by Dr Tariq Tahir.

Further work on validation of the model is necessary for the interactions of the angiopoietins with soluble Tie2 (sTie2). Experiments are required to examine the effect of increasing concentrations of sTie2 on Ang1-induced Tie2 phosphorylation without the use of vanadate. In addition the effect on Tie2 phosphorylation of adding increasing concentrations of sTie2 in the presence of both Ang1 and Ang2 at fixed concentrations is also required.

Once this has been achieved predictions on the state of Tie2 phosphorylation in pathological conditions such as sepsis, cancer and cardiovascular disease, can be determined. This can be conducted by changing the initial amounts of Ang1, Ang2 and sTie2 (found in healthy patients) in relation to the fold-changes found in pathological conditions. For example studies have suggested that the serum level of Ang2 in patients with sepsis increases between 4.6 and 6.6 fold (Parikh *et al.*, 2006; Siner *et al.*, 2009). Hence for simulations of sepsis the initial concentration of Ang2 should be increased by 4.6 to 6.6 fold to determine the relative change in Tie2 activation.

Other predictions can be made to generate hypotheses which can be verified experimentally. For example determining how much sTie2 would be required to sequester higher concentrations of Ang1 and or Ang2 in pathological conditions.

This model once fully validated has potential clinical relevance for personalised treatment. The model can be scaled for use in clinical settings, where the quantified levels

of Ang1, Ang2 and sTie2 from a patient's blood serum can be input and simulated to determine the optimal therapy. In addition the interactions of angiopoietins and Tie could potentially be integrated with recent models on VEGF receptor signalling (Tan *et al.*, 2013a; Tan *et al.*, 2013b) to support and advance research on the predictive modelling of angiogenesis (Bentley *et al.*, 2013). Conversely, if the model cannot be fully validated this can identify an area of the system which has importance to Tie2 regulation and should be explored and investigated experimentally.

Another important aspect of the computational model is the ability to identify the main regulatory parameters in the system. A sensitivity analysis can be performed on the rate constants and also the state concentrations at initial conditions. This analysis examines the robustness to variation for these parameters and can therefore determine which rate constants and states have the biggest effect on Tie2 activation. Once this has been determined the main states or parameters can be explored and further investigated. Synthetic biology approaches can then be used to modify the identified states (e.g. receptors) for therapeutic manipulation of signalling pathways relevant to pathological conditions.

Appendices

Appendix 1: Concentrations for Ang2 oligomeric forms

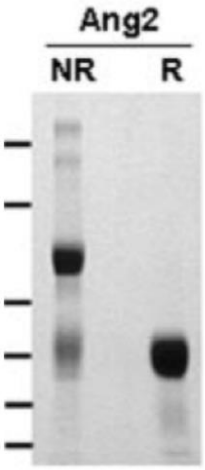

Figure taken from (Kim *et al.*, 2005)

	Density	**%**
Dimer (Ang2)2	463	75
Trimer (Ang2)3	55	9
Tetramer (Ang2)4	98	16
		100%

Total Ang2 ng/ml	**Dimer** 75% (nM)	**Trimer** 9% (nM)	**Tetramer** 16% (nM)
50	0.268	0.021	0.029
100	0.536	0.043	0.057
200	1.071	0.086	0.114
500	2.679	0.214	0.286
800	4.286	0.343	0.457
1000	5.357	0.429	0.571

Appendix 2: MATLAB scripts without dephosphorylation

```
%Script 1- Main script for Model- Ang-Tie interactions
%FULL MODEL - Ang1, Ang2, sTie2

% set parameters global, so they can be used in the ODE function.
global k1;
global k_1;
global k2;
global k_2;
global k3;
global k_3;
global k4;
global k_4;
global k5;
global k_5;
%global V6; %dephos
%global K6; %dephos
global k7;
global k8;

global k9;
global k10;
global k11;
global k12;

global k13;

global k14;
global k_14;

global k15;
global k_15;

global k16;
global k_16;
global k17;
global k_17;

global k18;
global k_18;
global k19;
global k_19;
global k20;
global k_20;

global k21;
global k_21;
global k22;
global k_22;
global k23;
global k_23;
global k24;
global k_24;
global k25;
global k_25;
%global V26; %dephos
%global K26; %dephos
```

```
global k27;
global k_27
global k28;
global k_28
global k29;
global k_29;

global k30;
global k_30;
global k31;
global k_31;
global k32;
global k_32;



% set parameter values
k1 = 0.0094; %Ang1 binding to Tie2 Monomer
k_1 = 0.0043;
k2 = 0.5; %Dimer
k_2 = 0.1;
k3 = 0.5; %Trimer
k_3 = 0.1;
k4 = 0.5; %Tetramer
k_4 = 0.1;
k5 = 1; %Phosphorylation
k_5 = 0.01;
%V6 = 13030.3; %dephosphorylation
%K6 = 104000; %dephosphorylation
k7 = 0.00684; %internalisation
k8 = 0.000684; % degradation

k9 = 0.00684; % Ang1 mono internalisation
k10 = 0.00684; % Ang1 di internalisation
k11 = 0.00684; % Ang1 tri internalisation
k12 = 0.00684; % Ang1 tetra internalisation

k13 = 0.00042; %Tie2 replenishment

k14 = 0.00000000000171; %Tie1:Tie2
k_14 = 0.1;

k15 = 0.0094; %Ang1 binding to sTie2 Monomer
k_15 = 0.0043;

k16 = 0.0094; %(Ang2)2 binding to Tie2 Monomer
k_16 = 0.0096;
k17 = 0.5; %Dimer
k_17 = 0.1;

k18 = 0.0094; %(Ang2)3 binding to Tie2 Monomer
k_18 = 0.0096;
k19 = 0.5; %Dimer
k_19 = 0.1;
k20 = 0.5; %Trimer
k_20 = 0.1;

k21 = 0.0094; %(Ang2)4 binding to Tie2 Monomer
```

```
k_21 = 0.0096;
k22 = 0.5; %Dimer
k_22 = 0.1;
k23 = 0.5; %Trimer
k_23 = 0.1;
k24 = 0.5; %Tetramer
k_24 = 0.1;
k25 = 1; %Phosphorylation
k_25 = 0.01;
%V26 = 13030.3; %dephosphorylation
%K26 = 104000; %dephosphorylation

k27 = 0.0094; %(Ang2)2 binding to Tie1:Tie2
k_27 = 0.0096;
k28 = 0.0094; %(Ang2)3 binding to Tie1:Tie2
k_28 = 0.0096;
k29 = 0.0094; %(Ang2)4 binding to Tie1:Tie2
k_29 = 0.0096;

k30 = 0.0094; %(Ang2)2 binding to sTie2
k_30 = 0.0096;
k31 = 0.0094; %(Ang2)3 binding to sTie2
k_31 = 0.0096;
k32 = 0.0094; %(Ang2)4 binding to sTie2
k_32 = 0.0096;


% set initial conditions
x = zeros(37,1);
x(1) = 0.179; %Ang1
x(2) = 0.01495; %Tie2
x(15) = 0.00745; %Tie1
x(16) = 0.01495; %Tie1:Tie2
x(14) = 0.0299; %new Tie2
%x(17) = 1; %sTie2
%x(19) = 1.071; %(Ang2)2
%x(22) = 0.086; %(Ang2)3
%x(26) = 0.114; %(Ang2)4



[T,Y] = ode23s(@ModelODEs_Thesis,[0 1800],x); %options;

figure;
title('Timecourse of Tie1 and Tie2 steady state', 'FontWeight',
'bold');
plot(T,Y(:,2), 'r', T,Y(:,15), 'b', T,Y(:,16), 'g');
legend('Tie2', 'Tie1', 'Tie1:Tie2');
xlabel('Time (sec.)');
ylabel('Concentration (nM)');

figure;
plot(T,Y(:,14));
legend('nTie2');
xlabel('Time (sec.)');
ylabel('Concentration (nM)');

figure;
title('Timecourse of Ang1-Tie2 Phosphorylation','FontWeight','bold');
```

```
plot(T,Y(:,7), 'r', T,Y(:,8), 'b', T,Y(:,9), 'g');
legend('Ang1-pTie2', 'i-pTie2', 'd-pTie2');
xlabel('Time (sec.)');
ylabel('Concentration (nM)');

figure;
title('Timecourse of (Ang2)4 induced
phosphorylation','FontWeight','bold');
plot(T,Y(:,31));
legend('(Ang2)4-pTie2');
xlabel('Time (sec.)');
ylabel('Concentration (nMol.)');
```

```
%Script 2 for Model- Ang-Tie interactions
%FULL MODEL - Ang1, Ang2, sTie2

function [ dx ] = ModelODEs_Thesis( t, x )
%function to return the derivatives of the state variables for the
Ang-Tie
%model

% parameters take values from main script (global)

global k1;
global k_1;
global k2;
global k_2;
global k3;
global k_3;
global k4;
global k_4;
global k5;
global k_5;
%global V6; %dephos
%global K6; %dephos
global k7;
global k8;

global k9;
global k10;
global k11;
global k12;

global k13;

global k14;
global k_14;

global k15;
global k_15;

global k16;
global k_16;
global k17;
global k_17;

global k18;
global k_18;
global k19;
global k_19;
global k20;
global k_20;

global k21;
global k_21;
global k22;
global k_22;
global k23;
global k_23;
global k24;
global k_24;
global k25;
```

```
global k_25;
%global V26; %dephos
%global K26; %dephos

global k27;
global k_27
global k28;
global k_28
global k29;
global k_29;

global k30;
global k_30;
global k31;
global k_31;
global k32;
global k_32;

% calculate reaction rates
r1 = k1*x(1)*x(2) - k_1*x(3); %Ang1 binding to Tie2 MONOMER
r2 = k2*(x(3)*2800000)*(x(2)*2800000) - k_2*x(4); %DIMER
r3 = k3*x(4)*(x(2)*2800000) - k_3*x(5); %TRIMER
r4 = k4*x(5)*(x(2)*2800000) - k_4*x(6);%TETRAMER
r5 = k5*x(6) - k_5*x(7); %PHOSPHORYLATION
%r6 = (V6*x(7))/(K6 + x(7)); %%%dephosphorylation%%%
r7 = k7*x(7); %internalization
r8 = k8*x(8); %degradation of pTie2

r9 = k9*x(3); %iTie2 mono Ang1
r10 = k10*x(4); %iTie2 di Ang1
r11 = k11*x(5); %iTie2 tri Ang1
r12 = k12*x(6); %iTie2 tetra Ang1

r13 = k13*x(14); %replenishment
r14 = k14*(x(15)*2800000)*(x(2)*2800000) - k_14*x(16); %Tie1:Tie2

r15 = k15*x(1)*x(17) - k_15*x(18); %Ang1 binding to sTie2 MONOMER

r16 = k16*x(19)*x(2) - k_16*x(20); %(Ang2)2 binding to Tie2 MONOMER
r17 = k17*(x(20)*2800000)*(x(2)*2800000) - k_17*x(21); %DIMER

r18 = k18*x(22)*x(2) - k_18*x(23); %(Ang2)3 binding to Tie2 MONOMER
r19 = k19*(x(23)*2800000)*(x(2)*2800000) - k_19*x(24); %DIMER
r20 = k20*x(24)*(x(2)*2800000) - k_20*x(25); %TRIMER

r21 = k21*x(26)*x(2) - k_21*x(27); %(Ang2)4 binding to Tie2 MONOMER
r22 = k22*(x(27)*2800000)*(x(2)*2800000) - k_22*x(28); %DIMER
r23 = k23*x(28)*(x(2)*2800000) - k_23*x(29); %TRIMER
r24 = k24*x(29)*(x(2)*2800000) - k_24*x(30);%TETRAMER
r25 = k25*x(30) - k_25*x(31); %PHOSPHORYLATION
%r26 = (V26*x(31))/(K26 + x(31)); %%%dephosphorylation%%%

r27 = k27*x(19)*(x(16)/2800000) - k_27*x(32); %(Ang2)2 binding to
Tie1:Tie2
r28 = k28*x(22)*(x(16)/2800000) - k_28*x(33); %(Ang2)3 binding to
Tie1:Tie2
r29 = k29*x(26)*(x(16)/2800000) - k_29*x(34); %(Ang2)4 binding to
Tie1:Tie2
```

```
r30 = k30*x(19)*x(17) - k_30*x(35); %(Ang2)2 binding to Tie1:Tie2
r31 = k31*x(22)*x(17) - k_31*x(36); %(Ang2)3 binding to Tie1:Tie2
r32 = k32*x(26)*x(17) - k_32*x(37); %(Ang2)4 binding to Tie1:Tie2

% calculate derivates
dx = zeros(37,1);
dx(1) = -r1-r15; % Ang1
dx(2) = -r1-r2-r3-r4+r13-r14-r16-r17-r18-r19-r20-r21-r22-r23-r24; %
Tie2

dx(3) = r1-r2-r9; % Monomer
dx(4) = r2-r3-r10; % Dimer
dx(5) = r3-r4-r11; % Trimer
%dx(6) = r4-r5+r6-r12; % Tetramer with dephos ++
dx(6) = r4-r5-r12; % Tetramer without dephos --
%dx(7) = r5-r6-r7; % Phosho-Tie2 with dephos ++
dx(7) = r5-r7; % Phosho-Tie2 without dephos --
dx(8) = r7-r8; % internalized pTie2
dx(9) = r8; % degraded pTie2

dx(10) = r9; % iTie2 mono Ang1
dx(11) = r10; % iTie2 di Ang1
dx(12) = r11; % iTie2 tri Ang1
dx(13) = r12; % iTie2 tetra Ang1

dx(14) = -r13; % New Tie2

dx(15) = -r14; % Tie1
dx(16) = r14-r27-r28-r29; % Tie1:Tie2

dx(17) = -r15-r30-r31-r32; % sTie2
dx(18) = r15; % Ang1-sTie2

dx(19) = -r16-r27-r30; % (Ang)2
dx(20) = r16-r17; % (Ang2)2 Monomer
dx(21) = r17; % Dimer

dx(22) = -r18-r28-r31; % (Ang)3
dx(23) = r18-r19; % (Ang2)3 Monomer
dx(24) = r19-r20; % Dimer
dx(25) = r20; % Trimer

dx(26) = -r21-r29-r32; % (Ang)4
dx(27) = r21-r22; % (Ang2)4 Monomer
dx(28) = r22-r23; % Dimer
dx(29) = r23-r24; % Trimer
%dx(30) = r24-r25+r26; % Tetramer with dephos ++
dx(30) = r24-r25; % Tetramer without dephos --
%dx(31) = r25-r26; % Phosho-Tie2 with dephos ++
dx(31) = r25; % Phosho-Tie2 without dephos --

dx(32) = r27; % (Ang2)2-Tie1:Tie2
dx(33) = r28; % (Ang2)3-Tie1:Tie2
dx(34) = r29; % (Ang2)4-Tie1:Tie2

dx(35) = r30; % (Ang2)2-sTie2
dx(36) = r31; % (Ang2)3-sTie2
dx(37) = r32; % (Ang2)4-sTie2
end
```

Appendix 3: MATLAB scripts with dephosphorylation

```
%Script 1- Main script for Model- Ang-Tie interactions
%FULL MODEL - Ang1, Ang2, sTie2

% set parameters global, so they can be used in the ODE function.
global k1;
global k_1;
global k2;
global k_2;
global k3;
global k_3;
global k4;
global k_4;
global k5;
global k_5;
global V6; %dephos
global K6; %dephos
global k7;
global k8;

global k9;
global k10;
global k11;
global k12;

global k13;

global k14;
global k_14;

global k15;
global k_15;

global k16;
global k_16;
global k17;
global k_17;

global k18;
global k_18;
global k19;
global k_19;
global k20;
global k_20;

global k21;
global k_21;
global k22;
global k_22;
global k23;
global k_23;
global k24;
global k_24;
global k25;
global k_25;
global V26; %dephos
global K26; %dephos
```

```
global k27;
global k_27
global k28;
global k_28
global k29;
global k_29;

global k30;
global k_30;
global k31;
global k_31;
global k32;
global k_32;



% set parameter values
k1 = 0.0094; %Ang1 binding to Tie2 Monomer
k_1 = 0.0043;
k2 = 0.5; %Dimer
k_2 = 0.1;
k3 = 0.5; %Trimer
k_3 = 0.1;
k4 = 0.5; %Tetramer
k_4 = 0.1;
k5 = 1; %Phosphorylation
k_5 = 0.01;
V6 = 13030.3; %dephosphorylation
K6 = 104000; %dephosphorylation
k7 = 0.00684; %internalisation
k8 = 0.000684; % degradation

k9 = 0.00684; % Ang1 mono internalisation
k10 = 0.00684; % Ang1 di internalisation
k11 = 0.00684; % Ang1 tri internalisation
k12 = 0.00684; % Ang1 tetra internalisation

k13 = 0.00042; %Tie2 replenishment

k14 = 0.00000000000171; %Tie1:Tie2
k_14 = 0.1;

k15 = 0.0094; %Ang1 binding to sTie2 Monomer
k_15 = 0.0043;

k16 = 0.0094; %(Ang2)2 binding to Tie2 Monomer
k_16 = 0.0096;
k17 = 0.5; %Dimer
k_17 = 0.1;

k18 = 0.0094; %(Ang2)3 binding to Tie2 Monomer
k_18 = 0.0096;
k19 = 0.5; %Dimer
k_19 = 0.1;
k20 = 0.5; %Trimer
k_20 = 0.1;

k21 = 0.0094; %(Ang2)4 binding to Tie2 Monomer
```

```
k_21 = 0.0096;
k22 = 0.5; %Dimer
k_22 = 0.1;
k23 = 0.5; %Trimer
k_23 = 0.1;
k24 = 0.5; %Tetramer
k_24 = 0.1;
k25 = 1; %Phosphorylation
k_25 = 0.01;
V26 = 13030.3; %dephosphorylation
K26 = 104000; %dephosphorylation

k27 = 0.0094; %(Ang2)2 binding to Tie1:Tie2
k_27 = 0.0096;
k28 = 0.0094; %(Ang2)3 binding to Tie1:Tie2
k_28 = 0.0096;
k29 = 0.0094; %(Ang2)4 binding to Tie1:Tie2
k_29 = 0.0096;

k30 = 0.0094; %(Ang2)2 binding to sTie2
k_30 = 0.0096;
k31 = 0.0094; %(Ang2)3 binding to sTie2
k_31 = 0.0096;
k32 = 0.0094; %(Ang2)4 binding to sTie2
k_32 = 0.0096;


% set initial conditions
x = zeros(37,1);
x(1) = 0.179; %Ang1
x(2) = 0.01495; %Tie2
x(15) = 0.00745; %Tie1
x(16) = 0.01495; %Tie1:Tie2
x(14) = 0.0299; %new Tie2
%x(17) = 1; %sTie2
%x(19) = 1.071; %(Ang2)2
%x(22) = 0.086; %(Ang2)3
%x(26) = 0.114; %(Ang2)4



[T,Y] = ode23s(@ModelODEs_Thesis,[0 1800],x); %options;

figure;
title('Timecourse of Tie1 and Tie2 steady state', 'FontWeight',
'bold');
plot(T,Y(:,2), 'r', T,Y(:,15), 'b', T,Y(:,16), 'g');
legend('Tie2', 'Tie1', 'Tie1:Tie2');
xlabel('Time (sec.)');
ylabel('Concentration (nM)');

figure;
plot(T,Y(:,14));
legend('nTie2');
xlabel('Time (sec.)');
ylabel('Concentration (nM)');

figure;
title('Timecourse of Ang1-Tie2 Phosphorylation','FontWeight','bold');
```

```
plot(T,Y(:,7), 'r', T,Y(:,8), 'b', T,Y(:,9), 'g');
legend('Ang1-pTie2', 'i-pTie2', 'd-pTie2');
xlabel('Time (sec.)');
ylabel('Concentration (nM)');

figure;
title('Timecourse of (Ang2)4 induced
phosphorylation','FontWeight','bold');
plot(T,Y(:,31));
legend('(Ang2)4-pTie2');
xlabel('Time (sec.)');
ylabel('Concentration (nMol.)');
```

```
%Script 2 for Model- Ang-Tie interactions
%FULL MODEL - Ang1, Ang2, sTie2

function [ dx ] = ModelODEs_Thesis( t, x )
%function to return the derivatives of the state variables for the
Ang-Tie
%model

% parameters take values from main script (global)

global k1;
global k_1;
global k2;
global k_2;
global k3;
global k_3;
global k4;
global k_4;
global k5;
global k_5;
global V6; %dephos
global K6; %dephos
global k7;
global k8;

global k9;
global k10;
global k11;
global k12;

global k13;

global k14;
global k_14;

global k15;
global k_15;

global k16;
global k_16;
global k17;
global k_17;

global k18;
global k_18;
global k19;
global k_19;
global k20;
global k_20;

global k21;
global k_21;
global k22;
global k_22;
global k23;
global k_23;
global k24;
global k_24;
global k25;
```

```
global k_25;
global V26; %dephos
global K26; %dephos

global k27;
global k_27
global k28;
global k_28
global k29;
global k_29;

global k30;
global k_30;
global k31;
global k_31;
global k32;
global k_32;

% calculate reaction rates
r1 = k1*x(1)*x(2) - k_1*x(3); %Ang1 binding to Tie2 MONOMER
r2 = k2*(x(3)*2800000)*(x(2)*2800000) - k_2*x(4); %DIMER
r3 = k3*x(4)*(x(2)*2800000) - k_3*x(5); %TRIMER
r4 = k4*x(5)*(x(2)*2800000) - k_4*x(6);%TETRAMER
r5 = k5*x(6) - k_5*x(7); %PHOSPHORYLATION
r6 = (V6*x(7))/(K6 + x(7)); %dephosphorylation
r7 = k7*x(7); %internalization
r8 = k8*x(8); %degradation of pTie2

r9 = k9*x(3); %iTie2 mono Ang1
r10 = k10*x(4); %iTie2 di Ang1
r11 = k11*x(5); %iTie2 tri Ang1
r12 = k12*x(6); %iTie2 tetra Ang1

r13 = k13*x(14); %replenishment
r14 = k14*(x(15)*2800000)*(x(2)*2800000) - k_14*x(16); %Tie1:Tie2

r15 = k15*x(1)*x(17) - k_15*x(18); %Ang1 binding to sTie2 MONOMER

r16 = k16*x(19)*x(2) - k_16*x(20); %(Ang2)2 binding to Tie2 MONOMER
r17 = k17*(x(20)*2800000)*(x(2)*2800000) - k_17*x(21); %DIMER

r18 = k18*x(22)*x(2) - k_18*x(23); %(Ang2)3 binding to Tie2 MONOMER
r19 = k19*(x(23)*2800000)*(x(2)*2800000) - k_19*x(24); %DIMER
r20 = k20*x(24)*(x(2)*2800000) - k_20*x(25); %TRIMER

r21 = k21*x(26)*x(2) - k_21*x(27); %(Ang2)4 binding to Tie2 MONOMER
r22 = k22*(x(27)*2800000)*(x(2)*2800000) - k_22*x(28); %DIMER
r23 = k23*x(28)*(x(2)*2800000) - k_23*x(29); %TRIMER
r24 = k24*x(29)*(x(2)*2800000) - k_24*x(30);%TETRAMER
r25 = k25*x(30) - k_25*x(31); %PHOSPHORYLATION
r26 = (V26*x(31))/(K26 + x(31)); %dephosphorylation

r27 = k27*x(19)*(x(16)/2800000) - k_27*x(32); %(Ang2)2 binding to
Tie1:Tie2
r28 = k28*x(22)*(x(16)/2800000) - k_28*x(33); %(Ang2)3 binding to
Tie1:Tie2
r29 = k29*x(26)*(x(16)/2800000) - k_29*x(34); %(Ang2)4 binding to
Tie1:Tie2
```

```
r30 = k30*x(19)*x(17) - k_30*x(35); %(Ang2)2 binding to Tie1:Tie2
r31 = k31*x(22)*x(17) - k_31*x(36); %(Ang2)3 binding to Tie1:Tie2
r32 = k32*x(26)*x(17) - k_32*x(37); %(Ang2)4 binding to Tie1:Tie2

% calculate derivates
dx = zeros(37,1);
dx(1) = -r1-r15; % Ang1
dx(2) = -r1-r2-r3-r4+r13-r14-r16-r17-r18-r19-r20-r21-r22-r23-r24; %
Tie2

dx(3) = r1-r2-r9; % Monomer
dx(4) = r2-r3-r10; % Dimer
dx(5) = r3-r4-r11; % Trimer
dx(6) = r4-r5+r6-r12; % Tetramer with dephos ++
%dx(6) = r4-r5-r12; % Tetramer without dephos --
dx(7) = r5-r6-r7; % Phosho-Tie2 with dephos ++
%dx(7) = r5-r7; % Phosho-Tie2 without dephos --
dx(8) = r7-r8; % internalized pTie2
dx(9) = r8; % degraded pTie2

dx(10) = r9; % iTie2 mono Ang1
dx(11) = r10; % iTie2 di Ang1
dx(12) = r11; % iTie2 tri Ang1
dx(13) = r12; % iTie2 tetra Ang1

dx(14) = -r13; % New Tie2

dx(15) = -r14; % Tie1
dx(16) = r14-r27-r28-r29; % Tie1:Tie2

dx(17) = -r15-r30-r31-r32; % sTie2
dx(18) = r15; % Ang1-sTie2

dx(19) = -r16-r27-r30; % (Ang)2
dx(20) = r16-r17; % (Ang2)2 Monomer
dx(21) = r17; % Dimer

dx(22) = -r18-r28-r31; % (Ang)3
dx(23) = r18-r19; % (Ang2)3 Monomer
dx(24) = r19-r20; % Dimer
dx(25) = r20; % Trimer

dx(26) = -r21-r29-r32; % (Ang)4
dx(27) = r21-r22; % (Ang2)4 Monomer
dx(28) = r22-r23; % Dimer
dx(29) = r23-r24; % Trimer
dx(30) = r24-r25+r26; % Tetramer with dephos ++
%dx(30) = r24-r25; % Tetramer without dephos --
dx(31) = r25-r26; % Phosho-Tie2 with dephos ++
%dx(31) = r25; % Phosho-Tie2 without dephos --

dx(32) = r27; % (Ang2)2-Tie1:Tie2
dx(33) = r28; % (Ang2)3-Tie1:Tie2
dx(34) = r29; % (Ang2)4-Tie1:Tie2

dx(35) = r30; % (Ang2)2-sTie2
dx(36) = r31; % (Ang2)3-sTie2
dx(37) = r32; % (Ang2)4-sTie2
end
```

References

Abdel-Malak, N.A., Mofarrahi, M., Mayaki, D., Khachigian, L.M., Hussain, S.N., 2009. Early growth response-1 regulates angiopoietin-1-induced endothelial cell proliferation, migration, and differentiation. *Arteriosclerosis, Thrombosis, and Vascular Biology.* **29,** 209-216.

Aldridge, B.B., Burke, J.M., Lauffenburger, D.A., Sorger, P.K., 2006. Physicochemical modelling of cell signalling pathways. *Nature Cell Biology.* **8,** 1195-1203.

Ashino, R., Nagase, M., Vaillancourt, R., 2000. Behind and Beyond the Matlab ODE Suite. *Computers and Mathematics with Applications.* **40,** 491-512.

Bai, E., Fotedar, S., Moy, A., 2008. Modeling and parameter estimation of endothelial cells. *Proceedings of the 17th World Congress the International Federation of Automatic Control.*

Bakker, B.M., Michels, P.A., Opperdoes, F.R., Westerhoff, H.V., 1997. Glycolysis in bloodstream form Trypanosoma brucei can be understood in terms of the kinetics of the glycolytic enzymes. *The Journal of Biological Chemistry.* **272,** 3207-3215.

Barton, W.A., Tzvetkova, D., Nikolov, D.B., 2005. Structure of the angiopoietin-2 receptor binding domain and identification of surfaces involved in Tie2 recognition. *Structure (London, England : 1993).* **13,** 825-832.

Barton, W.A., Tzvetkova-Robev, D., Miranda, E.P., Kolev, M.V., Rajashankar, K.R., Himanen, J.P., Nikolov, D.B., 2006. Crystal structures of the Tie2 receptor ectodomain and the angiopoietin-2-Tie2 complex. *Nature Structural & Molecular Biology.* **13,** 524-532.

Bentley, K., Jones, M., Cruys, B., 2013. Predicting the future: towards symbiotic computational and experimental angiogenesis research. *Experimental Cell Research.* **319,** 1240-1246.

Bogdanovic, E., Coombs, N., Dumont, D.J., 2009. Oligomerized Tie2 localizes to clathrin-coated pits in response to angiopoietin-1. *Histochemistry and Cell Biology.* **132,** 225-237.

Bogdanovic, E., Nguyen, V.P., Dumont, D.J., 2006. Activation of Tie2 by angiopoietin-1 and angiopoietin-2 results in their release and receptor internalization. *Journal of Cell Science.* **119,** 3551-3560.

Brindle, N.P., Saharinen, P., Alitalo, K., 2006. Signaling and functions of angiopoietin-1 in vascular protection. *Circulation Research.* **98,** 1014-1023.

Brown, K.D., Yeh, Y.C., Holley, R.W., 1979. Binding, internalization, and degradation of epidermal growth factor by balb 3T3 and BP3T3 cells: relationship to cell density and the stimulation of cell proliferation. *Journal of Cellular Physiology.* **100,** 227-238.

Brown, L.F., Dezube, B.J., Tognazzi, K., Dvorak, H.F., Yancopoulos, G.D., 2000. Expression of Tie1, Tie2, and angiopoietins 1, 2, and 4 in Kaposi's sarcoma and cutaneous angiosarcoma. *The American Journal of Pathology.* **156,** 2179-2183.

Carlson, T.R., Feng, Y., Maisonpierre, P.C., Mrksich, M., Morla, A.O., 2001. Direct cell adhesion to the angiopoietins mediated by integrins. *The Journal of Biological Chemistry.* **276,** 26516-26525.

Chang, A., Scheer, M., Grote, A., Schomburg, I., Schomburg, D., 2009. BRENDA, AMENDA and FRENDA the enzyme information system: new content and tools in 2009. *Nucleic Acids Research.* **37,** D588-92.

Cho, C.H., Kammerer, R.A., Lee, H.J., Steinmetz, M.O., Ryu, Y.S., Lee, S.H., Yasunaga, K., Kim, K.T., Kim, I., Choi, H.H., Kim, W., Kim, S.H., Park, S.K., Lee, G.M., Koh, G.Y., 2004. COMP-Ang1: a designed angiopoietin-1 variant with nonleaky angiogenic activity. *Proceedings of the National Academy of Sciences of the United States of America.* **101,** 5547-5552.

Cho, C.H., Kammerer, R.A., Lee, H.J., Steinmetz, M.O., Ryu, Y.S., Lee, S.H., Yasunaga, K., Kim, K.T., Kim, I., Choi, H.H., Kim, W., Kim, S.H., Park, S.K., Lee, G.M., Koh, G.Y., 2004. COMP-Ang1: a designed angiopoietin-1 variant with nonleaky angiogenic activity. *Proceedings of the National Academy of Sciences of the United States of America.* **101,** 5547-5552.

Cho, H., Krishnaraj, R., Itoh, M., Kitas, E., Bannwarth, W., Saito, H., Walsh, C.T., 1993. Substrate specificities of catalytic fragments of protein tyrosine phosphatases (HPTP beta, LAR, and CD45) toward phosphotyrosylpeptide substrates and thiophosphotyrosylated peptides as inhibitors. *Protein Science : A Publication of the Protein Society.* **2,** 977-984.

Chung, N.A., Makin, A.J., Lip, G.Y., 2003. Measurement of the soluble angiopoietin receptor tie-2 in patients with coronary artery disease: development and application of an immunoassay. *European Journal of Clinical Investigation.* **33,** 529-535.

Davis, S., Aldrich, T.H., Jones, P.F., Acheson, A., Compton, D.L., Jain, V., Ryan, T.E., Bruno, J., Radziejewski, C., Maisonpierre, P.C., Yancopoulos, G.D., 1996. Isolation of angiopoietin-1, a ligand for the TIE2 receptor, by secretion-trap expression cloning. *Cell.* **87,** 1161-1169.

Davis, S., Papadopoulos, N., Aldrich, T.H., Maisonpierre, P.C., Huang, T., Kovac, L., Xu, A., Leidich, R., Radziejewska, E., Rafique, A., Goldberg, J., Jain, V., Bailey, K., Karow, M., Fandl, J., Samuelsson, S.J., Ioffe, E., Rudge, J.S., Daly, T.J., Radziejewski, C., Yancopoulos, G.D., 2003. Angiopoietins have distinct modular domains essential for receptor binding, dimerization and superclustering. *Nature Structural Biology.* **10,** 38-44.

Di Ventura, B., Lemerle, C., Michalodimitrakis, K., Serrano, L., 2006. From in vivo to in silico biology and back. *Nature.* **443,** 527-533.

Dumont, D.J., Gradwohl, G., Fong, G.H., Puri, M.C., Gertsenstein, M., Auerbach, A., Breitman, M.L., 1994. Dominant-negative and targeted null mutations in the endothelial receptor tyrosine kinase, tek, reveal a critical role in vasculogenesis of the embryo. *Genes & Development.* **8,** 1897-1909.

Dumont, D.J., Yamaguchi, T.P., Conlon, R.A., Rossant, J., Breitman, M.L., 1992. Tek, a Novel Tyrosine Kinase Gene Located on Mouse Chromosome 4, is Expressed in Endothelial Cells and their Presumptive Precursors. *Oncogene.* **7,** 1471-1480.

Eungdamrong, N.J. & Iyengar, R., 2004. Computational approaches for modeling regulatory cellular networks. *Trends in Cell Biology.* **14,** 661-669.

Fagiani, E. & Christofori, G., 2013. Angiopoietins in angiogenesis. *Cancer Letters.* **328,** 18-26.

Felcht, M., Luck, R., Schering, A., Seidel, P., Srivastava, K., Hu, J., Bartol, A., Kienast, Y., Vettel, C., Loos, E.K., Kutschera, S., Bartels, S., Appak, S., Besemfelder, E., Terhardt, D., Chavakis, E., Wieland, T., Klein, C., Thomas, M., Uemura, A., Goerdt, S., Augustin, H.G., 2012. Angiopoietin-2 differentially regulates angiogenesis through TIE2 and integrin signaling. *The Journal of Clinical Investigation.* **122,** 1991-2005.

Fiedler, U. & Augustin, H.G., 2006. Angiopoietins: a link between angiogenesis and inflammation. *Trends in Immunology.* **27,** 552-558.

Fiedler, U., Krissl, T., Koidl, S., Weiss, C., Koblizek, T., Deutsch, U., Martiny-Baron, G., Marme, D., Augustin, H.G., 2003. Angiopoietin-1 and angiopoietin-2 share the same binding domains in the Tie-2 receptor involving the first Ig-like loop and the epidermal growth factor-like repeats. *The Journal of Biological Chemistry.* **278,** 1721-1727.

Fiedler, U., Scharpfenecker, M., Koidl, S., Hegen, A., Grunow, V., Schmidt, J.M., Kriz, W., Thurston, G., Augustin, H.G., 2004. The Tie-2 ligand angiopoietin-2 is stored in and rapidly released upon stimulation from endothelial cell Weibel-Palade bodies. *Blood.* **103,** 4150-4156.

Findley, C.M., Cudmore, M.J., Ahmed, A., Kontos, C.D., 2007. VEGF induces Tie2 shedding via a phosphoinositide 3-kinase/Akt dependent pathway to modulate Tie2 signaling. *Arteriosclerosis, Thrombosis, and Vascular Biology.* **27,** 2619-2626.

Folkman, J., 1995. Angiogenesis in cancer, vascular, rheumatoid and other disease. *Nature Medicine.* **1,** 27-31.

Fukuhara, S., Sako, K., Minami, T., Noda, K., Kim, H.Z., Kodama, T., Shibuya, M., Takakura, N., Koh, G.Y., Mochizuki, N., 2008. Differential function of Tie2 at cell-cell contacts and cell-substratum contacts regulated by angiopoietin-1. *Nature Cell Biology.* **10,** 513-526.

Fukuhara, S., Sako, K., Noda, K., Zhang, J., Minami, M., Mochizuki, N., 2010. Angiopoietin-1/Tie2 receptor signaling in vascular quiescence and angiogenesis. *Histology and Histopathology.* **25,** 387-396.

Funahashi, A., Matsuoka, Y., Jouraku, A., Morohashi, M., Kikuchi, N., Kitano, H., 2008. CellDesigner 3.5: a versatile modeling tool for biochemical networks. *Proceedings of the IEEE.* **96,** 1254–1265.

Funahashi, A., Tanimura, N., Morohashi, M., Kitano, H., 2003. CellDesigner: a process diagram editor for gene-regulatory and biochemical networks. *Biosilico.* **1,** 159-162.

Gex-Fabry, M. & DeLisi, C., 1984. Receptor-mediated endocytosis: a model and its implications for experimental analysis. *The American Journal of Physiology.* **247,** R768-79.

Griffioen, A.W. & Molema, G., 2000. Angiogenesis: potentials for pharmacologic intervention in the treatment of cancer, cardiovascular diseases, and chronic inflammation. *Pharmacological Reviews.* **52,** 237-268.

Haigler, H.T., Maxfield, F.R., Willingham, M.C., Pastan, I., 1980. Dansylcadaverine inhibits internalization of 125I-epidermal growth factor in BALB 3T3 cells. *The Journal of Biological Chemistry.* **255,** 1239-1241.

Hansen, T.M., Singh, H., Tahir, T.A., Brindle, N.P., 2010. Effects of angiopoietins-1 and -2 on the receptor tyrosine kinase Tie2 are differentially regulated at the endothelial cell surface. *Cellular Signalling.* **22,** 527-532.

Hatakeyama, M., Kimura, S., Naka, T., Kawasaki, T., Yumoto, N., Ichikawa, M., Kim, J.H., Saito, K., Saeki, M., Shirouzu, M., Yokoyama, S., Konagaya, A., 2003. A computational model on the modulation of mitogen-activated protein kinase (MAPK) and Akt pathways in heregulin-induced ErbB signalling. *The Biochemical Journal.* **373,** 451-463.

Holash, J., Maisonpierre, P.C., Compton, D., Boland, P., Alexander, C.R., Zagzag, D., Yancopoulos, G.D., Wiegand, S.J., 1999. Vessel cooption, regression, and growth in tumors mediated by angiopoietins and VEGF. *Science (New York, N.Y.).* **284,** 1994-1998.

Holash, J., Wiegand, S.J., Yancopoulos, G.D., 1999. New model of tumor angiogenesis: dynamic balance between vessel regression and growth mediated by angiopoietins and VEGF. *Oncogene.* **18,** 5356-5362.

Holmes, R.M., 2008. A Cell Biologist's Guide to Modeling and Bioinformatics. Center for Computational Science, Boston University, Boston, MA, USA: 57-74.

Hoops, S., Sahle, S., Gauges, R., Lee, C., Pahle, J., Simus, N., Singhal, M., Xu, L., Mendes, P., Kummer, U., 2006. COPASI--a COmplex PAthway SImulator. *Bioinformatics (Oxford, England).* **22,** 3067-3074.

Hubbard, S.R. & Till, J.H., 2000. Protein tyrosine kinase structure and function. *Annual Review of Biochemistry.* **69,** 373-398.

Hucka, M., Finney, A., Sauro, H.M., Bolouri, H., Doyle, J.C., Kitano, H., Arkin, A.P., Bornstein, B.J., Bray, D., Cornish-Bowden, A., Cuellar, A.A., Dronov, S., Gilles, E.D.,

Ginkel, M., Gor, V., Goryanin, I.I., Hedley, W.J., Hodgman, T.C., Hofmeyr, J.H., Hunter, P.J., Juty, N.S., Kasberger, J.L., Kremling, A., Kummer, U., Le Novere, N., Loew, L.M., Lucio, D., Mendes, P., Minch, E., Mjolsness, E.D., Nakayama, Y., Nelson, M.R., Nielsen, P.F., Sakurada, T., Schaff, J.C., Shapiro, B.E., Shimizu, T.S., Spence, H.D., Stelling, J., Takahashi, K., Tomita, M., Wagner, J., Wang, J., SBML Forum, 2003. The systems biology markup language (SBML): a medium for representation and exchange of biochemical network models. *Bioinformatics (Oxford, England).* **19,** 524-531.

Huyer, G., Liu, S., Kelly, J., Moffat, J., Payette, P., Kennedy, B., Tsaprailis, G., Gresser, M.J., Ramachandran, C., 1997. Mechanism of inhibition of protein-tyrosine phosphatases by vanadate and pervanadate. *The Journal of Biological Chemistry.* **272,** 843-851.

Jones, N., Chen, S.H., Sturk, C., Master, Z., Tran, J., Kerbel, R.S., Dumont, D.J., 2003. A unique autophosphorylation site on Tie2/Tek mediates Dok-R phosphotyrosine binding domain binding and function. *Molecular and Cellular Biology.* **23,** 2658-2668.

Keating, S.M., Bornstein, B.J., Finney, A., Hucka, M., 2006. SBMLToolbox: an SBML toolbox for MATLAB users. *Bioinformatics (Oxford, England).* **22,** 1275-1277.

Kell, D.B and Knowles, J.D., 2006. The role of modeling in systems biology. *In System Modeling in Cellular Biology: From Concepts to Nuts and Bolts.* 3-18.

Kholodenko, B.N., Demin, O.V., Moehren, G., Hoek, J.B., 1999. Quantification of short term signaling by the epidermal growth factor receptor. *The Journal of Biological Chemistry.* **274,** 30169-30181.

Kim, H.Z., Jung, K., Kim, H.M., Cheng, Y., Koh, G.Y., 2009. A designed angiopoietin-2 variant, pentameric COMP-Ang2, strongly activates Tie2 receptor and stimulates angiogenesis. *Biochimica Et Biophysica Acta.* **1793,** 772-780.

Kim, I., Kim, H.G., Moon, S.O., Chae, S.W., So, J.N., Koh, K.N., Ahn, B.C., Koh, G.Y., 2000. Angiopoietin-1 induces endothelial cell sprouting through the activation of focal adhesion kinase and plasmin secretion. *Circulation Research.* **86,** 952-959.

Kim, I., Kim, J.H., Moon, S.O., Kwak, H.J., Kim, N.G., Koh, G.Y., 2000. Angiopoietin-2 at high concentration can enhance endothelial cell survival through the phosphatidylinositol 3'-kinase/Akt signal transduction pathway. *Oncogene.* **19,** 4549-4552.

Kim, I., Kwak, H.J., Ahn, J.E., So, J.N., Liu, M., Koh, K.N., Koh, G.Y., 1999. Molecular cloning and characterization of a novel angiopoietin family protein, angiopoietin-3. *FEBS Letters.* **443,** 353-356.

Kim, I., Oh, J.L., Ryu, Y.S., So, J.N., Sessa, W.C., Walsh, K., Koh, G.Y., 2002. Angiopoietin-1 negatively regulates expression and activity of tissue factor in endothelial cells. *The FASEB Journal : Official Publication of the Federation of American Societies for Experimental Biology.* **16,** 126-128.

Kim, K.T., Choi, H.H., Steinmetz, M.O., Maco, B., Kammerer, R.A., Ahn, S.Y., Kim, H.Z., Lee, G.M., Koh, G.Y., 2005. Oligomerization and multimerization are critical for angiopoietin-1 to bind and phosphorylate Tie2. *The Journal of Biological Chemistry.* **280,** 20126-20131.

Kim, K.T., Choi, H.H., Steinmetz, M.O., Maco, B., Kammerer, R.A., Ahn, S.Y., Kim, H.Z., Lee, G.M., Koh, G.Y., 2005. Oligomerization and multimerization are critical for angiopoietin-1 to bind and phosphorylate Tie2. *The Journal of Biological Chemistry.* **280,** 20126-20131.

Kitano, H., 2002. Computational systems biology. *Nature.* **420,** 206-210.

Kitano, H., 2002. Systems biology: a brief overview. *Science (New York, N.Y.).* **295,** 1662-1664.

Kitano, H., Funahashi, A., Matsuoka, Y., Oda, K., 2005. Using process diagrams for the graphical representation of biological networks. *Nature Biotechnology.* **23,** 961-966.

Koh, G.Y., 2013. Orchestral actions of angiopoietin-1 in vascular regeneration. *Trends in Molecular Medicine.* **19,** 31-39.

Kontos, C.D., Stauffer, T.P., Yang, W.P., York, J.D., Huang, L., Blanar, M.A., Meyer, T., Peters, K.G., 1998. Tyrosine 1101 of Tie2 is the major site of association of p85 and is required for activation of phosphatidylinositol 3-kinase and Akt. *Molecular and Cellular Biology.* **18,** 4131-4140.

Korhonen, J., Partanen, J., Armstrong, E., Vaahtokari, A., Elenius, K., Jalkanen, M., Alitalo, K., 1992. Enhanced expression of the tie receptor tyrosine kinase in endothelial cells during neovascularization. *Blood.* **80,** 2548-2555.

Kriete, A. and Eils, R., 2005. *Computational Systems Biology.* San Diego, CA: Elsevier Academic Press.

Krohn, K.A. & Link, J.M., 2003. Interpreting enzyme and receptor kinetics: keeping it simple, but not too simple. *Nuclear Medicine and Biology.* **30,** 819-826.

Lauffenburger, L., 1993. Receptors: Models for Binding, Trafficking, and Signaling.

Lee, H.J., Cho, C.H., Hwang, S.J., Choi, H.H., Kim, K.T., Ahn, S.Y., Kim, J.H., Oh, J.L., Lee, G.M., Koh, G.Y., 2004. Biological characterization of angiopoietin-3 and angiopoietin-4. *The FASEB Journal : Official Publication of the Federation of American Societies for Experimental Biology.* **18,** 1200-1208.

Lee, S., Mandic, J., Van Vliet, K.J., 2007. Chemomechanical mapping of ligand-receptor binding kinetics on cells. *Proceedings of the National Academy of Sciences of the United States of America.* **104,** 9609-9614.

Li, C., Donizelli, M., Rodriguez, N., Dharuri, H., Endler, L., Chelliah, V., Li, L., He, E., Henry, A., Stefan, M.I., Snoep, J.L., Hucka, M., Le Novere, N., Laibe, C., 2010.

BioModels Database: An enhanced, curated and annotated resource for published quantitative kinetic models. *BMC Systems Biology.* **4,** 92.

Maisonpierre, P.C., Suri, C., Jones, P.F., Bartunkova, S., Wiegand, S.J., Radziejewski, C., Compton, D., McClain, J., Aldrich, T.H., Papadopoulos, N., Daly, T.J., Davis, S., Sato, T.N., Yancopoulos, G.D., 1997. Angiopoietin-2, a natural antagonist for Tie2 that disrupts in vivo angiogenesis. *Science (New York, N.Y.).* **277,** 55-60.

Maliba, R., Brkovic, A., Neagoe, P.E., Villeneuve, L.R., Sirois, M.G., 2008. Angiopoietin-mediated endothelial P-selectin translocation: cell signaling mechanisms. *Journal of Leukocyte Biology.* **83,** 352-360.

Marron, M.B., Hughes, D.P., Edge, M.D., Forder, C.L., Brindle, N.P., 2000. Evidence for heterotypic interaction between the receptor tyrosine kinases TIE-1 and TIE-2. *The Journal of Biological Chemistry.* **275,** 39741-39746.

Marron, M.B., Hughes, D.P., McCarthy, M.J., Beaumont, E.R., Brindle, N.P., 2000. Tie-1 receptor tyrosine kinase endodomain interaction with SHP2: potential signalling mechanisms and roles in angiogenesis. *Advances in Experimental Medicine and Biology.* **476,** 35-46.

Marron, M.B., Singh, H., Tahir, T.A., Kavumkal, J., Kim, H.Z., Koh, G.Y., Brindle, N.P., 2007. Regulated proteolytic processing of Tie1 modulates ligand responsiveness of the receptor-tyrosine kinase Tie2. *The Journal of Biological Chemistry.* **282,** 30509-30517.

Matthews, J.A., Batki, A., Hynds, C., Kricka, L.J., 1985. Enhanced chemiluminescent method for the detection of DNA dot-hybridization assays. *Analytical Biochemistry.* **151,** 205-209.

McCarthy, M.J., Crowther, M., Bell, P.R., Brindle, N.P., 1998. The endothelial receptor tyrosine kinase tie-1 is upregulated by hypoxia and vascular endothelial growth factor. *FEBS Letters.* **423,** 334-338.

Moss, A., 2013. The angiopoietin:Tie 2 interaction: A potential target for future therapies in human vascular disease. *Cytokine & Growth Factor Reviews.*

Murray, B.W., Padrique, E.S., Pinko, C., McTigue, M.A., 2001. Mechanistic effects of autophosphorylation on receptor tyrosine kinase catalysis: enzymatic characterization of Tie2 and phospho-Tie2. *Biochemistry.* **40,** 10243-10253.

Nishimura, M., Miki, T., Yashima, R., Yokoi, N., Yano, H., Sato, Y., Seino, S., 1999. Angiopoietin-3, a novel member of the angiopoietin family. *FEBS Letters.* **448,** 254-256.

Onimaru, M., Yonemitsu, Y., Suzuki, H., Fujii, T., Sueishi, K., 2010. An autocrine linkage between matrix metalloproteinase-14 and Tie-2 via ectodomain shedding modulates angiopoietin-1-dependent function in endothelial cells. *Arteriosclerosis, Thrombosis, and Vascular Biology.* **30,** 818-826.

Orton, R.J., Sturm, O.E., Gormand, A., Wolch, W., Gilbert, D.R., 2008. Computational modelling reveals feedback redundancy within the epidermal growth factor receptor/extracellular-signal regulated kinase signalling pathway. *IET Systems Biology.* **2,** 173-183.

Orton, R.J., Sturm, O.E., Vyshemirsky, V., Calder, M., Gilbert, D.R., Kolch, W., 2005. Computational modelling of the receptor-tyrosine-kinase-activated MAPK pathway. *The Biochemical Journal.* **392,** 249-261.

Papin, J.A., Price, N.D., Wiback, S.J., Fell, D.A., Palsson, B.O., 2003. Metabolic pathways in the post-genome era. *Trends in Biochemical Sciences.* **28,** 250-258.

Parikh, S.M., 2013. Dysregulation of the angiopoietin-Tie-2 axis in sepsis and ARDS. *Virulence.* **4,** 517-524.

Parikh, S.M., Mammoto, T., Schultz, A., Yuan, H.T., Christiani, D., Karumanchi, S.A., Sukhatme, V.P., 2006. Excess circulating angiopoietin-2 may contribute to pulmonary vascular leak in sepsis in humans. *PLoS Medicine.* **3,** e46.

Peters, K.G., Coogan, A., Berry, D., Marks, J., Iglehart, J.D., Kontos, C.D., Rao, P., Sankar, S., Trogan, E., 1998. Expression of Tie2/Tek in breast tumour vasculature provides a new marker for evaluation of tumour angiogenesis. *British Journal of Cancer.* **77,** 51-56.

Procopio, W.N., Pelavin, P.I., Lee, W.M., Yeilding, N.M., 1999. Angiopoietin-1 and -2 coiled coil domains mediate distinct homo-oligomerization patterns, but fibrinogen-like domains mediate ligand activity. *The Journal of Biological Chemistry.* **274,** 30196-30201.

Resat, H., Ewald, J.A., Dixon, D.A., Wiley, H.S., 2003. An integrated model of epidermal growth factor receptor trafficking and signal transduction. *Biophysical Journal.* **85,** 730-743.

Reusch, P., Barleon, B., Weindel, K., Martiny-Baron, G., Godde, A., Siemeister, G., Marme, D., 2001. Identification of a soluble form of the angiopoietin receptor TIE-2 released from endothelial cells and present in human blood. *Angiogenesis.* **4,** 123-131.

Robinson, J.M. & Vandre, D.D., 2001. Antigen retrieval in cells and tissues: enhancement with sodium dodecyl sulfate. *Histochemistry and Cell Biology.* **116,** 119-130.

Saharinen, P., Eklund, L., Miettinen, J., Wirkkala, R., Anisimov, A., Winderlich, M., Nottebaum, A., Vestweber, D., Deutsch, U., Koh, G.Y., Olsen, B.R., Alitalo, K., 2008. Angiopoietins assemble distinct Tie2 signalling complexes in endothelial cell-cell and cell-matrix contacts. *Nature Cell Biology.* **10,** 527-537.

Saharinen, P., Kerkela, K., Ekman, N., Marron, M., Brindle, N., Lee, G.M., Augustin, H., Koh, G.Y., Alitalo, K., 2005. Multiple angiopoietin recombinant proteins activate the Tie1 receptor tyrosine kinase and promote its interaction with Tie2. *The Journal of Cell Biology.* **169,** 239-243.

Sato, T.N., Qin, Y., Kozak, C.A., Audus, K.L., 1993. Tie-1 and tie-2 define another class of putative receptor tyrosine kinase genes expressed in early embryonic vascular system. *Proceedings of the National Academy of Sciences of the United States of America.* **90,** 9355-9358.

Sato, T.N., Tozawa, Y., Deutsch, U., Wolburg-Buchholz, K., Fujiwara, Y., Gendron-Maguire, M., Gridley, T., Wolburg, H., Risau, W., Qin, Y., 1995. Distinct roles of the receptor tyrosine kinases Tie-1 and Tie-2 in blood vessel formation. *Nature.* **376,** 70-74.

Scharpfenecker, M., Fiedler, U., Reiss, Y., Augustin, H.G., 2005. The Tie-2 ligand angiopoietin-2 destabilizes quiescent endothelium through an internal autocrine loop mechanism. *Journal of Cell Science.* **118,** 771-780.

Schmidt, H. & Jirstrand, M., 2006. Systems Biology Toolbox for MATLAB: a computational platform for research in systems biology. *Bioinformatics (Oxford, England).* **22,** 514-515.

Schneider, C.A., Rasband, W.S., Eliceiri, K.W., 2012. NIH Image to ImageJ: 25 years of image analysis. *Nature Methods.* **9,** 671-675.

Schnurch, H. & Risau, W., 1993. Expression of tie-2, a member of a novel family of receptor tyrosine kinases, in the endothelial cell lineage. *Development (Cambridge, England).* **119,** 957-968.

Schoeberl, B., Eichler-Jonsson, C., Gilles, E.D., Muller, G., 2002. Computational modeling of the dynamics of the MAP kinase cascade activated by surface and internalized EGF receptors. *Nature Biotechnology.* **20,** 370-375.

Schutz-Geschwender, A., Zhang, Y., Holt, T., McDermitt, D., Olive, D., 2004. Quantitative, two-color Western blot detection with infrared fluorescence. *LI-COR Biosciences.*

Seegar, T.C., Eller, B., Tzvetkova-Robev, D., Kolev, M.V., Henderson, S.C., Nikolov, D.B., Barton, W.A., 2010. Tie1-Tie2 interactions mediate functional differences between angiopoietin ligands. *Molecular Cell.* **37,** 643-655.

Shankaran, H., Resat, H., Wiley, H.S., 2007. Cell surface receptors for signal transduction and ligand transport: a design principles study. *PLoS Computational Biology.* **3,** e101.

Shaw, J.P., Basch, R., Shamamian, P., 2004. Hematopoietic stem cells and endothelial cell precursors express Tie-2, CD31 and CD45. *Blood Cells, Molecules & Diseases.* **32,** 168-175.

Siner, J.M., Bhandari, V., Engle, K.M., Elias, J.A., Siegel, M.D., 2009. Elevated serum angiopoietin 2 levels are associated with increased mortality in sepsis. *Shock (Augusta, Ga.).* **31,** 348-353.

Singh, H., Tahir, T.A., Alawo, D.O., Issa, E., Brindle, N.P., 2011. Molecular control of angiopoietin signalling. *Biochemical Society Transactions.* **39,** 1592-1596.

Starbuck, C. & Lauffenburger, D.A., 1992. Mathematical model for the effects of epidermal growth factor receptor trafficking dynamics on fibroblast proliferation responses. *Biotechnology Progress.* **8,** 132-143.

Steele, K., 2013. Directed Evolution of Angiopoietin-Binding Proteins by Somatic Hypermutation and Cell Surface Display. PhD Thesis ed. University of Leicester, UK.

Stoll, M., Cowley, A.W.,Jr, Tonellato, P.J., Greene, A.S., Kaldunski, M.L., Roman, R.J., Dumas, P., Schork, N.J., Wang, Z., Jacob, H.J., 2001. A genomic-systems biology map for cardiovascular function. *Science (New York, N.Y.).* **294,** 1723-1726.

Stratmann, A., Risau, W., Plate, K.H., 1998. Cell type-specific expression of angiopoietin-1 and angiopoietin-2 suggests a role in glioblastoma angiogenesis. *The American Journal of Pathology.* **153,** 1459-1466.

Sugimachi, K., Tanaka, S., Taguchi, K., Aishima, S., Shimada, M., Tsuneyoshi, M., 2003. Angiopoietin switching regulates angiogenesis and progression of human hepatocellular carcinoma. *Journal of Clinical Pathology.* **56,** 854-860.

Suri, C., Jones, P.F., Patan, S., Bartunkova, S., Maisonpierre, P.C., Davis, S., Sato, T.N., Yancopoulos, G.D., 1996. Requisite role of angiopoietin-1, a ligand for the TIE2 receptor, during embryonic angiogenesis. *Cell.* **87,** 1171-1180.

Suri, C., McClain, J., Thurston, G., McDonald, D.M., Zhou, H., Oldmixon, E.H., Sato, T.N., Yancopoulos, G.D., 1998. Increased vascularization in mice overexpressing angiopoietin-1. *Science (New York, N.Y.).* **282,** 468-471.

Tait, C.R. & Jones, P.F., 2004. Angiopoietins in tumours: the angiogenic switch. *The Journal of Pathology.* **204,** 1-10.

Takagi, H., Koyama, S., Seike, H., Oh, H., Otani, A., Matsumura, M., Honda, Y., 2003. Potential role of the angiopoietin/tie2 system in ischemia-induced retinal neovascularization. *Investigative Ophthalmology & Visual Science.* **44,** 393-402.

Takahama, M., Tsutsumi, M., Tsujiuchi, T., Nezu, K., Kushibe, K., Taniguchi, S., Kotake, Y., Konishi, Y., 1999. Enhanced expression of Tie2, its ligand angiopoietin-1, vascular endothelial growth factor, and CD31 in human non-small cell lung carcinomas. *Clinical Cancer Research : An Official Journal of the American Association for Cancer Research.* **5,** 2506-2510.

Tan, W.H., Popel, A.S., Mac Gabhann, F., 2013. Computational Model of Gab1/2-Dependent VEGFR2 Pathway to Akt Activation. *PloS One.* **8,** e67438.

Tan, W.H., Popel, A.S., Mac Gabhann, F., 2013. Computational model of VEGFR2 pathway to ERK activation and modulation through receptor trafficking. *Cellular Signalling.* **25,** 2496-2510.

Tanaka, S., Mori, M., Sakamoto, Y., Makuuchi, M., Sugimachi, K., Wands, J.R., 1999. Biologic significance of angiopoietin-2 expression in human hepatocellular carcinoma. *The Journal of Clinical Investigation.* **103,** 341-345.

Teichert-Kuliszewska, K., Maisonpierre, P.C., Jones, N., Campbell, A.I., Master, Z., Bendeck, M.P., Alitalo, K., Dumont, D.J., Yancopoulos, G.D., Stewart, D.J., 2001. Biological action of angiopoietin-2 in a fibrin matrix model of angiogenesis is associated with activation of Tie2. *Cardiovascular Research.* **49,** 659-670.

Thomas, M. & Augustin, H.G., 2009. The role of the Angiopoietins in vascular morphogenesis. *Angiogenesis.* **12,** 125-137.

Thurston, G. & Daly, C., 2012. The complex role of angiopoietin-2 in the angiopoietin-tie signaling pathway. *Cold Spring Harbor Perspectives in Medicine.* **2,** a006550.

Thurston, G., Rudge, J.S., Ioffe, E., Zhou, H., Ross, L., Croll, S.D., Glazer, N., Holash, J., McDonald, D.M., Yancopoulos, G.D., 2000. Angiopoietin-1 protects the adult vasculature against plasma leakage. *Nature Medicine.* **6,** 460-463.

Thurston, G., Suri, C., Smith, K., McClain, J., Sato, T.N., Yancopoulos, G.D., McDonald, D.M., 1999. Leakage-resistant blood vessels in mice transgenically overexpressing angiopoietin-1. *Science (New York, N.Y.).* **286,** 2511-2514.

Tsai, J.H. & Lee, W.M., 2009. Tie2 in tumor endothelial signaling and survival: implications for antiangiogenic therapy. *Molecular Cancer Research : MCR.* **7,** 300-310.

Valenzuela, D.M., Griffiths, J.A., Rojas, J., Aldrich, T.H., Jones, P.F., Zhou, H., McClain, J., Copeland, N.G., Gilbert, D.J., Jenkins, N.A., Huang, T., Papadopoulos, N., Maisonpierre, P.C., Davis, S., Yancopoulos, G.D., 1999. Angiopoietins 3 and 4: diverging gene counterparts in mice and humans. *Proceedings of the National Academy of Sciences of the United States of America.* **96,** 1904-1909.

Vikkula, M., Boon, L.M., Carraway, K.L.,3rd, Calvert, J.T., Diamonti, A.J., Goumnerov, B., Pasyk, K.A., Marchuk, D.A., Warman, M.L., Cantley, L.C., Mulliken, J.B., Olsen, B.R., 1996. Vascular dysmorphogenesis caused by an activating mutation in the receptor tyrosine kinase TIE2. *Cell.* **87,** 1181-1190.

Waterman, H. & Yarden, Y., 2001. Molecular mechanisms underlying endocytosis and sorting of ErbB receptor tyrosine kinases. *FEBS Letters.* **490,** 142-152.

Winderlich, M., Keller, L., Cagna, G., Broermann, A., Kamenyeva, O., Kiefer, F., Deutsch, U., Nottebaum, A.F., Vestweber, D., 2009. VE-PTP controls blood vessel development by balancing Tie-2 activity. *The Journal of Cell Biology.* **185,** 657-671.

Yabkowitz, R., Meyer, S., Black, T., Elliott, G., Merewether, L.A., Yamane, H.K., 1999. Inflammatory cytokines and vascular endothelial growth factor stimulate the release of soluble tie receptor from human endothelial cells via metalloprotease activation. *Blood.* **93,** 1969-1979.

Yabkowitz, R., Meyer, S., Yanagihara, D., Brankow, D., Staley, T., Elliott, G., Hu, S., Ratzkin, B., 1997. Regulation of tie receptor expression on human endothelial cells by protein kinase C-mediated release of soluble tie. *Blood.* **90,** 706-715.

Yacyshyn, O.K., Lai, P.F., Forse, K., Teichert-Kuliszewska, K., Jurasz, P., Stewart, D.J., 2009. Tyrosine phosphatase beta regulates angiopoietin-Tie2 signaling in human endothelial cells. *Angiogenesis.* **12,** 25-33.

Yu, X., Seegar, T.C., Dalton, A.C., Tzvetkova-Robev, D., Goldgur, Y., Rajashankar, K.R., Nikolov, D.B., Barton, W.A., 2013. Structural basis for angiopoietin-1-mediated signaling initiation. *Proceedings of the National Academy of Sciences of the United States of America.* **110,** 7205-7210.

Yuan, H.T., Khankin, E.V., Karumanchi, S.A., Parikh, S.M., 2009. Angiopoietin 2 is a partial agonist/antagonist of Tie2 signaling in the endothelium. *Molecular and Cellular Biology.* **29,** 2011-2022.

Yuan, H.T., Venkatesha, S., Chan, B., Deutsch, U., Mammoto, T., Sukhatme, V.P., Woolf, A.S., Karumanchi, S.A., 2007. Activation of the orphan endothelial receptor Tie1 modifies Tie2-mediated intracellular signaling and cell survival. *The FASEB Journal : Official Publication of the Federation of American Societies for Experimental Biology.* **21,** 3171-3183.

Zi, Z., 2011. Sensitivity analysis approaches applied to systems biology models. *IET Systems Biology.* **5,** 336-336.